RELIABILITY ASSESSMENT OF REHABILITATED BUILDINGS OF MODERATE HEIGHT

RELIABILITY ASSESSMENT OF REHABILITATED BUILDINGS OF MODERATE HEIGHT

BY

Ahmed Hassanein, M.Sc.

A Project
Submitted to the School of Graduate Studies
in Partial Fulfilment of the requirements
for the degree of
Master of Engineering

McMaster University

Master of Engineering (1997)
(Civil Engineering)

McMaster University
Hamilton, Ontario

Title: Reliability Assessment of Rehabilitated Buildings of Moderate Height
Author: Ahmed Hassanein, M.Sc.
Supervisor: Professor A. Ghobarah
Number of Pages: xi, 136

ABSTRACT

Buildings that were designed according to earlier codes tend to have limited lateral load-carrying capacity when compared to buildings built in accordance with current seismic codes. This deficiency caused severe damage to existing buildings when subjected to earthquake loading. Over the past three decades, building codes have been updated with more stringent seismic demand requirements.

The objective of the current study is to evaluate the seismic behaviour of an existing nine-storey office building, designed according to the ACI-318-63 code. Pushover static analysis, as well as seismic analysis of the building behaviour were conducted.

Uncertainties in both the demand (load) on the structural system as well as capacity (resistance) were taken into account. An ensemble of synthetically-generated ground motion time history records was used to simulate earthquakes on both soft soil and rock sites using both stationary and non-stationary approaches. Randomness in structural capacity was modelled by selecting appropriate probability distributions for variations in both element dimensions and material strength. Aging of concrete was also taken into account. The Monte Carlo Simulation was used to incorporate various sources of uncertainty into the analysis.

The performance of the existing building was evaluated. Different performance levels were defined for the structure in terms of the damage levels. The damage state of the building was quantified using the damage index proposed by Park et al. (1985) and modified by Kunnath et al. (1992). The results of the dynamic analysis were related to the damage index, story drift, roof drift and the static pushover analysis.

The reliability approach was used to evaluate the effectiveness of different retrofitting schemes for the reinforced concrete columns of the existing building. The retrofitting schemes considered included increasing strength, ductility, stiffness and both strength and stiffness simultaneously.

ACKNOWLEDGMENTS

I would like to express my deep appreciation and gratitude to my supervisor, Dr. Ahmed Ghobarah, for his continued guidance and cooperation during the process of this work. His advice and comments were most valuable. His cooperation went far beyond the call of duty.

I would also like to express my gratitude to Dr. Brian Baetz, Chair of the Department of Civil Engineering, and Dr. Brian Allen for their sincere cooperation when the going got tough.

I'd also like to thank Dr. Mohamed El-Attar, University of Western Ontario, for his invaluable advice throughout the progress of this work. The cooperation of Maged Youssef and Hamdy Abou ElFath is also greatly acknowledged. I would like to thank Gail Britton and Deborah Smaluck for their patience and cooperation.

Last, but in no way least, I'd like to thank my wife for her patience and understanding, and putting up with the long hours I spent at the computer.

TABLE OF CONTENTS

LIST OF TABLES

LIST OF FIGURES

CHAPTER ONE

INTRODUCTION

1.1 BACKGROUND

Existing structures that were built before the 1970's tend to perform rather poorly during earthquakes when compared to structures built in accordance with current seismic codes. This is because many of the structures that exist today were designed and constructed before seismic codes were in effect or were designed according to earlier, inadequate seismic codes. Compared to structures built according to the current code provisions, earlier structures tend to have insufficient lateral load-carrying capacity. Over the past few decades, design codes have been regularly updated, often imposing more stringent seismic demands. Other important factors that also affect the performance of existing structures are aging and deterioration with time and use.

It is recommended that the state of existing structures be inspected immediately following major earthquakes. This assessment, which could be conducted either analytically or experimentally, would help decide whether any retrofitting is necessary. Analytical investigation methods include the examination of the design calculations and drawings, reviewing applicable specifications, and

analysing the structure aided by additional field observations. Experimental investigation is normally concerned with determining the locations of plastic hinging and failure (if any), as well as detecting any defective structural elements (Yao, 1981). Non-destructive testing techniques (NDT) have been frequently used to help assess the lateral load-carrying capacity of different structures. From the experimental assessment, the stiffness and dynamic characteristics of structures could be estimated. Visible damage features such as cracks and permanent deformations can be detected by inspectors. Smaller cracks could be detected by the use of advanced NDT equipment.

Due to the lack of well-defined criteria for evaluating the state of existing structures, testing the building for compliance with current code provisions may be a logical criterion. However, the problem with such an approach is that codes are being updated on regular basis, and that there are no explicit provisions available for older materials, outdated methods, or structural elements that do not comply with current detailing requirements (Holmes, 1996). Another disadvantage is that the performance criterion in recent codes is difficult to adjust for aging structures. In addition, upgrading existing structures in order to comply with new codes may not be necessary or economical.

Several researchers have attempted to evaluate the seismic capacity of existing structures. However, no method has developed into a universally-accepted standard procedure. An earlier attempt to suggest procedures for evaluating existing buildings was presented in the report by FEMA (1992a and b). It was based on an earlier

report: *Evaluating the Seismic Resistance of Existing Buildings* (ATC, 1987). Another document (NRC, 1992a) was published in Canada (Allen and Rainer, 1996). After the 1968 Tokachi-Oki Earthquake in Japan, an extensive effort was made to evaluate and enhance the performance of existing structures. Special attention was paid to structures that were damaged during the earthquake. A comprehensive standard for reinforced concrete buildings is available in Japan. This standard is applicable to existing as well as damaged structures (Hirosawa et al., 1994: as reported by Holmes, 1996).

Guidelines and procedures for the evaluation of seismic performance of existing buildings were developed in the U.S. (ATC, 1987; Rojahn, 1986). The methodology is mainly concerned with life safety, which can be defined as the potential for both structural and non-structural damage that may cause death or injury to occupants. This methodology classifies existing buildings into 15 model building types, depending on the type of construction, construction material, and the lateral load-resisting elements. Seismic hazard maps are used to estimate the expected level of seismic loading. Certain characteristics of the building that would render it particularly vulnerable to seismic damage are identified. These characteristics include shear capacity of columns, load paths, and performance during previous earthquakes.

The FEMA (1992b) guidelines aim at achieving a wide range of performance by adopting a rehabilitation objective which is based on a desired performance level for a given hazard (ground motion). Figure 1.1 shows the performance levels in terms of damage. The four principal adopted performance levels are:

i) operational,

ii) immediate occupancy,

iii) life safety, and

iv) collapse prevention.

Ghobarah et al. (1997) proposed the use of the level of damage as a measure of the performance level. The damage levels are;

i) no damage,

ii) minor damage,

iii) repairable damage,

iv) unrepairable damage, and

v) excessive damage.

When investigating the performance of existing structures, one approach could be to use damage assessment criterion as an indicator of the behaviour of the structure during seismic loading. Some of the available damage models, and retrofitting techniques, will be presented.

1.2 DAMAGE MODELS

Several damage models are available to determine the state of a structure when subjected to seismic loading. In an attempt to quantify the damage suffered by the structure, the idea of a damage index was introduced. The damage index is a

measure of the damage state of the structure. Local damage indices quantify the damage state of individual members or connections, while global damage indices relate to the overall damage state of the structure. Some of the common damage indices are reviewed.

1.2.1 Banon et al.

Inter-storey drift and ductility were used as measures for damage in earlier models. Banon et al. (1981) defined the rotation ductility, μ_θ, as follows:

$$\mu_\theta = \frac{\theta_{max}}{\theta_y} \tag{1.1}$$

where θ_{max} is the maximum rotation and θ_y is the rotation at first yielding of the steel reinforcement. The rotation ductility measure as defined by Equation 1.1 does not account for load reversal under seismic loading. In order to overcome this problem, Banon et al. (1981) suggested the use of the flexural damage ratio. Flexural damage ratio is defined as the ratio of the initial tangent stiffness to a reduced secant stiffness at maximum deformation.

1.2.2 Park and Ang

A local damage index that incorporates the combined effects of damage due to both deformation and fatigue was introduced by Park et al. (1984) and Park and Ang (1985). This damage model accounts for the element ductility and the hysteretic

energy dissipated by the element during seismic loading. The damage index for a structural element is defined as:

$$DI = \frac{\delta_m}{\delta_u} + \frac{\beta}{\delta_u P_y} \int dE_h \qquad (1.2)$$

where δ_m is the maximum deformation of the element,

δ_u is the ultimate deformation of the element,

P_y is the yield strength of the element,

$\int dE_h$ is the hysteretic energy absorbed by the element during the seismic loading, and

β is the model constant parameter.

A value of 0.1 was suggested for the model constant (β) for nominal strength deterioration (Park et al., 1987). This damage model accounts for the damage caused by maximum inelastic strains due to the deformation history. The global damage index is the weighted average of the local damage indices of the elements of the structure. The global damage index, *D*, is given by:

$$D = \sum_{i=1}^{N} \lambda_i D_i \qquad (1.3)$$

$$\text{where} \quad \lambda_i = E_i / \sum_{i=1}^{N} E_i \qquad (1.4)$$

D_i is the local damage index of element i,

N is the number of elements, and

E_i is the energy dissipated in element i.

The global damage index could be calculated for the whole structure or part of the structure such as a specific floor in a moment-resisting frame. The Park et al. (1985) damage index was later modified by Kunnath et al. (1992) as

$$DI = \frac{\theta_m - \theta_r}{\theta_u - \theta_r} + \frac{\beta}{M_y \theta_u} E_h \qquad (1.5)$$

where θ_m is the maximum rotation attained during the loading history,

θ_u is the ultimate rotation capacity of the section,

θ_r is the recoverable rotation when unloading,

M_y is the yield moment, and

E_h is the dissipated energy in the section.

1.2.3 Roufael and Meyer

Roufael and Meyer (1987) closely observed the relationship between the roof displacement and the change in the structure's fundamental frequency. They developed a model based on the concept of structural softening. Their proposed damage index, D, is given by:

$$D = \frac{\delta_r - \delta_y}{\delta_f - \delta_y} = \frac{14.2\ \delta_y\ (\sqrt{\omega_e/\omega} - 1)}{\delta_f - \delta_y} \qquad (1.6)$$

where δ_r is the maximum roof displacement caused by the earthquake,

δ_y is the roof displacement when the first steel reinforcement starts to yield,

δ_f is the roof displacement at failure,

ω_e is the fundamental frequency of the undamaged structure, and

ω is the fundamental frequency of the damaged structure.

Roufael and Meyer's (1987) damage model provides little information regarding the distribution of damage sustained by the various members of the structure. Other drawbacks are that the damage index does not account for the dissipation of hysteretic energy, and the difficulty in determining the roof displacement at failure.

The model developed by Roufael and Meyer (1987) was based on the concept of structural softening. However, the model implements the concept of overall softening of the structure. Thus, the model does not account for locally-sustained damage by different elements.

1.2.4 DiPasquale and Cakmak

DiPasquale and Cakmak (1990) developed two damage indices. Both models

were based on the concept of structural softening; the maximum (δ_m) and final (δ_f) softening indices. They are computed using the following formulae;

$$\delta_m = 1 - \frac{T_0}{T_{max}} \tag{1.7}$$

and

$$\delta_f = 1 - \frac{T_0^2}{T_f^2} \tag{1.8}$$

where δ_m is the maximum softening index,

δ_f is the final softening index,

T_0 is the initial natural period,

T_{max} is the longest natural period of an equivalent linear system, and

T_f is the final natural period of an equivalent linear system.

As the square of the period is inversely-proportional to the stiffness, the final softening index δ_f is closely related to the average reduction in the structure's stiffness. On the other hand, the value of maximum softening index, δ_m, depends mainly on the degree of degradation of stiffness, and plastic deformation caused by the seismic loading.

The model developed by DiPasquale and Cakmak (1987) is similar to that of by Roufael and Meyer (1987) in that it's based on the concept of structural softening.

1.2.5 Bracci et al.

Bracci et al. (1989) developed a damage index based on the damage state of an element compared to its ultimate damage potential. The damage potential is computed from the area enveloped by the monotonic load-deformation curve and the fatigue failure envelope. The damage sustained by an element can be related to either;

i) strength deterioration and dissipated hysteretic energy, or

ii) permanent deformations.

Bracci et al. (1989) calibrated their damage index using a series of tests performed on columns and frame models. The damage model proved to be a relatively good indicator of the damage state of the structure. The model is simple, as it uses a simplified bilinear moment-curvature relationship. However, its level of complexity may be increased if a more sophisticated relationship is implemented.

1.2.6 Fragility Analysis

The ATC-13 report (ATC, 1985) proposed a methodology for developing the motion-damage relationships for 78 different categories of structures. Since the available data was somewhat limited, the report mainly relied on expertise, and data that was provided by a study of the probabilities of damage occurrence to each structure type at different levels of seismic activity. The peak ground acceleration (PGA) is used as a measure of the level of seismic activity.

Motion-damage relationships are frequently expressed as either damage

probability matrices (DPMs) or fragility curves. A DPM contains values of the probabilities of the structure being at a certain level of damage at specific levels of seismic activity. On the other hand, a fragility curve is a plot of the conditional probabilities versus the level of seismic activity. Thus, both approaches provide information on the probability of experiencing some level of damage under a specified level of ground motion.

1.3 REHABILITATION TECHNIQUES

The selection of a particular technique for structural rehabilitation should be guided by a well-defined objective and strategy. Engineering judgement might favour one technique over another depending on the situation. Among the most widely used rehabilitation techniques for concrete buildings are jacketing of columns, addition of structural walls, and steel bracing. Many buildings were heavily damaged by the 1968 Tokachi-Oki Earthquake, Japan. The Japan Concrete Institute compiled data on 157 existing reinforced concrete buildings in Japan that were constructed between the early 1930's and mid-1970's (Edno et al., 1984). The investigated sample included both damaged and undamaged buildings that had been upgraded to enhance their lateral load-carrying capacity. The study concluded that in the majority of cases undamaged buildings had been upgraded. On the other hand, in a few cases, buildings that experienced some damage by an earthquake were previously rehabilitated structures. The survey showed that adding shear walls was the most common retrofitting technique. In 35% of the cases, column jacketing was the second most

common method of choice.

An experimental investigation was carried out by Sugano (1981) to determine the effect of using different retrofitting techniques. A portal frame was tested both before and after strengthening using eight retrofitting strategies. Figure 1.2 (Sugano, 1981) presents typical load-displacement relationships for the studied structures. Sugano (1981) pointed out that the figure should only be used as a qualitative indicator of the order of strength and ductility that might be attained by adopting each technique. The figure indicates that adding a monolithic wall provides the highest increase in strength, however, loss of ductility is associated with the increase in strength.

When rehabilitating a structure, the normal practice is to retrofit the weak elements and potential damage regions. No established procedures exist for developing a rational rehabilitation strategy which would favour one retrofitting technique over another. Moreover, the effect of the rehabilitating scheme on the performance of a structure remains an area that cannot yet be accurately predicted.

Previous researchers have examined different rehabilitation techniques and their effect on the performance of structures (Bertero, 1992; Anicic, 1994; and Rodriguez 1994). Some of the common rehabilitation schemes are reviewed.

1.3.1 Wall Elements

The lateral load-carrying capacity of structures could be enhanced by providing structural wall elements. These could either be infill walls that are cast in

place reinforced concrete, precast panels or steel plates. In general, the flexural capacity of infill walls depends on the strength of the boundary or framing elements. However, practical reasons might prevent the use of infill walls, due to required openings or the difficulties involved with placing concrete in an existing frame. Ensuring that the proper connection is established between the existing frame members and the wall could also prove to be difficult. Lengthy reinforced concrete construction time may be a source of inconvenience to the building occupants. The use of steel plate panels as structural walls has two main advantages over concrete walls;

i) the structural steel wall panels cause no significant increase in the overall weight of the structure which is not expected to modify the dynamic characteristics of the structure, and

ii) short installation time.

1.3.2 Steel Braces

The addition of steel bracing systems to enhance the lateral load-carrying capacity of reinforced concrete moment-resisting frames is a common rehabilitation technique. A typical bracing system is shown in figure 1.3 (Jirsa, 1996). Steel braces consist of wide-flange sections to resist buckling under compressive loads. In addition to the steel braces, collector members are installed at the floor levels, as well as along the columns to sustain shear forces from the floor. Grouted anchor bolts are used to connect all collector elements to concrete elements of the structure. If the

collector members are not used, the brace joints with the existing concrete frame should be carefully designed and detailed. In addition, the column should be checked to ensure that no shear failure would occur due to the presence of the bracing.

The results of the testing of steel bracing showed that the retrofitted system performed reasonably well (Bush et al., 1991; Garcia, 1996). The response of the retrofitted structure was linear up to levels almost twice the code design forces. When the braces finally buckled, the load was transferred to columns and they eventually failed due to shear. This retrofitting scheme has the advantages of low weight as well as relatively short construction time. The steel bracing may cause obstructions to openings such as windows and doors. In the case of openings, eccentric steel bracing systems have been tested and shown to perform well. A link element is designed to yield and provide sufficient ductility before failure.

1.3.3 Cable Braces

Cable braces are mainly used to overcome the problems of buckling of the steel bracing system. The cable bracing system may span one to three floors. The cables may stretch from the top of a column on the last floor to the fixed end of the bottom column in a three-storey structure. This technique greatly enhances both the stiffness and strength of the structure. This rehabilitation scheme is normally used for low-rise concrete buildings, and was widely used in Mexico City following the 1985 Earthquake. In few situations, the cable bracing was used in wall panels to span each floor in high-rise buildings. The performance of this rehabilitation technique has not

been adequately tested during earthquakes. Jirsa (1996) recommended improving the behaviour of the structure by strengthening its elements, rather than concentrating the modifications in a few locations.

1.3.4 Strengthening of Columns

Jacketing is one of the most common techniques used to enhance the strength or increase the stiffness of reinforced concrete columns. Both concrete and steel jackets could be used. The concrete jacket is constructed by adding both longitudinal and transverse reinforcement enveloping the existing columns. The concrete is then poured to form the jacket. The jacket may be anchored to the original column so that both elements work as a composite member. Another alternative would be to isolate the jacket from the column. In this case each element would act separately in resisting the applied loads. Steel jackets are formed from welded steel plates, enveloping the existing columns. Non-shrink grout is then poured to fill the gap between the column and the jacket to ensure bonding (Ghobarah et al., 1996a, b and c).

Similar to the steel bracing technique, jacketing does not significantly increase the weight of the structure. Partial jacketing of the column increases its ductility but not its stiffness or strength. In this case, there is no need for strengthening the foundation. In the case where the full column is jacketed using reinforced concrete, the need for strengthening the foundations should be investigated. Concrete jacketing is labour-intensive, and requires careful design, detailing and construction.

Two techniques exist to strengthen concrete columns using steel jacketing;

complete covering, and using steel straps and angles. Both techniques are shown in figure 1.4 (Rodriguez and Park, 1991). The use of steel straps and angles may not be reliable because the steel is pre-heated and installed hot. As the steel cools, the straps are prestressed. This process is difficult to control in the field. Two methods for retrofitting the column-base connection were suggested by Ghobarah et al (1997) and Mahgoub (1997). These techniques are shown in Figure 1.5 (Mahgoub, 1997).

1.3.5 Strengthening of Beams

Many of the reinforced concrete structures built in accordance with earlier design codes share common problems. These include insufficient anchor length of the bottom (positive) reinforcement of beams, and inadequate shear reinforcement. One procedure to rehabilitate the length of anchorage of the bottom reinforcement is by using steel plates attached to the bottom end of the beam at the column joint. Epoxy-grouted dowels are normally used as anchors. This technique is schematically shown in figure 1.6 (Estrada, 1990). The steel plates relieve the bottom reinforcement of excess tensile forces that could otherwise cause bond failure. Although theoretically feasible, this rehabilitation system has not been tested in use in actual earthquakes.

1.4 THE RELIABILITY APPROACH

Much of the data used in the analysis and design of structures include various degrees of uncertainty. Thus neither the reliability nor the safety of the structure could be established in absolute terms. Reliability is addressed as the probability of

a certain level of structural performance under actual loading conditions. During the design phase, the uncertainties are taken into account in the form of a factor of safety.

Several modern design codes include the reliability-based load and resistance factor (LRFD). Wen et al, (1994), observed that this approach yields over-conservative estimates of both the load and resistance. However, the level of damage sustained by a structure designed using this approach with respect to its overall performance and the level of expected damage during severe earthquake events has not been clearly established.

Recently, several researchers, such as Veneziano (1976) and Shinozuka (1974), have been investigating reliability-based analysis (Wen et al., 1994). The probability of failure of a structure can be evaluated by employing either the First or Second Order Reliability Methods (FORM, or SORM) (Ang and Tang, 1984, and Madsen, 1986). Both methods are based on a first or second order approximation of the limit state function. The Monte Carlo Simulation technique can be applied for the same purpose to more complex structures.

1.5 OBJECTIVES

There is a need to develop performance-based design approaches in order to design the structure to a given level of expected performance. Performance-based design is also applicable in the case of rehabilitation of existing structures.

The objective of this study is to evaluate the performance of an existing reinforced concrete building of moderate height when subjected to various levels of

ground motion. The performance of the same building when rehabilitated using different techniques is investigated in order to determine the effectiveness of various rehabilitation strategies.

1.6 METHODOLOGY

The seismic response of a typical nine-story office building designed in accordance with ACI 318-63 (ACI, 1963) is investigated. The program IDARC2D (Valles et al., 1996) is used in the analysis. The damage state of the building is estimated by quantifying the performance of the structure when subjected to a large number of ground motion time history records. Uncertainties in both structural capacity and demand are included in the proposed methodology. Since ground motion is, by nature, a random process, intuition would suggest employing a probabilistic approach to incorporate some key random variables. Structural capacity is modelled by considering probability distributions for variations in both;

i) dimensions of the structural elements, and

ii) strength of materials.

The building is subjected to a set of ground motions scaled to different PGA levels. The Monte Carlo Simulation, paired with the Latin Hypercube sampling technique, is used to carry out the statistical sampling process. Quantification of the damage sustained by the structure is achieved by adopting a suitable damage index.

1.7 ORGANIZATION OF THE REPORT

Chapter one includes a brief summary of the research programs carried out to date regarding damage indices, as well as a review of the different rehabilitation schemes. The reliability approach is outlined.

Chapter Two presents the deterministic aspect of the adopted methodology. The design features of the investigated building are described. Chapter Three details the adopted probabilistic approach.

Chapter Four presents the response of the building to various levels of earthquake ground motion. Chapter Five presents the response of the building when rehabilitated using various techniques. The conclusions and recommendations for future investigation are summarized in Chapter Six.

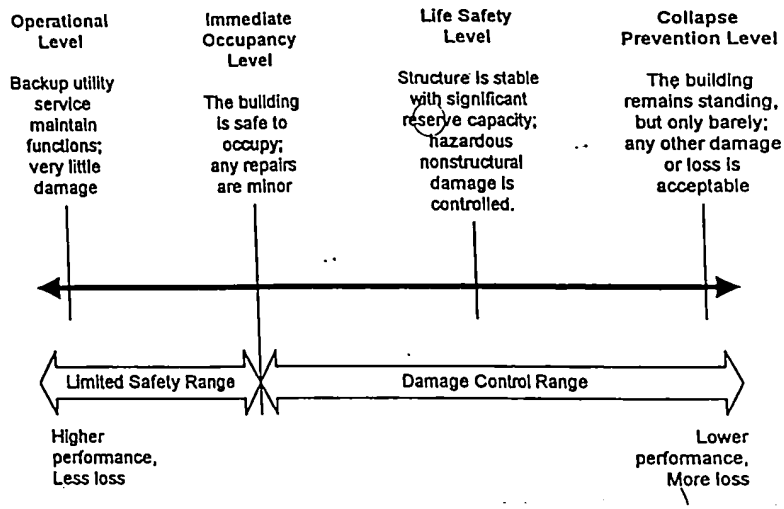

Figure 1.1 Performance levels (FEMA, 1992b)

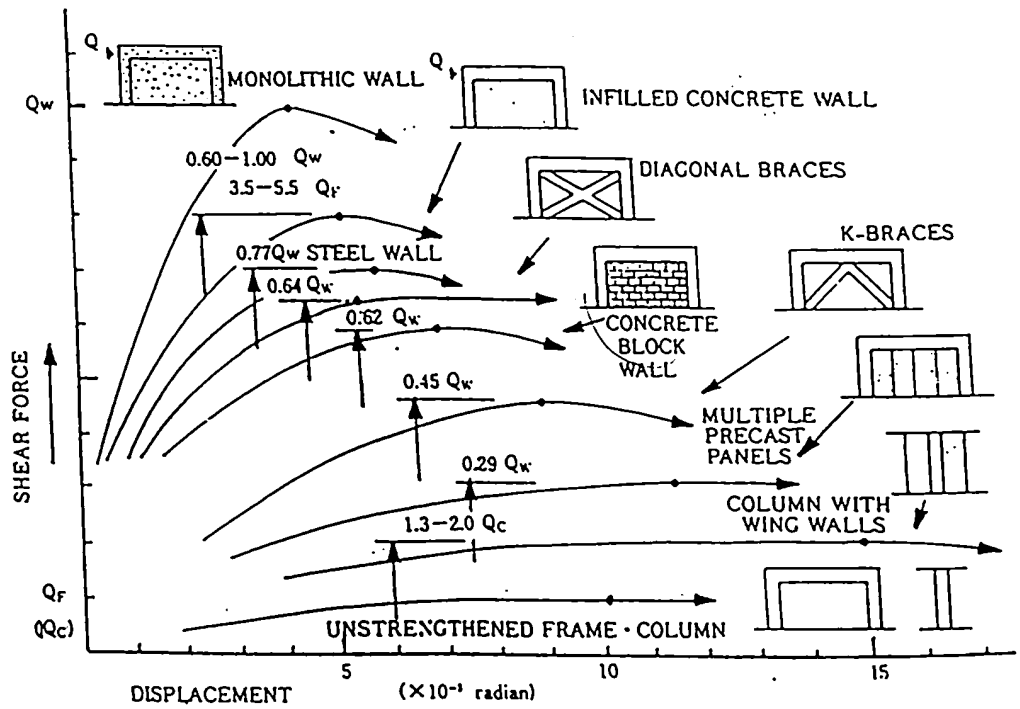

Figure 1.2 Load-displacement relationships for various rehabilitation techniques (Sugano, 1981)

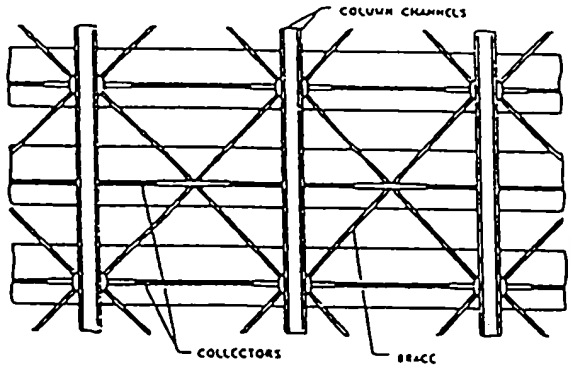

Figure 1.3 Typical bracing system (Jirsa, 1996)

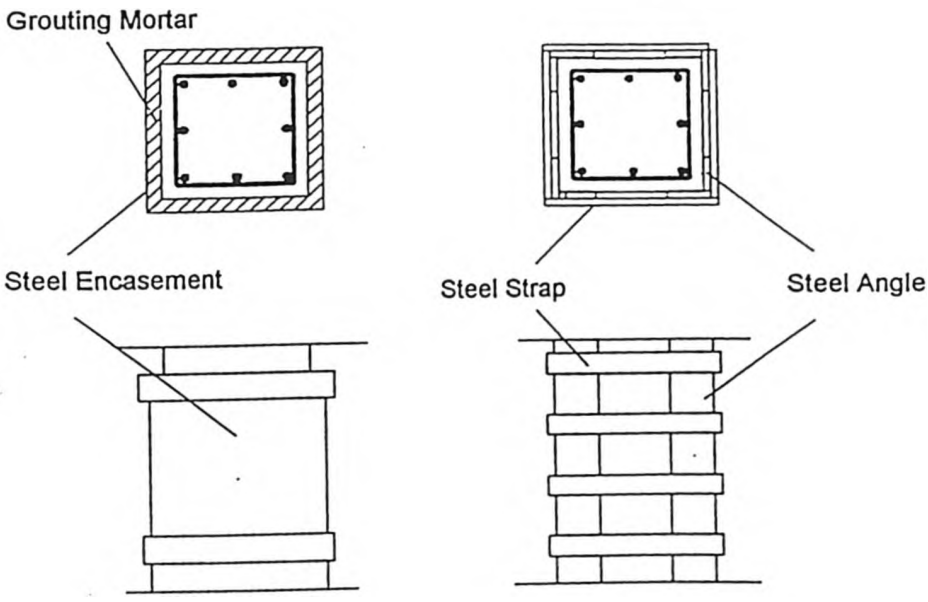

Figure 1.4 Column-strengthening techniques (Rodriguez and Park, 1991)

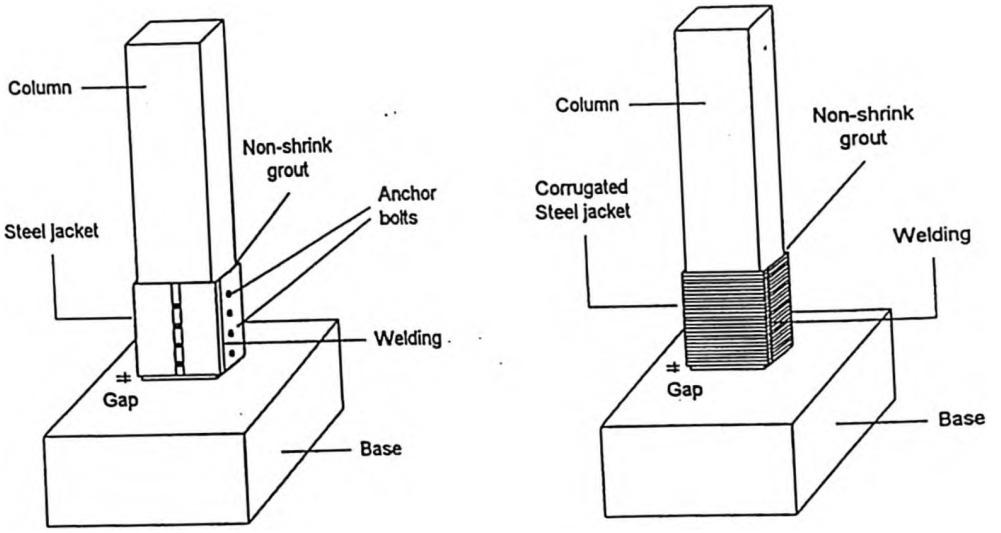

Figure 1.5 Column-base connection retrofitting techniques (Mahgoub, 1997)

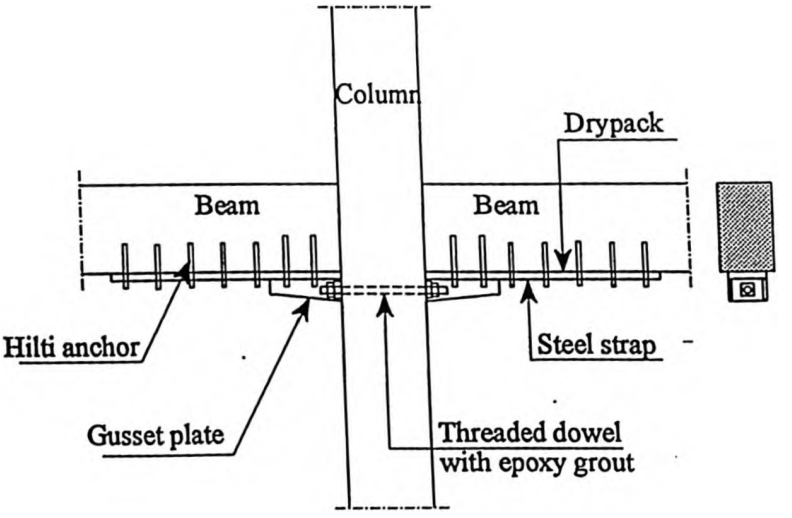

Figure 1.6 Beam strengthening technique (Estrada, 1990)

CHAPTER TWO

DETERMINISTIC ASPECTS

2.1 INTRODUCTION

One of the major challenges associated with the rehabilitation practice is to realistically assess the capacity of an existing structure. When the performance of the structure is determined, the designer is required to select a suitable rehabilitation technique. The proposed evaluation scheme quantifies the performance of the structure based on its deformation and the sustained level of damage. The adopted probabilistic approach enables investigating the significance of various uncertainties inevitably present in structures and the applied load.

2.2 METHODOLOGY

A 30-year-old nine-storey building, designed in accordance with one of the applicable codes at the time (ACI 318-63, 1963), is used in the analysis. The structure is modelled using the program IDARC2D. The two types of analyses conducted are nonlinear dynamic analysis and nonlinear static pushover analysis. The three-parameter Park model is used to model the hysteretic behaviour of the structure. Damage is quantified using the criterion developed by Park et al. (1985) as discussed

in Chapter One. It was decided to adopt a probabilistic approach because of the randomness and uncertainties inevitably present in both structural capacity and demand. The Monte Carlo simulation technique is employed to incorporate such variations into the analysis.

2.3 BASIC ASSUMPTIONS

The following simplifying assumptions were made in the analysis:

i) Plane sections remain plane in flexure.

ii) The tensile strength of concrete is ignored beyond its tensile cracking capacity.

iii) The effect of bond-slip between the reinforcing bars and concrete is considered.

iv) The concrete properties are assumed identical in the confined core and cover.

v) The stress-strain properties for concrete and steel are as shown in figures 2.1 and 2.2 (Aly, 1997), respectively.

vi) The axial force is considered to be uniformly applied over the entire section.

vii) The degree of confinement is the sole factor affecting the ultimate deformation capacity of a section.

Figure 2.3 (Aly, 1997) shows a typical cross section subjected to both an axial load, N, and a bending moment, M.

2.4 STRUCTURAL ASPECTS OF THE BUILDING

The study was conducted on a nine-storey reinforced concrete office building. a typical floor plan and an elevation view of the building are shown in figures 2.4 and 2.5, respectively (Biddah, 1997). The structure is composed of three six-metres bays in one direction, and four bays of similar span in the other. Moment resisting reinforced concrete frames sustain both gravity and lateral loads. The structure is designed in accordance with the American Concrete Institute standard 318-63 (ACI, 1963a). The dimensions and reinforcement details of the columns and beams are presented in figure 2.6 and 2.7 (Biddah, 1997), while the reinforcement details of a typical beam-column connection is presented in figure 2.8 (Biddah, 1997).

As a common practice of the 1950's and early 1960's, structures of moderate height were designed for gravity loads only (Sause et al, 1996). The generated design may be checked for lateral wind loads only. One of the most common design codes then was the ACI-318-63 (1963). Assuming the thickness of the slab to be 150 mm (typical value), and the density of the slab to be 24 kN/m^3, the dead loads were computed. The roof snow load was assumed to be 1.6 kN/m^2. Both the beam and slab design forces were computed by employing the approximate ACI moment coefficients method. The compressive strength of the concrete and the yield strength of the steel reinforcement were assumed to be 25 MPa and 300 MPa, respectively. The ultimate strength design method was employed to design the cross section dimensions. The dead and live load factors were assumed to be 1.5 and 1.8, respectively, while an average value of 0.9 was assigned to the capacity reduction

factor. The reinforcement details of the frame exhibit the following drawbacks when compared to buildings designed in accordance with the current code:

i) Inadequate shear reinforcement in the beams in the vicinity of the columns.

ii) Inadequate confinement reinforcement in the columns.

iii) No shear reinforcement in the beam-column connection.

iv) Lap-splices of the longitudinal reinforcement of the column traditionally occur immediately above the slab and foundation levels.

v) Inadequate anchorage of the positive reinforcement of the beam at the beam-column joint.

2.5 RESPONSE PREDICTION

The computer program IDARC2D, version 4.0, is selected for the analysis of the building. The program was developed by Valles et al. (1996) for reinforced concrete frame-wall structures. The program is capable of performing three types of analyses; free vibration analysis, pushover analysis, and dynamic time-history analysis. The structural capacities and demands are specified stochastically. The Monte Carlo simulation method is employed for statistical sampling. Uncertainties due to variations in both member dimensions and material strength were considered. Aging of concrete was also included in the analysis. A generated ensemble of ground motion time history records is used to represent seismic loading. The variations within these records introduces another source of uncertainty in the analysis. These numerous sources of variation deem a probabilistic analysis inevitable.

The floors were assumed to behave as infinitely-rigid diaphragms. The building was modelled as a series of plane frames linked by rigid horizontal diaphragms. Torsional effects on the frames were neglected. Identical frames were lumped together, and the stiffness contribution of each frame was factored by the number of frames. The viscous damping matrix is computed using mass proportional damping.

2.5.1 Elements Details

Both column and beam elements were modelled using the same basic macro formulation. Flexural, shear and axial deformations of the column elements were taken into account. Axial deformations in the beam element were neglected. Typical column and beam elements, along with their corresponding degrees of freedom, are presented in figures 2.9 and 2.10 (Aly, 1997). The three-parameter Park model (Park et al, 1987) was employed to model the hysteretic behaviour of both flexural and shear springs. Axial deformations in column elements were modelled using a linear elastic spring element, uncoupled from the flexural and shear spring elements. A rigid length zone was introduced at the ends of both column and beam elements to simulate the enhanced stiffness of the elements through the joints to the centre-line. The length of the rigid zone is shown in figure 2.11 (Aly, 1997).

2.5.2 The Three-Parameter Park Hysteretic Model

The three-parameter Park hysteretic model (Park et al., 1987) incorporates stiffness degradation, strength deterioration, pinching, non-symmetric response, and a trilinear monotonic loading envelope. Depending on the deformation history, the model traces the hysteretic behaviour of an element as it passes from one linear stage to another. Figures 2.12 and 2.13 (Kunnath et al., 1992) display the influence of different degrading parameters on the shape of the hysteretic loops. The control parameters could be calibrated to accommodate a range of hysteretic patterns typical of reinforced concrete elements. The main characteristics represented in the model are: stiffness degradation, strength deterioration and pinching.

2.5.2.1 Stiffness Degradation Parameter (HC)

This parameter quantifies the level of stiffness decay as a function of the attained ductility. As figure 2.12 shows, the unloading paths on the primary curve converge to a single point. This incorporates the effect of lower stiffness at higher levels of deformation. This parameter can readily be obtained from experimental data that are typical of the structure being investigated. Based on observations of test data, typical values of the stiffness degradation parameters were found to range between 1.5 and 3.0 (Kunnath et al, 1992).

2.5.2.2 Strength Deterioration Model

The loss in strength shown in figure 2.12, is determined using the formula:

$$F_{new} = F_{max} (1 - HBE \times \bar{E} - HBD \times \mu_c) \qquad (2.3)$$

where *HBE* and *HBD* are control parameters that determine the degree of decay in strength as a function of dissipated energy and ductility,

$$\bar{E} = A_T / M_y \phi_u \qquad (2.4)$$

$$\mu_c = \phi_{max} / \phi_y \qquad (2.5)$$

where A_T is the area enclosed by the M-ϕ loops, and

ϕ_y and ϕ_{max} are the yield and maximum attained curvatures, respectively.

The advantage of this formulation is that strength decay can be controlled in terms of ductility, energy, or a combination of both. When data is scarce, *HBE* and *HBD* could be assumed as 0.1 and zero, respectively. For high levels of strength degradation, either (or both) parameters may be increased up to a maximum value of 0.5. This would cause a severe stiffness deterioration response (Kunnath et al, 1992).

2.5.2.3 Slip or Pinching Control Representation (HS)

In the element model shown in figure 2.12, the unloading path crosses the zero moment axis and continues to a lower target point. This point is specified by either (HS × PYP) or (HS × PYN), where *PYP* and *PYN* are the positive and negative moments at yield, respectively. The loading path retains this lower stiffness until it reaches the cracking deformation state. Upon crossing the point of cracking deformation, the loading path passes through the previous maximum point, unless strength deterioration is specified. In this case, a lower target point is introduced. a value of 0.5 for *HS* simulates effects typical of crack opening and closing (Kunnath et al, 1992).

The influence of the degrading parameters on the hysteretic behaviour is illustrated in figure 2.13. By proper choice of the control parameters, a wide range of hysteretic shapes that are typical of most reinforced concrete sections could be produced.

2.5.3 Ultimate Deformation Capacity

The ultimate curvature of the section was employed to express the ultimate deformation capacity. The moment applied to the section was incrementally increased until either;

i) the specified ultimate compressive strain of the concrete is reached, or

ii) the specified ultimate tensile strength of the reinforcement is reached.

According to the defined failure criteria, the model does not account for failure modes such as shear failure or bond slip of anchored reinforcement or lap splices. These are some of the limitations of the IDARC2D program employed in the analysis.

2.5.4 P-Delta Effect

The term "P-Δ effect" refers to the additional overturning moments generated by the relative inter-story drifts. Such moments are caused by eccentric gravity loads, and are taken into account by evaluating the axial forces in the columns.

In the program IDARC2D, P-Δ effects are represented by equivalent lateral forces. These lateral forces are equal in magnitude to the overturning moments caused by the eccentricity of gravity loads due to inter-story drift (Wilson and Habibullah, 1987).

2.6 ANALYSIS TYPES

The designed nine-storey frame was subjected to static and dynamic analyses. The analysis techniques that were employed in the current study are detailed in the following sections:

2.6.1 Pushover Analysis

The nonlinear static pushover analysis is a simple-yet efficient-technique that could be employed to predict the seismic response of structures prior to a full dynamic

analysis. A pushover analysis can be used to determine the capacity curve, sequence of yielding of elements, the potential ductility capacity, and whether the lateral strength of the building. The capacity curve is a plot relating the base shear, normalized by the building weight with a measure of the floor or roof displacement in terms of drift. The story drift is defined as the maximum relative story displacement normalized by the story height. The roof drift is the roof displacement normalized by the building height.

This analysis technique is performed by subjecting the structure to a distribution of monotonically-increasing lateral loads and determining the corresponding lateral displacements. Several options are present in the program IDARC2D. The distribution of lateral forces could be;

i) assumed as point load acting at roof level,

ii) assumed an inverted triangle, similar to the distribution of lateral seismic load in the code provisions, or

iii) assumed as a modal-adaptive loading.

Several other options are present in the program IDARC2D, but the above-mentioned cases were the ones considered. The pushover analysis has its own limitations when applied to structures. Depending on the model used, the pushover analysis may not be capable of establishing the failure of the structure. The type of loading used to account for higher mode contribution remains a question. Research is currently underway to develop procedures for three-dimensional pushover analysis,

and to take the torsional behaviour of the structure into account.

2.6.2 Nonlinear Dynamic Analysis

Nonlinear dynamic analysis is carried out using a combination of the Newmark-Beta integration and the pseudo-force methods in incremental form. The dynamic equation of the system is solved using the Newmark-Beta algorithm that assumes a linear variation of the acceleration between different time steps. The solution is performed incrementally assuming that the properties of the structure remain constant during each time step. This might cause some potential equilibrium problems, as the stiffness of some elements is likely to change during the time step. This is overcome by a compensation procedure that is adopted to minimize the resulting error. The compensation procedure, illustrated in figure 2.14 (Aly, 1997), applies a one-step correction for the unbalanced force. At the end of time step "i", an unbalanced force might result. This force is due to the difference between the restoring force calculated using the hysteretic model discussed earlier, and the restoring force (computed assuming no change in stiffness during time step "i"). This difference is then applied at the following time step (i+1) of the analysis. Generally, such a procedure works best when small unbalanced forces are developed. The magnitude of the unbalanced forces could be minimized by using a time step that is sufficiently small. The solution stability is ensured by the addition of numeric damping.

2.7 DAMAGE ANALYSIS

The Park et al (1985) damage model, modified by Kunnath et al. (1992), was selected for use in the current study. This damage model takes into account both element ductility and hysteretic energy dissipated by each element during the response history. Since the rate of strength degradation is directly related to the parameter β incorporated in the damage index, this damage model was found to be convenient to be incorporated as an integral part of the three parameter models controlling the hysteretic behaviour. Three damage indices are computed using this damage model, namely;

i) element damage index (column or beam elements),

ii) storey damage index (vertical and horizontal components and overall storey damage), and

iii) global damage index for the whole structure.

Direct application of this model to a structural element, storey, or building requires the determination of the corresponding overall element, story, or building peak deformation. Since inelastic behaviour tends to be confined to plastic zones near the ends of some members, the relationship between element, story or roof deformation and the local plastic rotations might prove difficult to establish. For the element end section damage, the following formula developed by Kunnath et al. (1992) was employed:

$$DI = \frac{\theta_m - \theta_r}{\theta_u - \theta_r} + \frac{\beta}{M_y \theta_u} E_h \qquad (2.6)$$

where θ_m is the maximum rotation attained during the loading history,

θ_u is the ultimate rotation capacity of the section,

θ_r is the recoverable rotation when unloading,

M_y is the yield moment, and

E_h is the dissipated energy in the section.

The damage index of each element is then selected as the higher of the damage indices at both ends of the element.

The two additional indices, story and global damage indices are computed using weighting factors. The weighting factors are based on dissipated hysteretic energy at the component and story levels. The storey and global damage indices are given by;

$$DI_{storey} = \sum (\lambda_i)_{component} (DI_i)_{component} \; ; \; (\lambda_i)_{component} = \sum (\frac{E_i}{\sum E_i})_{component} \qquad (2.7)$$

$$DI_{global} = \sum (\lambda_i)_{storey} (DI_i)_{storey} \; ; \; (\lambda_i)_{storey} = \sum (\frac{E_i}{\sum E_i})_{storey} \qquad (2.8)$$

where λ_i is the energy weighting factor, and

E_i is the total energy absorbed by element or storey "*i*".

This damage model has been calibrated with observed structural damage of reinforced concrete buildings (Park et al, 1985). Table 2.1, as well as figure 2.15 (Park et al., 1987) present an interpretation of the calibrated damage index with the degree of observed damage in the structure.

2.8 SUMMARY

The methodology for evaluating the capacity of existing buildings was presented. The assumptions made and the limitations of the analysis were discussed. A nine-storey office building was designed in accordance with earlier codes. The computer program IDARC2D was employed to predict the nonlinear static pushover and dynamic response of the building. The elements used were reviewed.

Quantifying the performance of this building when subjected to seismic excitation is a rather complex problem, as many uncertainties may be involved. Consideration of the uncertainties inherent in both loading, as well as structural resistance, is necessary to carry out a reliability assessment investigation. The probabilistic approach was therefore adopted to evaluate the performance of the building. The Monte Carlo simulation was used to incorporate the various sources of uncertainty into the analysis.

Table 2.1 Damage criteria in terms of overall damage index (Park et al., 1987)

Limit State Damage Index	Degree of Damage	Damage (Service) State	Usability	Appearance
0.00	None	Undamaged		Undeformed / Uncracked
			Usable	
0.20 - 0.30	Slight	Serviceable		Moderate to severe cracking
0.30 - 0.50	Minor	Repairable	Temporarily	Spalling of concrete cover
0.50 - 0.60	Moderate		unusable	
0.60 - 1.00	Severe	Unrepairable		Buckled bars, exposed core
> 1.00				
	Collapse	Collapse	Unusable	Loss of shear / axial capacity

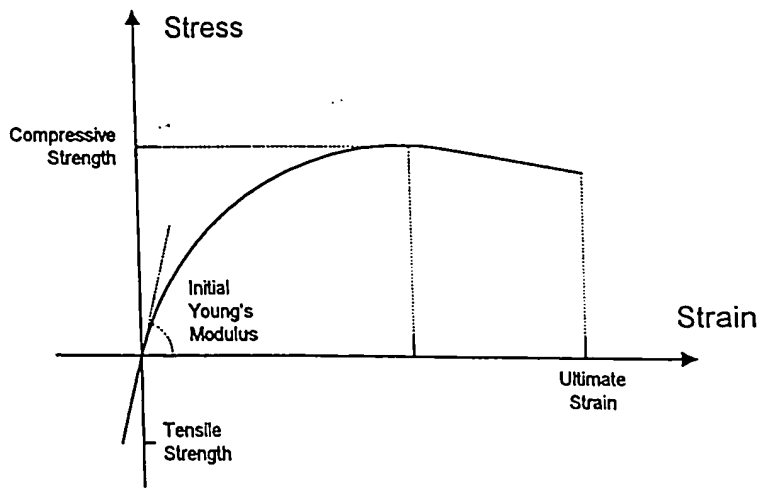

Figure 2.1 The stress-strain properties for concrete (Aly, 1997).

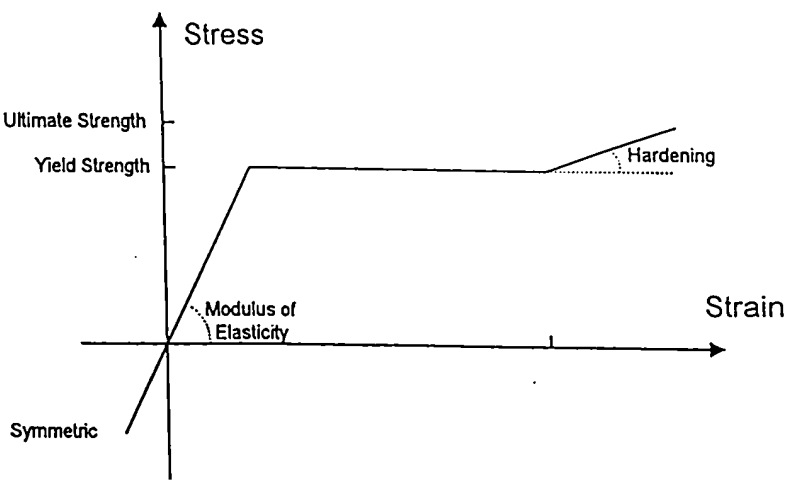

Figure 2.2 The stress-strain properties for steel (Aly, 1997)

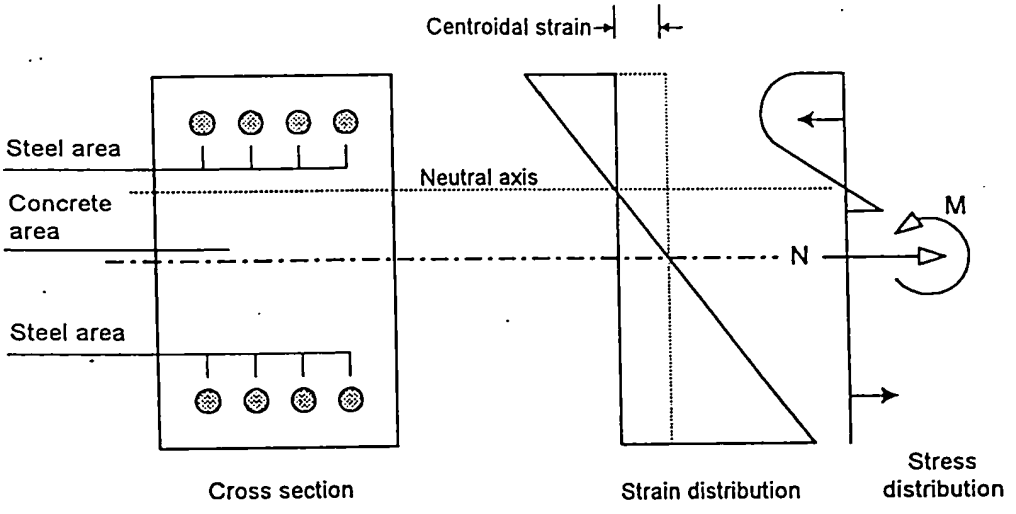

Figure 2.3 Typical cross section subjected to both an axial load, N, and a bending moment, M (Aly, 1997)

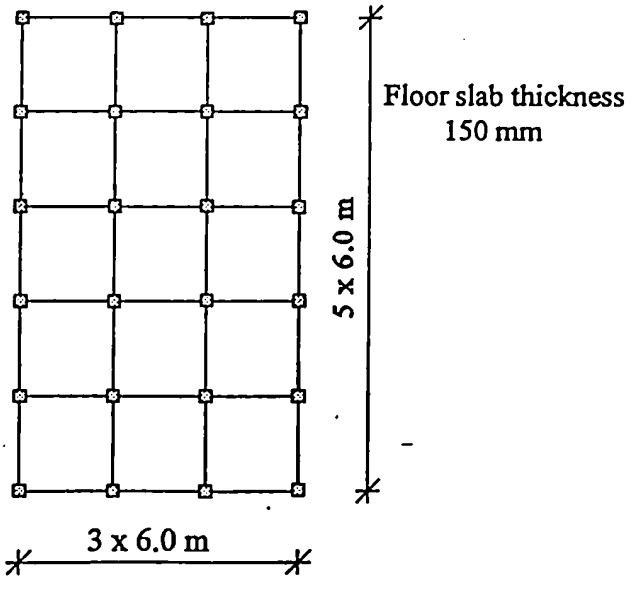

Figure 2.4 Typical floor plan of the building (Biddah, 1997)

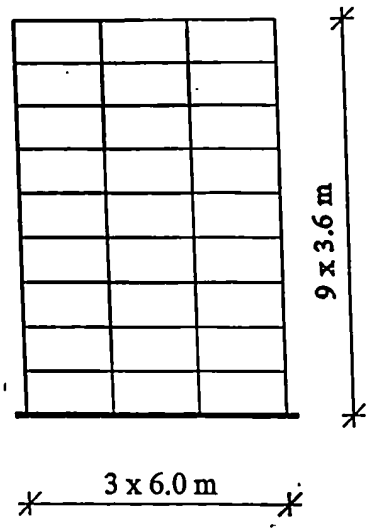

Figure 2.5 Elevation view of the building (Biddah, 1997)

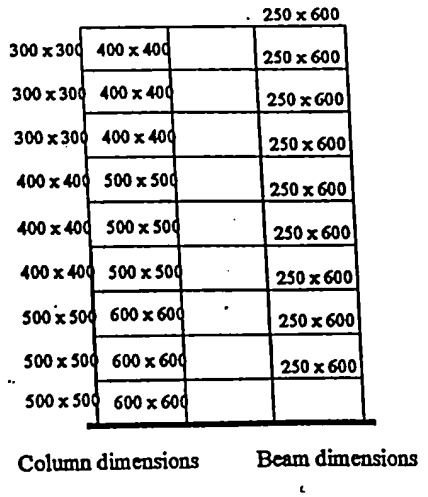

Figure 2.6 The dimensions of the columns and beams (Biddah, 1997)

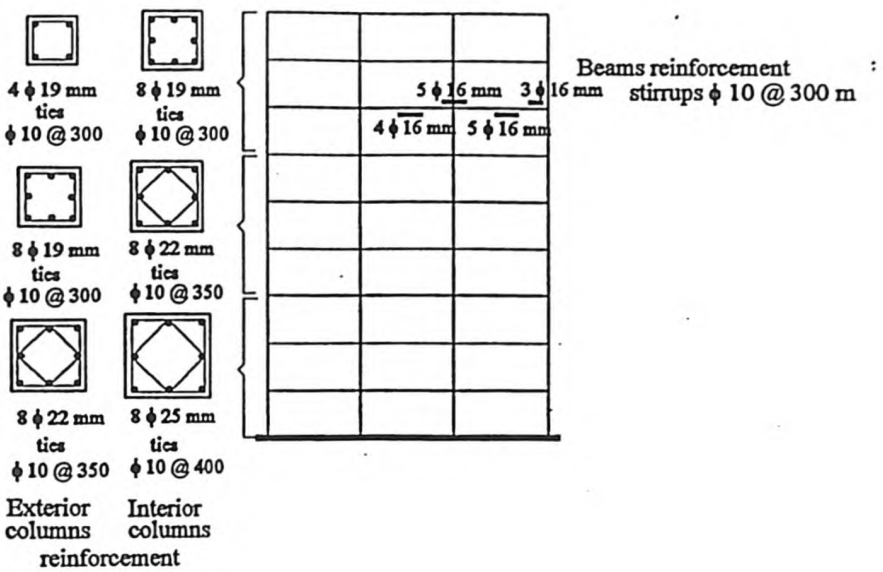

Figure 2.7 The reinforcement of the columns and beams (Biddah, 1997)

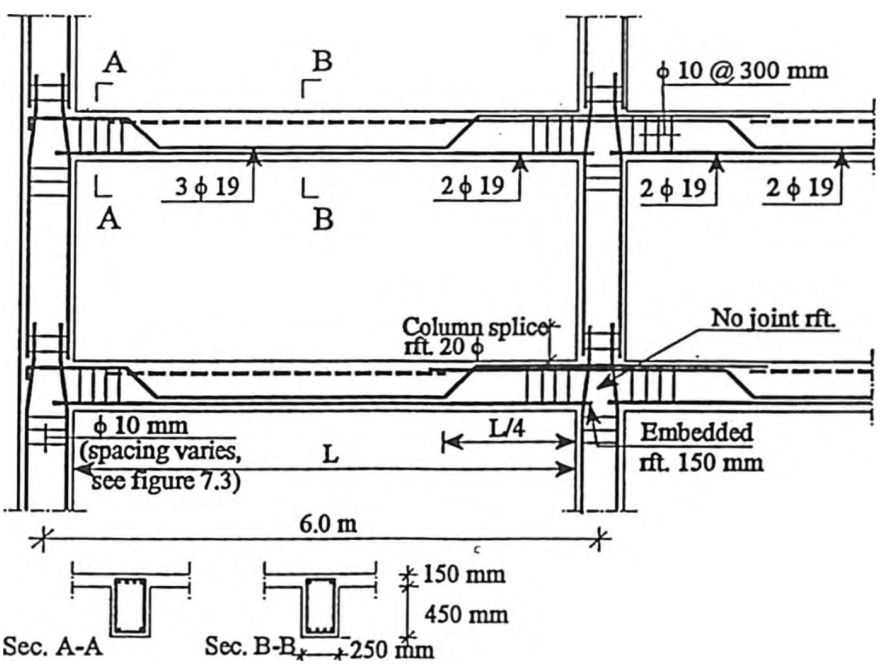

Figure 2.8 Reinforcement details (Biddah, 1997)

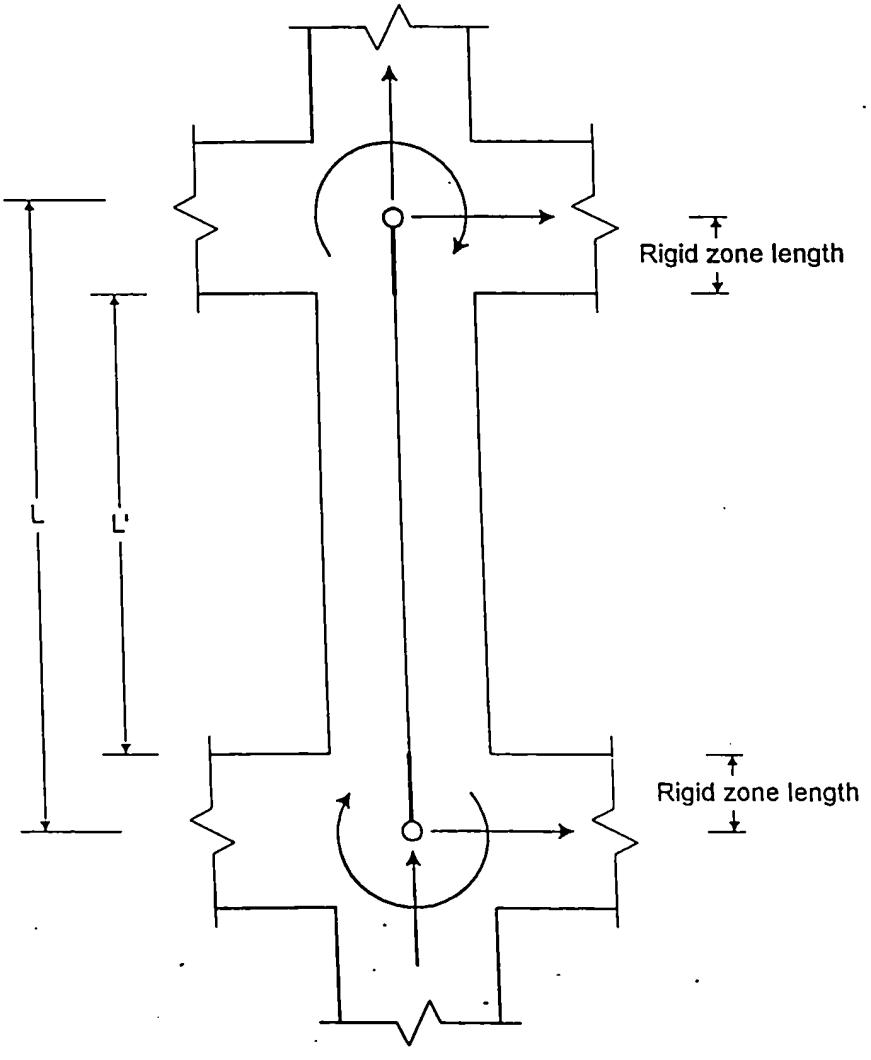

Figure 2.9 Typical column element and degrees of freedom (Aly, 1997)

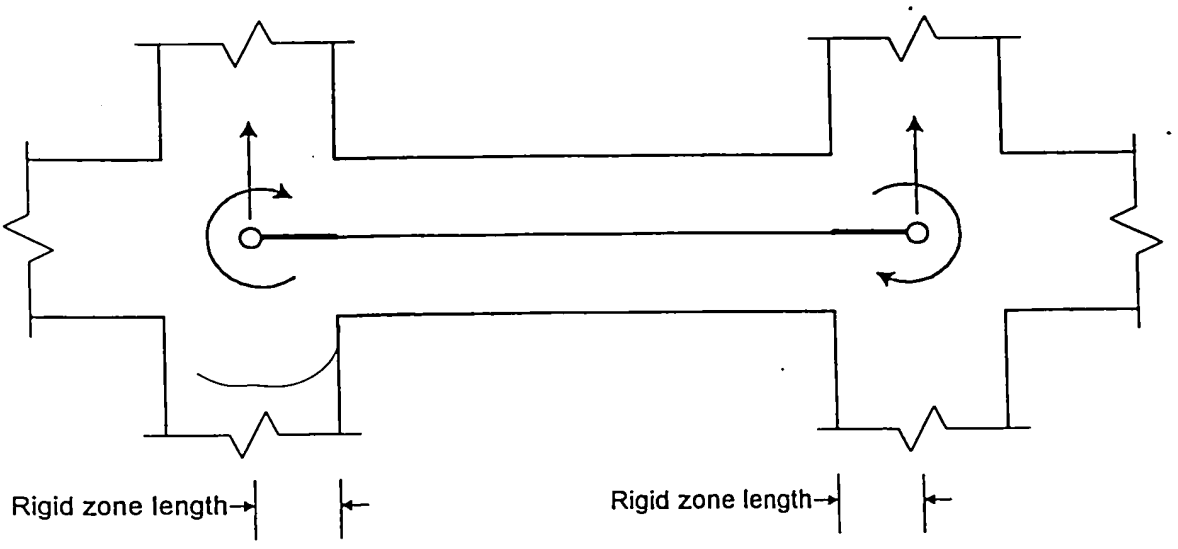

Figure 2.10 Typical beam element and degrees of freedom (Aly, 1997)

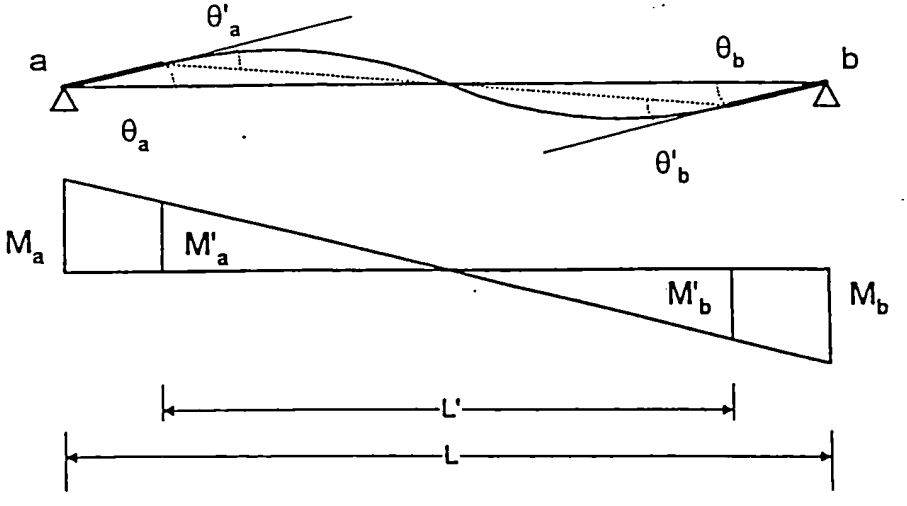

Figure 2.11 Effect of the rigid zone (Aly, 1997)

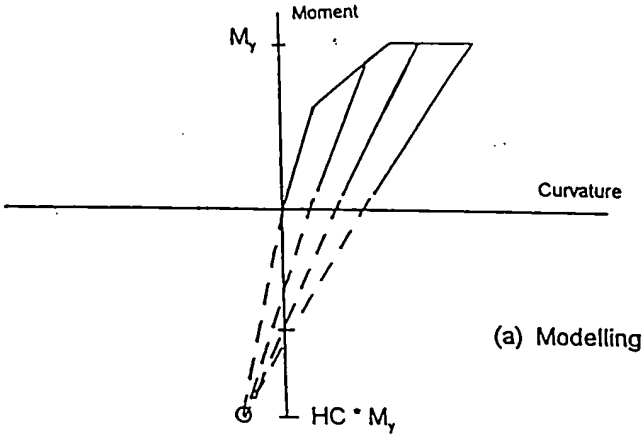

(a) Modelling of stiffness degradation

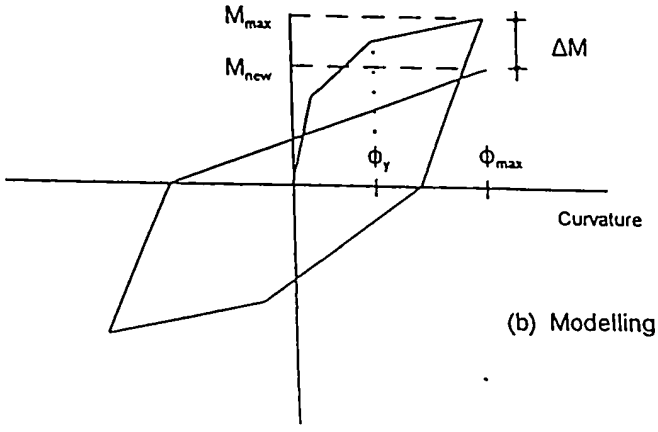

(b) Modelling of strength deterioration

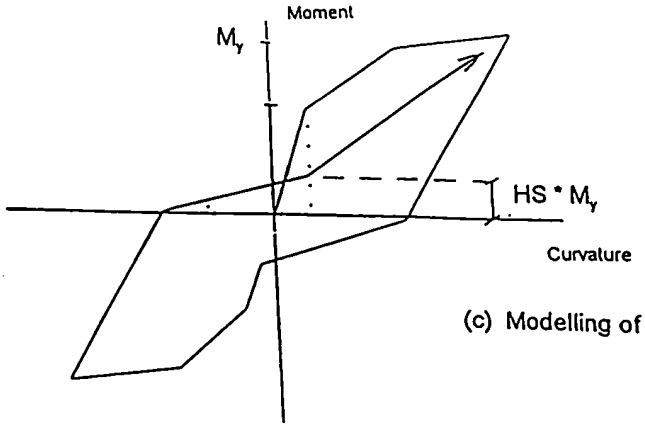

(c) Modelling of pinching behaviour

Figure 2.12 Control parameters for the hysteretic model (Park et al., 1987)

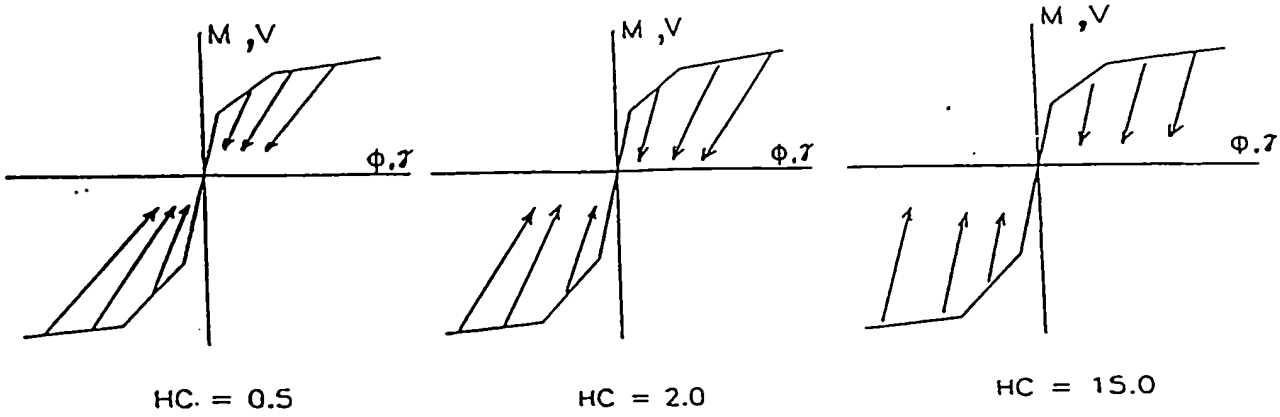

(a) Stiffness degrading parameter

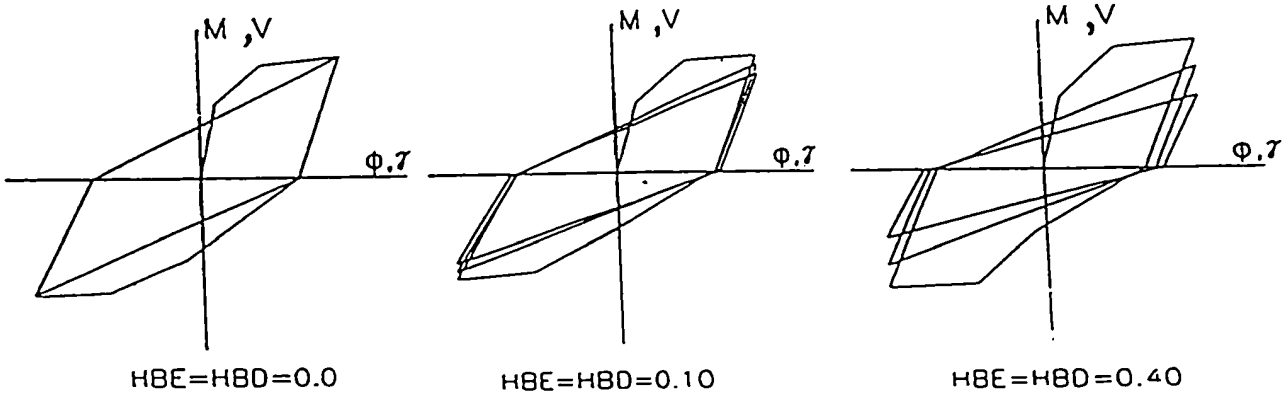

(b) Strength deterioration parameter

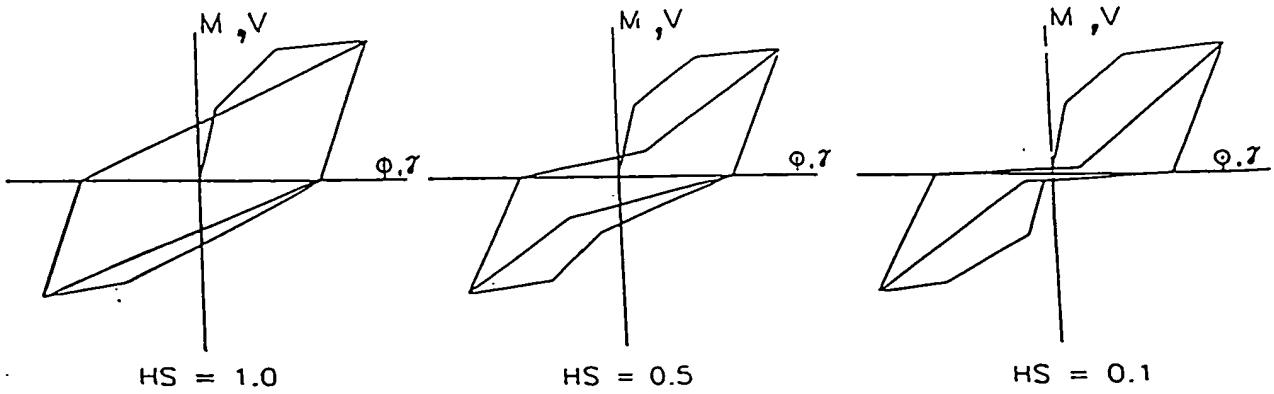

(c) Slip control parameter

Figure 2.13 Effect of degrading parameters on hysteretic loops (Park et al., 1987)

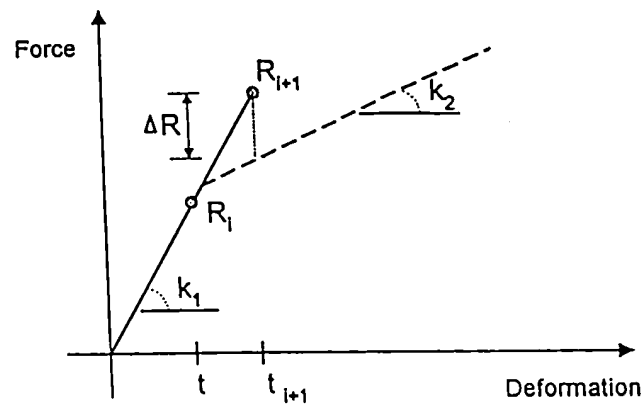

Figure 2.14 The compensation procedure (Aly, 1997)

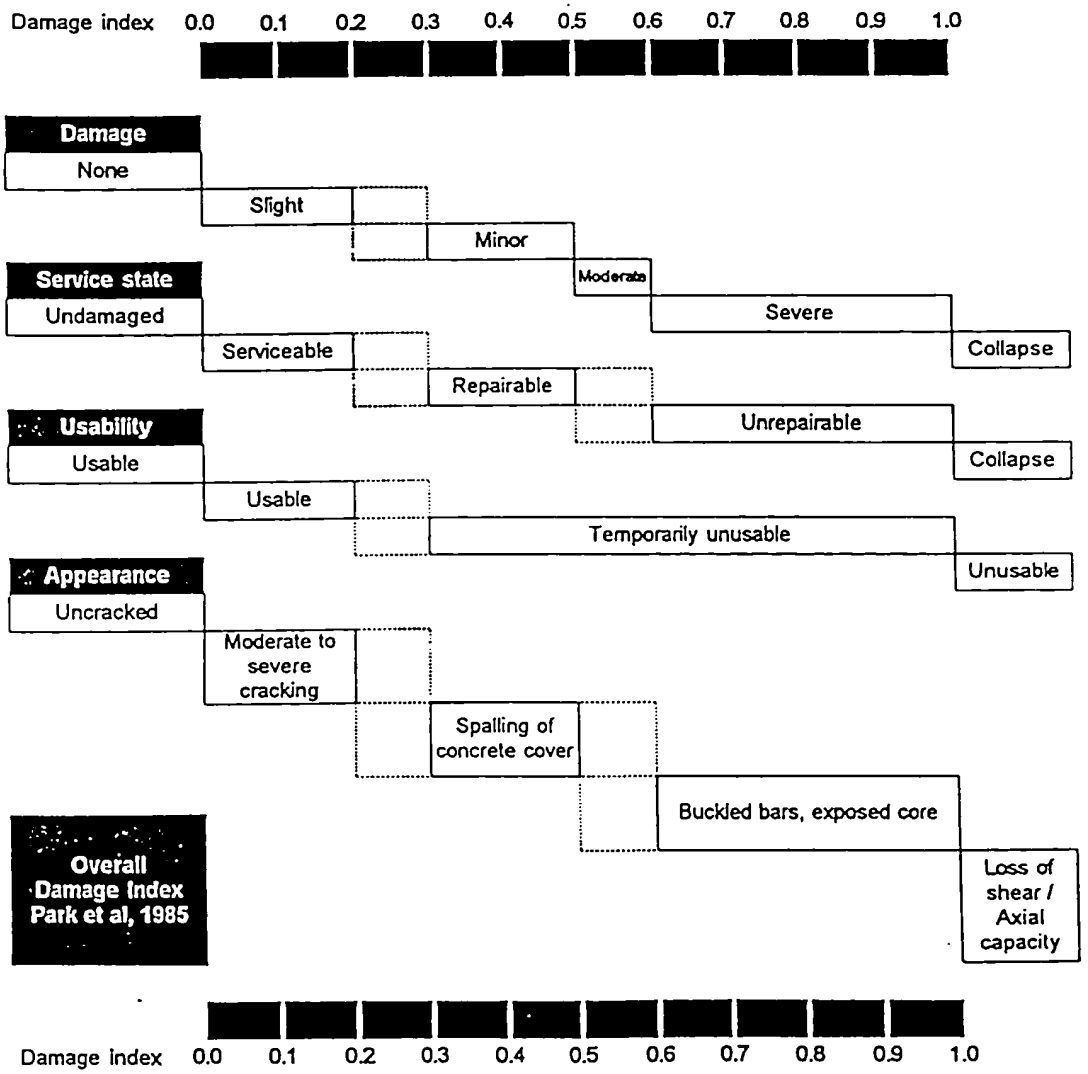

Figure 2.15 Interpretation of the calibrated damage index (Park et al., 1987)

CHAPTER THREE

PROBABILISTIC ANALYSIS

3.1 INTRODUCTION

Both structural capacity and ground motion characteristics are random quantities. The damage to the structure is based on the given ground motion and the estimated capacity of the structure. A probabilistic methodology would thus be the logical approach for evaluating the seismic performance of existing structures. Ground motion characteristics, material strength, and structure dimensions were considered random variables in the current study. Details of the probabilistic approach adopted in the current study will be outlined. There are other sources of uncertainties in the design that contribute to the variability in the seismic response of structures. These may include the rotation capacity of sections and the interaction between flexural and shear capacities of the section. These other sources of uncertainties are recognized, but are not included in the present analysis.

3.2 UNCERTAINTIES IN STRUCTURAL CAPACITY

Nilson and Winter (1991) noted that the capacity of the entire structure can be considered to be a random variable. Many design, materials and construction

factors affect the capacity of a structure. The minimum strength of the materials used in the structure such as masonry, concrete and reinforcing steel, are specified. However, no limits are imposed on the mean or the variation of the material strength. The exact values of the strength of different materials rely on issues of the manufacturing process and quality control. This introduces randomness in the values assigned to material strength.

The strength of a structure depends on the quality of construction. Member dimensions are bound to vary from the specified values. Issues of quality of construction affect the variance of the values from the specified dimensions. In a poorly-constructed structure reinforcement might also be poorly placed, or the concrete may contain voids. The values of the member dimensions and material strength are significant sources of uncertainty, and are considered as random variables.

From the time of pouring, the concrete strength increases with time. Over many years, a gain in concrete strength of 5-15% above the 28-day strength is not unusual. On the other hand, the concrete strength deteriorates with time. This time-related loss of strength is caused by use, creep, freezing and thawing cycles and chemical and pollutant attacks. The variation of concrete strength with time will be taken into account in the current analysis.

3.2.1 Variation in Material Strength

Based on the results of their investigations, Mirza and MacGregor (1979a and b) suggested modelling the compressive strength of the concrete in the form of a normal distribution. Mirza and MacGregor (1979a and b) suggested the following equation to determine the mean value of the distribution (f_m):

$$f_m = 0.675\, f_c' + 7.59 \leq 1.15\, f_c' \quad \text{(MPa)} \qquad (3.1)$$

where f_c' is the nominal compressive strength of the concrete.

Ellingwood (1977), and Mirza and MacGregor (1979) recommended certain values for the variability of concrete compressive strength, depending on the quality of the construction. In the current analysis, the coefficient of variation of the concrete compressive strength is taken to be 0.15, which represents average quality control conditions.

Ellingwood (1977) investigated the variability of the steel yield strength. He concluded that it should be modelled following a Log-normal probability distribution. Following his methodology, the mean and coefficient of variation of the yield strength for 300 MPa reinforcement steel were 366 MPa and 0.107, respectively. For 400 MPa reinforcement, the mean and coefficient of variation were 473 MPa and 0.093, respectively. He also stated that the variability in the reinforcement bar area could be modelled following a normal distribution with a mean equal to its nominal value, and a coefficient of variation of 0.024.

3.2.2 Variation in Member Dimensions

Member dimensions depend on the level of quality control during construction. Several researchers (Tso and Zelman, 1970; Mirza and MacGregor, 1979a and b; Lu et al., 1994) suggested assuming the variation in member dimensions to be a normal distribution. They, recommended a ratio of mean to nominal values of unity. The values suggested for use by Ellingwood (1977) and Mirza and MacGregor (1979a and b) are presented in table 3.1.

3.2.3 Concrete Aging

After the concrete is mixed and poured in place, its strength continues to increase with time due to the continuing process of hydration, but at a decreasing rate. On the other hand, reinforced concrete structures are affected by aging which causes deterioration of the concrete strength with time. It is rather difficult to quantify the deterioration of concrete strength with time. This is because of the difficulty of simulating all the factors that could potentially affect the strength of the concrete in the laboratory. In assessing the performance of an existing reinforced concrete structure, aging of concrete was found to depend on the construction quality of the building, its location and its use. Among the most effective factors are the cycles of freeze and thaw, sulfate attack and corrosion of reinforcement.

One of the main reasons for aging is creep. The term "creep" refers to the increasing deformation of a material at constant stress conditions. The nature of the creep process is shown schematically in figure 3.1 (Nilson and Winter, 1991).

Creep has been a topic of research interest for many years. Branson (1977) recommended an empirical formula to predict the compressive strength of concrete as a function of elapsed time:

$$(f_c') = \frac{t}{a + bt} (f_c)_{28d} \qquad (3.2)$$

where $(f'_c)_{28d}$ is 28-day compressive strength of the concrete,

t is elapsed time, and

a and b are constants which depend on the type of cement used, aggregate type and curing method.

Values of a were found to range between 0.50 to 8.00, while b was found to range between 0.67 and 1.10. The above relationship might yield an increase in the long term concrete strength ranging from 2 to 18 percent (Branson, 1977).

Like most materials, the fatigue strength of concrete is considerably smaller than its static strength. The fatigue strength of concrete depends on many factors, including moisture condition, age, and rate of loading (ACI SP-75, 1982). Nilson and Winter (1991) observed that the fatigue limit of concrete is in the range of 55 percent of the static strength. This value was suggested for flexural loading.

Mori and Ellingwood (1993) suggested using either a linear, parabolic or square root degradation function. The strength of a 40-years-old building would typically range between 0.7 to 0.9 of the original strength. In this current study, a linear degradation function was used. The rate of degradation was assumed to be

mild, resulting in the structure's strength being 90 percent of its original strength after 40 years. The building under investigation was assumed to be 30 years old. Accordingly, the concrete strength was estimated to be 93 percent of its original strength. This figure is considered to take into account both the gain and the deterioration of concrete strength with time.

3.3 LOADING UNCERTAINTIES

In a probabilistic analysis, a large number of ground motion time history records are needed to obtain accurate results. Many of the available records of actual earthquakes are not well categorized as recorded on either soil or rock sites. Moreover, many of the available records cannot be considered representative of free field conditions. This is because the recording instruments are normally mounted on structures (basement, intermediate, or roof floor). The recorded time history would thus be affected by the response of the structure. This limits the number of available usable earthquake records. For this reason, actual recorded earthquake ground motions would not form adequate data for a reliable probabilistic analysis. Artificially-generated ground motion time history records represent a viable alternative for generating input data in the current study.

There are numerous approaches for ground motion modelling. Two approaches are presented below. The first approach is employed to model ground motion for a general site, while the second is used to model ground motion for a specific location.

3.3.1 Modelling General Ground Motion

Artificial ground motion time history records can be generated using both stationary and non-stationary approaches. Clough-Penzien (1975) suggested using a power spectral density function for the ground acceleration to generate the ground motion. The power spectral density function is defined as:

$$S_g(\omega) = S_0 \frac{1 + 4\zeta^2_g (\omega/\omega_g)^2}{[1 - (\omega/\omega_g)^2]^2 + 4\zeta^2_g (\omega/\omega_g)^2} \frac{(\omega/\omega_f)^4}{[1 - (\omega/\omega_f)^2]^2 + 4\zeta^2_f (\omega/\omega_f)^2} \quad (3.3)$$

where S_0 is the amplitude of the white noise bedrock excitation,

ω_g and ω_f are the first and second filters' frequencies, respectively, and

ζ_g and ζ_f are the damping ratios of the first and second filters, respectively.

Several attempts have since been made to estimate the values of these parameters (Lai, 1982; Elghadamsi et al, 1988). Lai (1982) studied records on 118 soil-sites and 22 rock-site. Table 3.2. presents values for both the mean and the coefficient of variation for ω_g and ζ_g, as suggested by Lai (1982). The value of ω_f was assumed as 0.1 ω_g and ζ_f and ζ_g were assumed equal. Figure 3.2 (Aly, 1997) schematically illustrates the power spectral density function for a set of assumed parameters. The figure shows that a normal distribution could be assumed for the probability distribution of the filter parameters.

Shinozuka (1974) suggested that a stationary acceleration time history record can be generated using the following expression:

$$\ddot{u}_g(t) = \sum_{k=1}^{n} \sqrt{2\, S_g(\omega_k)\, \Delta\omega}\, \sin(\omega_k t + \phi_k) \qquad (3.4)$$

where $S_g(\omega_k)$ is the value of the power spectral function for the ground acceleration, as defined by Equation 3.2, calculated at ω_k;

$\Delta\omega = \omega_{k+1} - \omega_k$,

ω_k is the frequency corresponding to the power spectral ordinate,

k is the number of frequencies considered in the analysis (200).

ϕ_k is a random phase angle distributed uniformly between zero and 2π.

Generating the artificial ground motion records for rock and soil sites is achieved by assigning random values for both ω_g and ζ_g using the mean, standard deviation, and probability distribution type for every parameter as listed in Table 3.2. Equation 3.3 is employed to generate different power spectral density functions, while equation. 3.4 is used to generate different ground motion records for both rock and soil sites.

The acceleration time history record obtained from Equ. 3.4 is multiplied by a suitable envelope nonstationary function $\Psi(t)$ to model the variation of intensity inherent in a typical earthquake. Sues et al. (1985) suggested an envelope in the

following form:

$$\psi(t) = \begin{cases} \left(\frac{t}{t_1}\right)^2 & \text{for } t \le t_1, \\ 1 & \text{for } t_1 \le t \le t_2, \\ e^{-c(t - t_2)} & \text{for } t_2 \le t \end{cases} \qquad (3.5)$$

where t_1 is the rise time of the ground motion,

t_2 is the decay time of the ground motion, and

c is a decay parameter.

The duration of strong shaking is (t_2-t_1). The non-stationary envelope function is shown in figure 3.3. Sues et al. (1985) assigned a value of 1.5 sec for the rise time, and a value of 0.18 for the decay parameter. They recommended a strong shaking duration of 10.0 sec for soft soil sites, and 5.5 sec for rock sites. The duration of the strong ground was considered deterministic in the current study.

3.3.2 Modelling Zone-Specific Ground Motion

Modern seismic design codes utilize the design response spectra to specify the expected level of ground motion. This approach yields approximate and conservative estimates of the seismic loads. In linear dynamic analysis of a structure subjected to earthquake ground motion, the response spectrum approach could be employed in conjunction with modal combination rules. However, for high PGA levels of ground motion, where nonlinear response is expected, the spectral approach yields inaccurate

results. A time history analysis should be carried out to determine the nonlinear behaviour of the structure.

The seismic loads specified by the code are based on the design spectrum for the zone where the structure is located. Ground motion time histories could be simulated by generating acceleration time histories that are compatible with the specified design spectrum of the region.

In the inelastic analysis of structures, the nonlinear response varies significantly with the input ground motion. Therefore, a large enough set of ground motion records should be used in the analysis. The number of useable ground motion time history records is insufficient to carry out a reliable probabilistic analysis. Therefore, generated spectrum-compatible acceleration time histories may be used to carry out the probabilistic analysis. The suppression and raising technique (Tsai, 1972, as reported by Ahmadi, 1979) can be used to generate the time history records needed for the analysis. In this method, the original ground motion is modified by passing the record through a set of spectrum-suppressing filters of the frequencies at which the spectrum is higher than the design response spectrum. The motion was further modified by locally raising the spectrum without altering the remainder of the spectrum. The numerical algorithm SYNTH (Naumoski, 1996) was used to generate spectrum-compatible time histories.

It should be noted that the generated spectrum-compatible records do not represent actual earthquakes. The process by which these records were generated might distort the records in a manner that the corresponding velocity and

displacement components become unrealistic (Marshall and Farzad, 1996).

For example, if the city of Victoria, British Columbia is selected as a site, the artificial ground motion records are generated to fit the NBCC (1995) response spectrum for the city of Victoria shown in figure 3.4 (NBCC, 1995). The records should be checked to ensure realistic velocity and displacement time history components. The response spectra of the generated records can then be compared to the target spectrum to ensure accuracy.

3.4 THE MONTE CARLO SIMULATION

The Monte Carlo Simulation technique involves random sampling to artificially simulate a large number of experiments and observe their results. In structural reliability analysis, this involves randomly sampling each random variable to obtain a sample value. The damage criteria are then checked. The experiment was repeated, each time with a new randomly chosen set of the sample values, which were generated according to their respective probability distributions. A conclusion was then reached based on statistical evaluation of the results (Melchers, 1987).

In order to apply the Monte Carlo techniques to practical problems, it is necessary to develop a systematic methodology for numerical sampling of the basic variables. If the simple random sampling technique had been used to generate samples, the required sample size would have been excessively large. In the current study, the Latin Hypercube sampling technique (Imam and Conover, 1980) was selected to establish samples of the earthquake input and the response of the structure

system for nonlinear time history analysis. The Latin Hypercube sampling technique is a method of random sampling that, for a fixed number of samples, ensures that the entire range of each control parameter is sampled and thus an efficient estimate of the dependant variable could be determined. Given a reasonable number of samples, the Latin Hypercube sampling technique can provide response statistics. The values for all variables were matched randomly in sets containing one value for each random variable. These sets were then matched to the earthquake time histories to construct 200 samples of the earthquake-structure system. The damage states are then estimated based on the damage model develped by Park et al. (1985), which is integrated in the program IDARC2D.

The aim of current codes is designing buildings that would be able to resist minor earthquakes without significant damage, moderate earthquakes with repairable damage and major earthquakes without collapse. During recent earthquakes, reinforced concrete structures designed in accordance with current seismic codes performed satisfactorily. Steel structures suffered joint and weld failures. However, the economic loss because of the sustained damage during earthquakes was substantial. Performance based design would provide structures with controlled and predictable damage potential.

The concept of target performance definitions is useful in the design of new structures, as well as retrofitting existing buildings (SEAOC, 1995). It provides a better vision of the expected behaviour of the structure, which may assist in

increasing the safety levels at lower costs. Recently, performance-based design has become more popular among seismic engineers. In modern seismic codes, it has been realized that different levels of performance can be expected depending on the ground motion level. Several researchers have attempted to identify the expected performance levels of structures. The following limits were suggested by Hamburger et al. (1996):

i) Collapse Prevention which allows a little margin of safety against collapse during severe earthquakes.

ii) Life Safety which allows significant damage to the building's lateral force resisting system but keeping a substantial margin against collapse.

iii) Immediate Occupancy where relatively minor damage occurs to the building.

Although these design objectives may be understood by engineers, they might imply a guarantee for immediate occupancy or for life safety. It is therefore recommended to link the performance levels to various drift ratios and damage stages of the structure, as this would be a more viable approach. The performance of the structure would be defined in terms of five ranges of damage states. These are: the elastic no damage state, minor, repairable, unrepairable damage and ultimately the structure is in the state of extensive damage and progressive collapse.

3.5 APPROACH FOR DESIGN EVALUATION

When discussing performance levels, it is natural to focus on displacement- and drift-related criteria as well as the state of damage of the structure. The identified

levels of damage to a structure include five states (Ghobarah et al, 1997). These states represent:

i) No damage, up to the *Elastic Limit*;

ii) Minor damage, up to the minor *Damage Limit*;

iii) Repairable damage, up to the *Repair Limit*;

iv) Unrepairable damage up to the *Collapse Prevention Limit* at which the structure is on the verge of collapse; and

v) Extensive damage where the structure starts a phase of *Progressive Collapse* until ultimate failure.

The proposed levels of damage are shown in figure 3.5 superimposed on a typical performance curve. Relating the damage level to life safety and immediate occupancy definitions, as proposed by SEAOC (1995) involves some judgement.

For each category of structures, a probabilistic analysis could be performed to correlate the expected behaviour of the structure as given by the pushover analysis with the dynamic performance in terms of damage potential. For different earthquake records of low peak ground acceleration, PGA, the behaviour of the structure is independent of the earthquake characteristics. In the non-linear stage, the behaviour of the structure strongly relies on the specifics of the ground motion record. Therefore, a probabilistic approach was adopted. A large number of ground motion time history records was used to assess the structure's response.

The dynamic analysis would relate the ground motion characteristic

parameters such as PGA to storey and roof drifts. The relationship between drift and damage level could be established based on the response of the structure. The defined damage limits in terms of drift could be correlated with the results of the static pushover analysis. The expected damage levels are correlated to the force-drift relationship obtained using the pushover analysis. The drift from the pushover analysis is related to the dynamic performance level of the structure in terms of levels of damage potential. This relationship can be used in the performance evaluation process.

3.6 SUMMARY

Uncertainties in the structural capacity were evaluated in terms of the strength of concrete and steel, the dimensions of the various members, and the aging of the concrete. The process of ground motion modelling is described in terms of general and zone-specific regions. The general ground motion was modelled using the power spectral density approach, while the zone-specific ground motion records were generated using design spectrum-compatible acceleration time histories. The structural response was evaluated statistically using the Monte Carlo simulation technique. The reliability analysis procedure presented in this Chapter will be used in the response analysis and damage evaluation of the designed nine-storey frame.

Table 3.1 Random variables characteristics (Ellingwood, 1977; Mirza and MacGregor, 1979a and b)

Random variable	Probability distribution	Coefficient of variation
Steel yield strength	Lognormal	0.093 - 0.107
Concrete compressive strength	Normal	0.150
Slab thickness	Normal	0.070
Beam width	Normal	0.020
Beam height	Normal	0.010
Beam depth	Normal	0.020
Column dimension	Normal	0.020
Steel rebar area	Normal	0.024

Table 3.2 Mean and the coefficient of variation for ω_g and ζ_g (Lai, 1982)

Ground condition	ω_g (rad/sec)		ζ_g	
	Mean	Coefficient of variation	Mean	Coefficient of variation
Rock	26.70	0.398	0.350	0.391
Soil	19.10	0.425	0.320	0.426

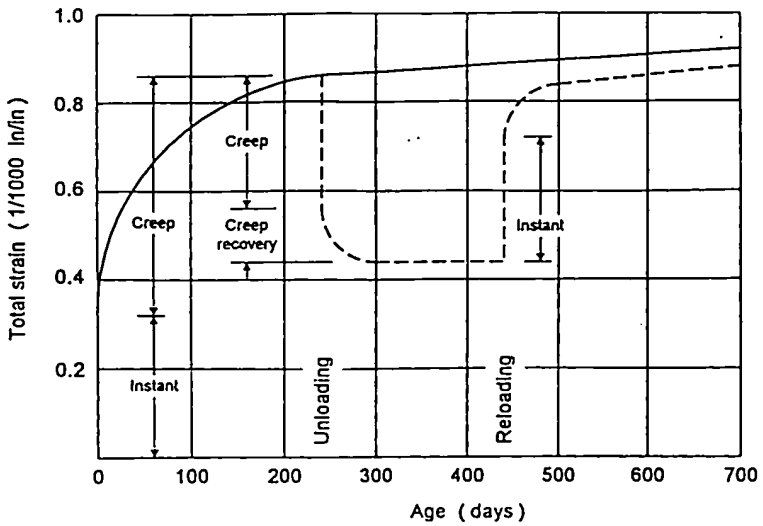

Figure 3.1 Typical creep curve for concrete (Nilson and Winter, 1991)

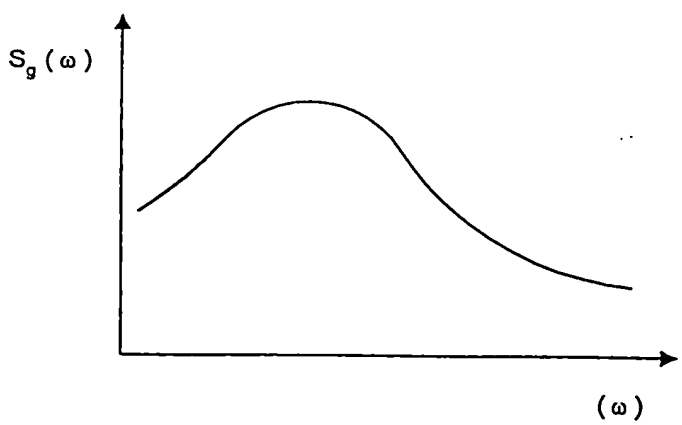

Figure 3.2 General shape of the power-spectral density function (Aly, 1997)

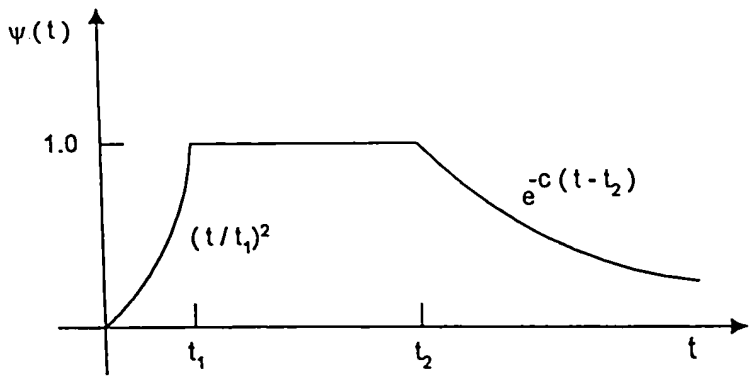

Figure 3.3 Intensity function for non-stationary process (Aly, 1997)

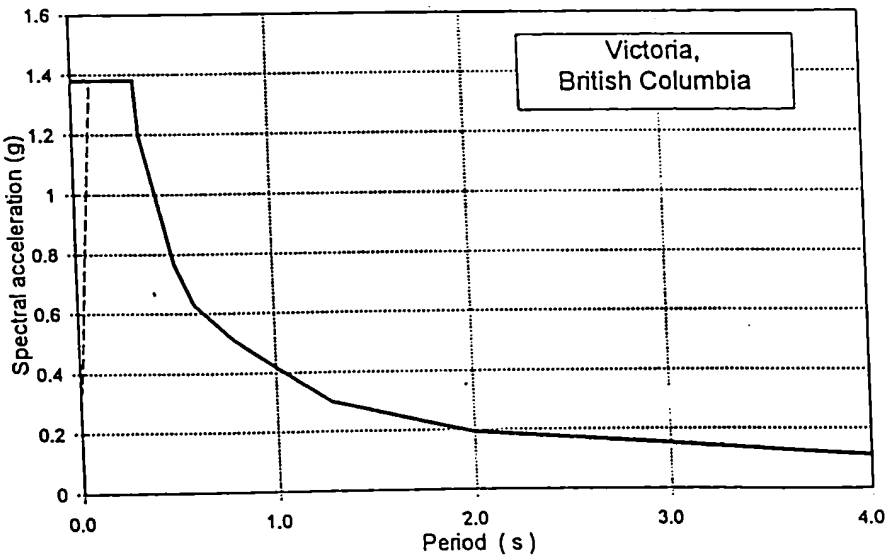

Figure 3.4 Design response spectrum for Victoria, B.C. (NBCC, 1995)

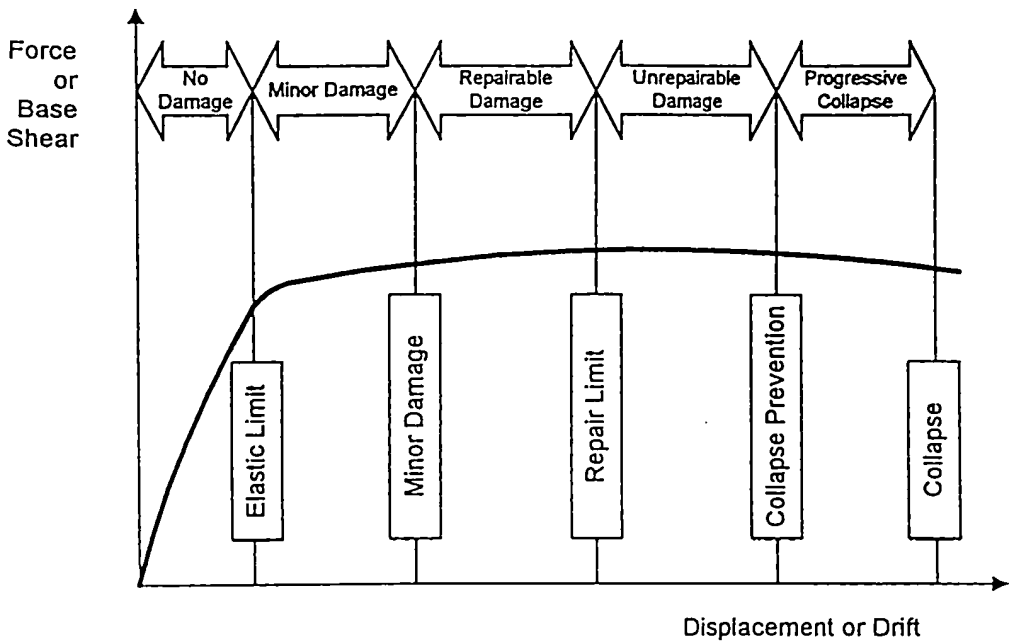

Figure 3.5 Proposed levels of damage (Aly, 1997)

CHAPTER FOUR

PERFORMANCE OF EXISTING BUILDING

4.1 INTRODUCTION

Many of the existing buildings were designed in accordance with earlier codes, where the design was to lower levels of seismic loads when compared to current codes. Structures designed to resist gravity loads might have inadequate lateral capacity, which renders them more vulnerable to earthquakes. The seismic design of new buildings is intended to provide adequate protection for life safety during severe seismic events. During recent earthquakes, the behaviour of reinforced concrete buildings designed in accordance with the recent seismic codes was found to be satisfactory. However, structures designed in accordance with earlier codes sustained severe damage. A major challenge facing seismic engineers is evaluating the seismic capacity of existing buildings and predicting their behaviour during earthquakes. Methods to assess the seismic capacity of structures range from rapid visual inspection (ATC, 1987) to sophisticated analyses. A common approach to evaluate the seismic capacity of structures is to conduct a nonlinear pushover analysis (Ghobarah et al., 1997, and others).

The main deficiencies in existing reinforced concrete frame structures include,

but are not limited to:

i) Inadequate column shear capacity due to lack of confinement.

ii) Weak joints due to limited shear capacity caused by inadequate transverse reinforcement.

iii) Poor reinforcement details.

iv) Lack of rotational capacity at beam ends due to inadequate anchorage of positive reinforcement.

v) Column side-sway mechanisms at the lower levels due to the horizontal joint shear failures that prevent the columns from reaching their full capacity.

The seismic performance of a nine-storey reinforced concrete building designed in accordance with the ACI 318-63 (ACI, 1963a) code was assessed. The details of the design of the building are presented in Chapter Two. The performance of the building was evaluated using the results of a static pushover analysis, as well as a dynamic analysis. The computer program IDARC2D was employed in the analysis. The roof drift, inter-storey drift and damage index were determined for ground motion with different levels of PGA. The variations in member dimensions, material strength, and seismic loading were considered in the analysis. For each set of ground motion records, a study was carried out to determine the mean, μ and (mean + standard deviation, $\mu + \sigma$) values of the drift and damage index.

4.2 PUSHOVER ANALYSIS

A nonlinear static pushover analysis was conducted to estimate the potential ductility of the building and determine its lateral load-carrying capacity. The pushover analysis was carried out using the force control option in the program IDARC2D. Two lateral load distributions were considered, namely;

i) a single point load at the roof,

ii) an inverted triangular load distribution, and

iii) a modal-adaptive load distribution.

The results of the pushover analysis for concentrated triangular and modal-adaptive loadings are presented in figures 4.1 through 4.4. The figures show the different performance levels with respect to the relation between the base shear and the roof displacement in a nonlinear static analysis. For example, the elastic limit occurs just before yielding of the structure which would ensure that no damage would occur to the non-structural elements.

4.2.1 Single Point Load

The results of the pushover analysis for single point load at roof level were as shown in Figure 4.1. The figure shows that the building sustained a yield load equal to about 0.05W, and an ultimate load of 0.065W, where W is the weight of the building. These values are considered rather low when compared to current code requirements, indicating that lateral resistance of the building is inadequate.

4.2.2 Triangular Loading

Figure 4.2 shows that the building sustained a yield load equal to about 0.069W, and an ultimate lateral load of 0.102W, where W is the weight of the building. These values are considered rather low when compared to current code requirements, indicating that lateral resistance of the building is not sufficient to resist the seismic demand in many parts of the country.

4.2.3 Modal Adaptive Loading

Figure 4.3 shows that the existing frame sustained yield and ultimate lateral loads of 0.054W and 0.0723W, respectively. These values are also considered rather low when compared to current code requirements, indicating that the lateral load-carrying capacity of the building is inadequate.

A comparison of the loading cases is presented in figure 4.4. The figure shows that the building sustained a higher lateral load when subjected to the triangular load. The difference in results between the loading cases could be attributed to the participation of the higher modes. In the case of the inverted triangular loading, only the first mode is significantly contributing to the overall behaviour of the building. On the other hand, when the modal-adaptive loading was used, the contribution of the higher modes was pronounced, which reduced the lateral capacity of the building.

4.3 SEISMIC ANALYSIS

The response of the building was determined when subjected to the generated ground motion time history records. The frequencies of free vibration of the building are presented in table 4.1. Two hundred ground motion time history records were employed in the analysis. Half these records was simulating time history records on soft soil sites, while one hundred records were simulating time history records on rock sites. The Monte Carlo Simulation was used to analyse the characteristics of the response of the frames.

Figures 4.5 and 4.6 show the variation of the mean, μ, and (mean + standard deviation, $\mu+\sigma$) of the roof drift and maximum storey drift, respectively, with PGA for the whole ensemble of generated earthquakes. Figures 4.7 and 4.8 show a comparison between the roof and maximum storey drifts of the building when subjected to earthquakes simulating soft soil and rock ground motion, respectively. A statistical study was carried out to determine whether the response of the building in the two cases was significantly different. The details of the statistical study and the results of the dynamic analysis are presented in the following sections.

Figure 4.9 shows the variation of the average storey drift with the height of the nine-storey building for PGA=0.4. The figure shows that the maximum storey drift occurs in the fourth or fifth storey. This pattern was observed for other values of PGA. Figure 4.10 shows the variation of the storey shear with the height of the building. Figures 4.9 and 4.10 show that more than one mode contribute to the overall behaviour of the building. The sequence of hinging is shown in figure 4.11.

4.3.1 Statistical Study

When comparing two populations of known mean (μ) and standard deviation (σ), it is important to determine if the two populations are significantly different. The distribution of the populations will be assumed to be normal (Gaussian). Figure 4.11 (Box et al., 1987) shows normal distributions with different means and variances (σ^2).

The method of statistical inference is called "Hypothesis Testing", or "Significance Testing". In the general approach to hypothesis testing, one acts as the devil's advocate and introduce the null hypothesis (H_0). This is the hypothesis that the two mean values are identical. That is to say;

$$H_0: \mu_1 = \mu_2 \tag{4.1}$$

Where μ_1 is the mean of population 1, and

μ_2 is the mean of population 2.

The quantity D_0 is equal to the difference between the means of the two populations. Thus, if H_0 is true, then D_0 is equal to zero.

The alternative hypothesis (H_1), is that the two mean values are different. That is;

$$H_1: \mu_1 \neq \mu_2 \tag{4.2}$$

Where μ_1 and μ_2 are as defined in Equation 4.1.

This would be considered a two-tailed test, as the alternative hypothesis doesn't state that either mean is larger than the other ($\mu_1 \prec \mu_2$, or $\mu_1 \succ \mu_2$).

The test is carried out at a particular significance level (α). The significance level normally termed "Type I Error", and is defined as the probability of rejecting H_0 when it is actually true. The value normally chosen for α varies from 0.05 to 0.01. In the current study, the value chosen for α was 0.05. This means that the possibility of accepting H_1 when it is in fact wrong was only 5%.

The next step in the testing procedure would be to compute the quantity (Z_{calc}), defined as:

$$Z_{calc} = \frac{x - D_0}{S_p} \qquad (4.3)$$

Where x is the difference between the means of the two populations (μ_2-μ_1),

D_0 is equal to zero, and

S_p is the pooled standard deviation of the two populations, given by

$$S_p = \frac{(N_1 - 1)\,\sigma_1^2 + (N_2 - 1)\,\sigma_2^2}{N_1 + N_2 - 2} \qquad (4.4)$$

Where N_1 and N_2 are the number of readings of the first and second populations, respecitvely, and σ_1 and σ_2 are the standard variations of the first and second populations, respectively.

The next step is to compare the calculated value, Z_{calc}, to the tabulated value, Z_{tab}. The value of Z_{tab} is obtained from statistical tables corresponding to the required significance level ($\alpha = 0.5$). If the value of Z_{calc} is greater than Z_{tab}, then the null hypothesis is rejected, which means that the two populations are significantly different.

4.3.2 Seismic Response of the Building

The results of the study showed that, at 95% confidence, the response of the building was significantly higher for soil sites than rock sites at high levels of ground shaking (PGA≥0.2 g). This difference in response could be attributed to the building's fundamental frequency being closer to the predominant frequency of soft soil site records. Earthquakes occurring on soft soil sites tend to have a lower frequency content than earthquakes occurring on rock sites. This is due to the filtering of the higher frequencies as the seismic wave propagates through layers of soft soil. The investigated nine-storey building was quite flexible, as it had a fundamental period of 1.21 sec. This would render the building more vulnerable to earthquakes with relatively low frequency contents.

The results in figures 4.6 and 4.8 show that the inter-storey drift could exceed

the 1% and 2% limits specified in the new seismic codes for high levels of ground shaking. For soil site records, the mean value of the inter-storey drift exceeded 1% for values of peak ground acceleration larger than 0.2 g and exceeded 2% for values of peak ground acceleration larger than 0.33 g. For rock site records, the mean value of the inter-storey drift exceeded 1% for values of peak ground acceleration larger than 0.24g and exceeded 2% for values of peak ground acceleration larger than 0.35g.

4.4 PERFORMANCE EVALUATION

The damage model developed by Park et al. (1985) was calibrated on the basis of the observed damage sustained by reinforced concrete buildings during earthquakes. Singhal and Kiremidjian (1996) suggested that a damage index value between 0.1 and 0.2 corresponds to minor damage, between 0.2 and 0.5 corresponds to moderate damage, and a damage index of 1.0 represents total collapse. In the present study, it was proposed to use damage levels related to the inter-storey drift. The elastic limit and the minor damage limit were taken to correspond to a storey drift of 0.3% and 1%, respectively. The moderate damage limit was taken to correspond to a storey drift of 2% and the collapse prevention limit was assumed at a damage index of 0.6. The actual collapse was assumed to occur at a damage index equal to unity. These damage values could potentially be updated based on new experimental evidence or observations following future earthquakes.

The *Elastic limit*, *Minor Damage limit* and the *Repair limit* corresponded to storey drift values of 0.3%, 1.0%, and 2.0%, respectively, while the *Collapse*

Prevention corresponded to a damage index of 0.6. Identical damage index limit values were adopted for both the soil and rock sites. These limits were 0.18, 0.24, 0.36 and 0.60 for the *Elastic limit*, *Minor damage limit*, *Repair limit*, and the *Collapse prevention limit*, respectively.

4.5 DAMAGE ANALYSIS

The results from the dynamic analysis were evaluated to assess the level of damage sustained by the building. The damage index developed by Park et al. (1985) and modified by Kunnath et al. (1992) was used in this analysis.

Figure 4.12 shows the damage index for different values of peak ground acceleration when subjected to the whole ensemble of generated earthquakes. Figure 4.13 shows a comparison between the effect of soil and rock sites on the damage sustained by the building. This figure shows that, for high levels of ground shaking (PGA≥ 0.2g), the value of the damage index for soil site records is higher than rock site records for the same level of ground shaking. The statistical study was carried out to determine if the results of the damage analysis were significantly different for rock and soil sites. The study verified that the damage sustained by the structure was significantly higher in the case when soil site records were used. This difference in damage predictions could be attributed to the building's fundamental frequency being closer to the predominant frequency of soft soil site records.

4.6 CONCLUSIONS

The performance of a reinforced concrete building designed according to the ACI (1963) was evaluated. Different performance levels were defined for the structure in terms of the damage level. The results of the dynamic analysis were related to the damage index, storey drift, roof drift and the pushover analysis.

The results of the analysis indicated various degrees of damage were to be expected when the building was subjected to various ground motion levels. The developed methodology provided a procedure to relate the performance levels to the static pushover analysis which could provide the required assessment of existing structures.

The study also showed that the earthquakes simulating soft soil sites caused higher drift and damage values than those simulating rock sites. This could be explained by the flexibility of the building, and the lower frequency content of earthquakes occurring on soft soil sites.

Table 4.1 Natural modes of vibration of the building.

Mode Number	Frequency (Hz)	Period (sec.)
1	0.82	1.21
2	2.24	0.45
3	3.79	0.26
4	5.24	0.19
5	7.34	0.14
6	9.11	0.11
7	11.94	0.08
8	15.23	0.07
9	21.02	0.05

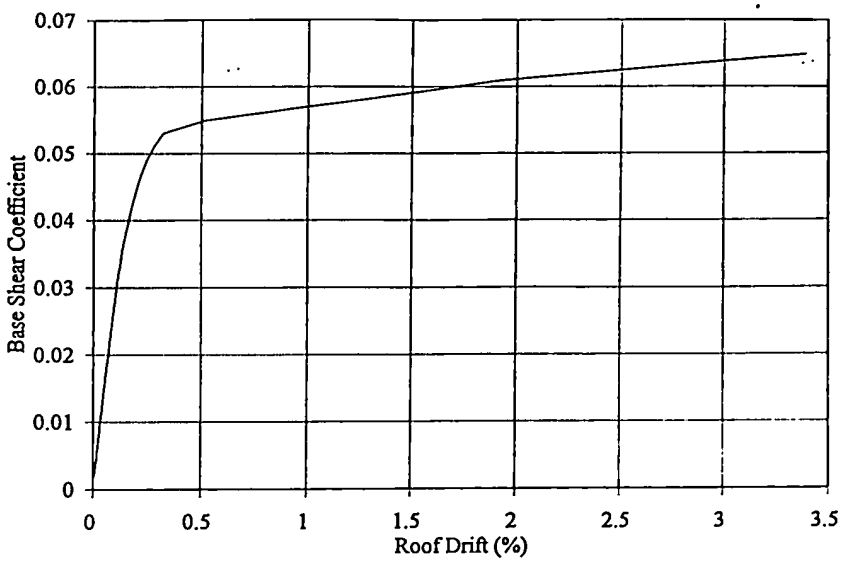

Figure 4.1 Pushover analysis with point load at roof level

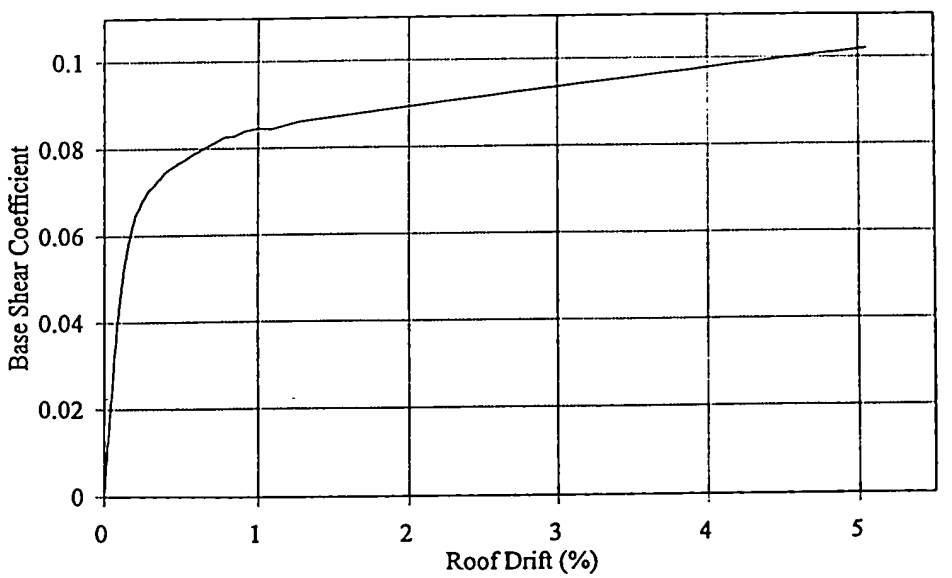

Figure 4.2 Pushover analysis with triangular loading

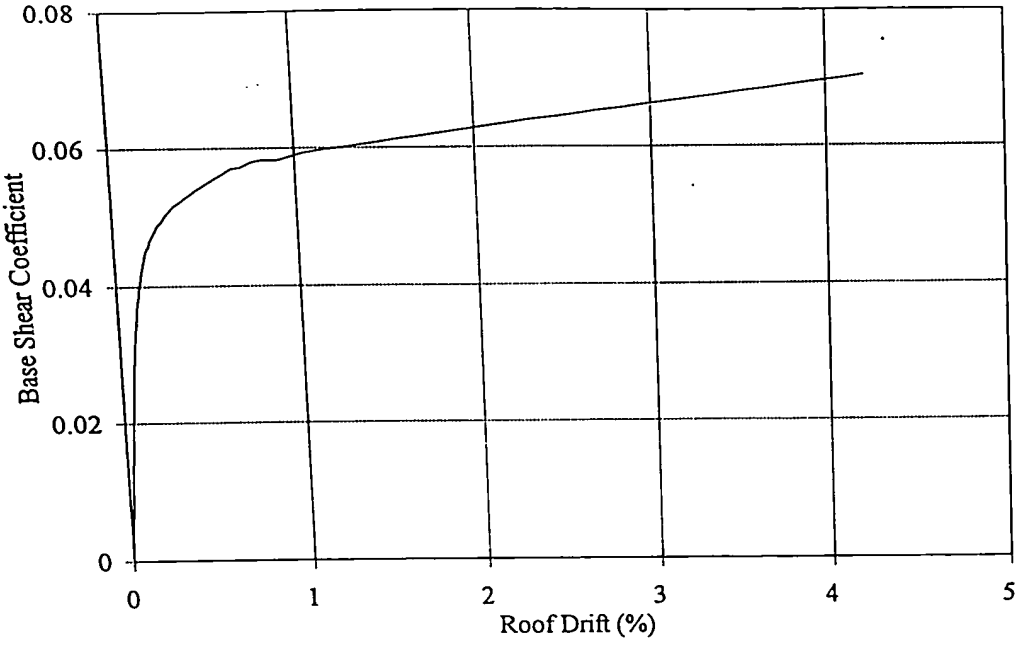

Figure 4.3 Pushover analysis for modal-adaptive loading

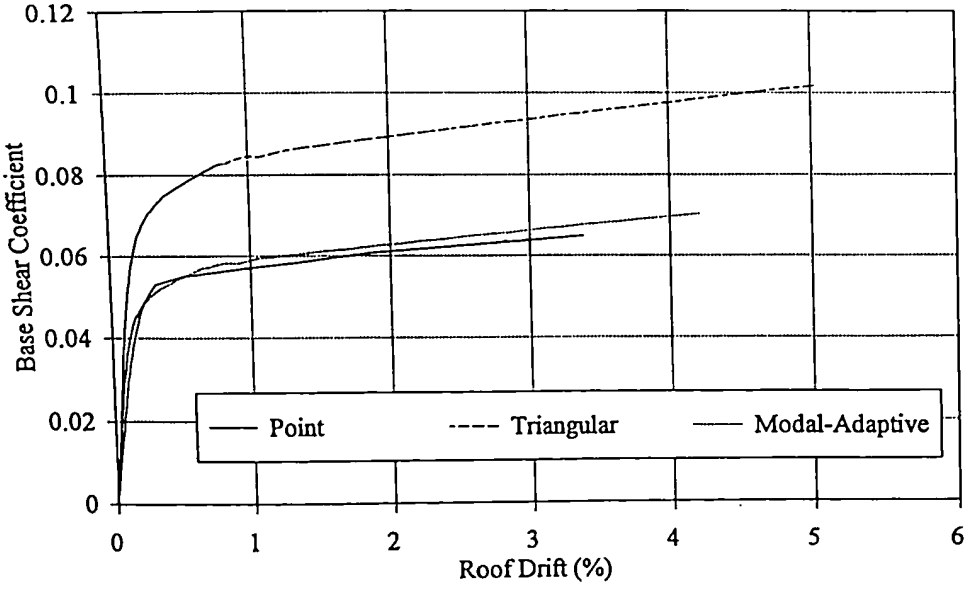

Figure 4.4 Comparison between point, triangular and modal-adaptive loading

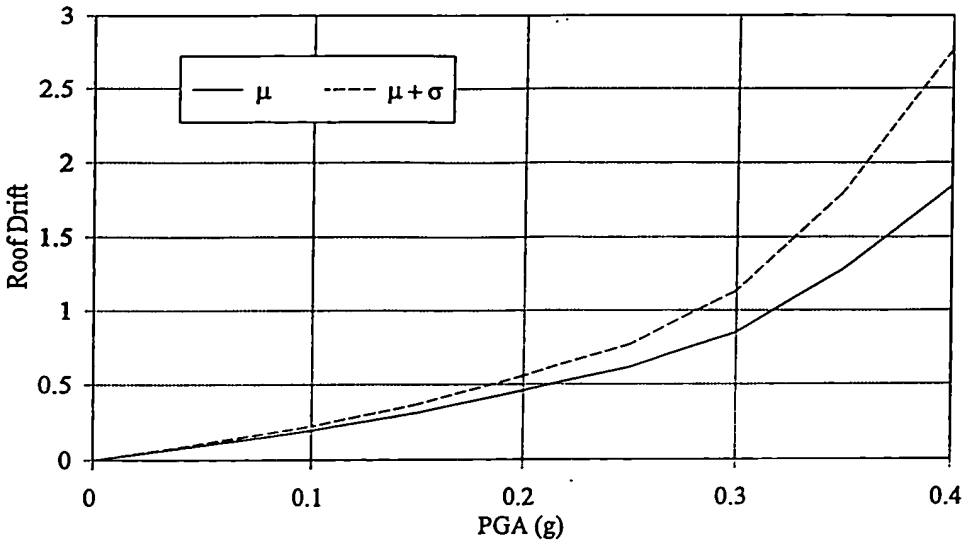

Figure 4.5 Variation of the mean and (mean + standard deviation) of the roof drift with PGA

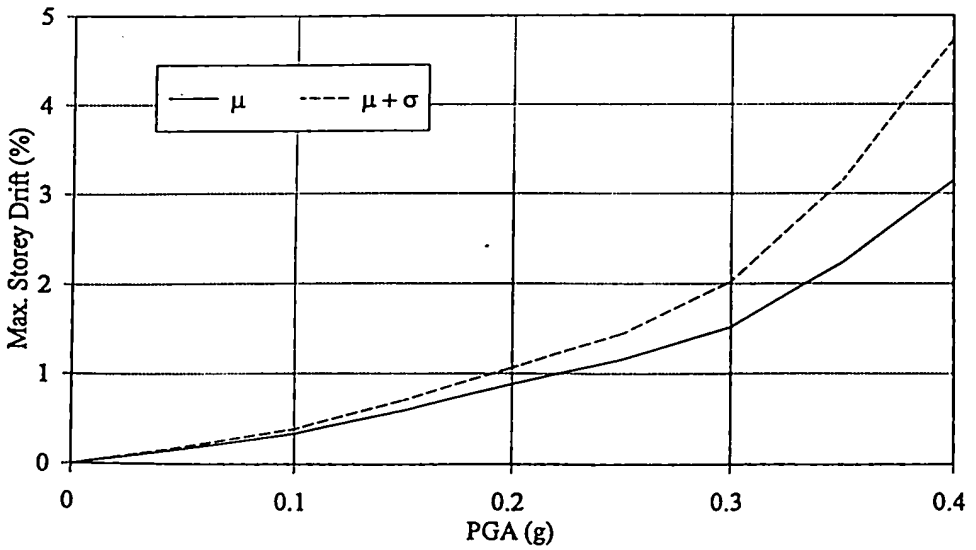

Figure 4.6 Variation of the mean and (mean + standard deviation) of the maximum storey drift with PGA

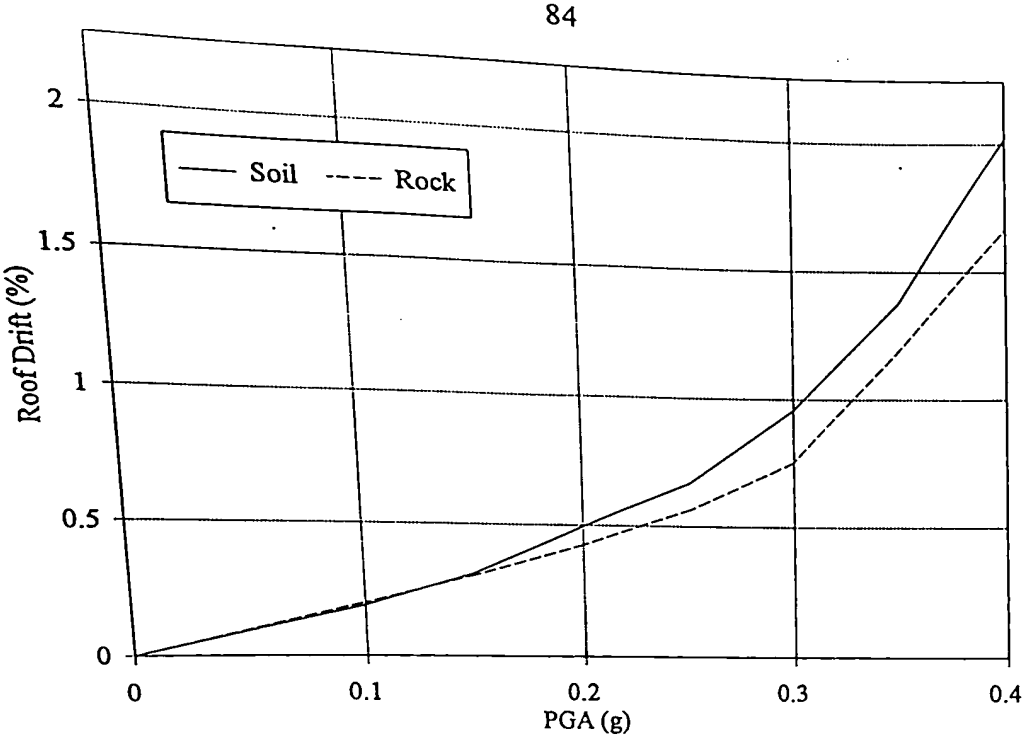

Figure 4.7 Comparison between the roof drift of the building when subjected to earthquakes simulating soft soil and rock ground motion

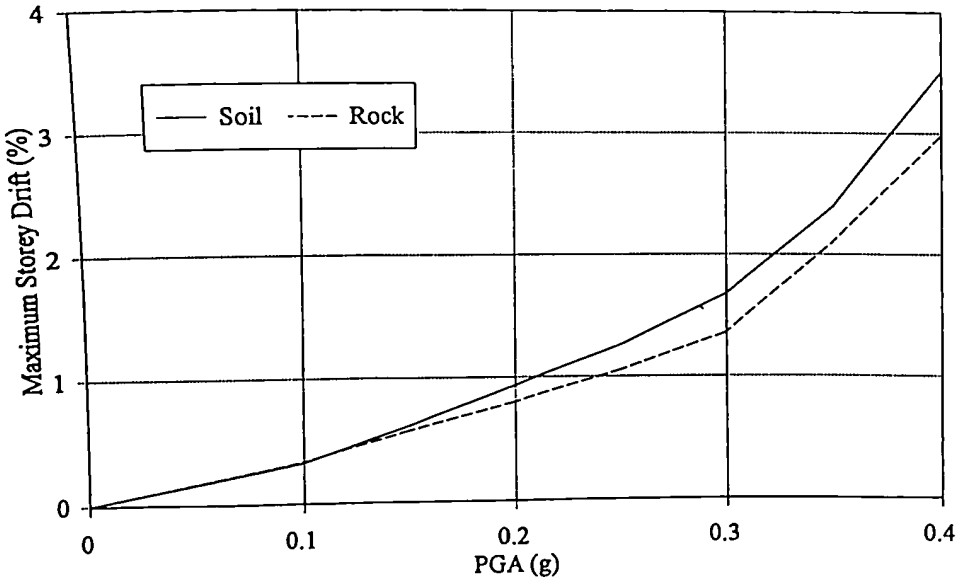

Figure 4.8 Comparison between the maximum storey drift of the building when subjected to earthquakes simulating soft soil and rock ground motion

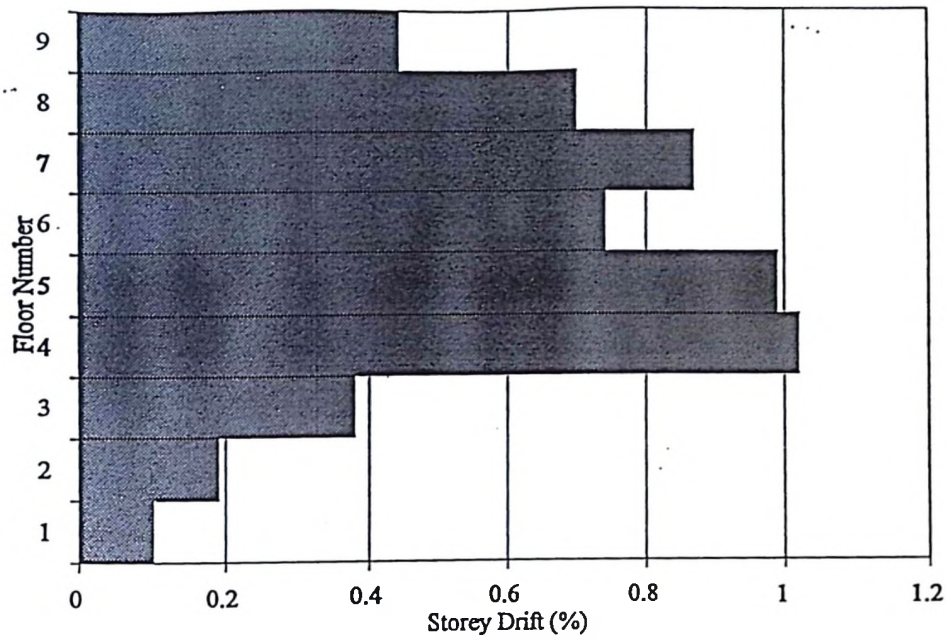

Figure 4.9 Variation of average storey drift with height of building

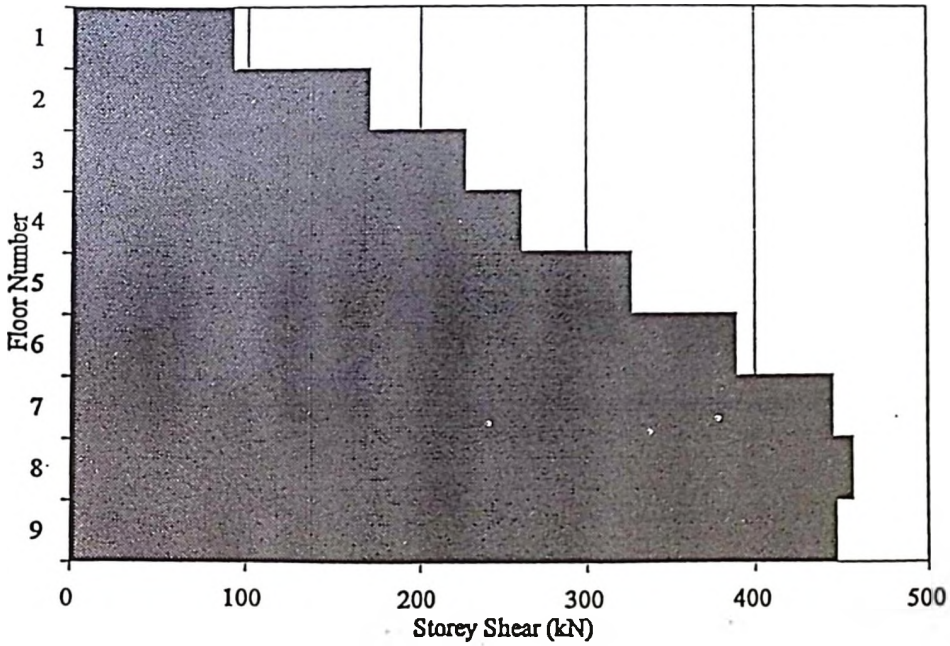

Figure 4.10 Variation of storey shear with height of building

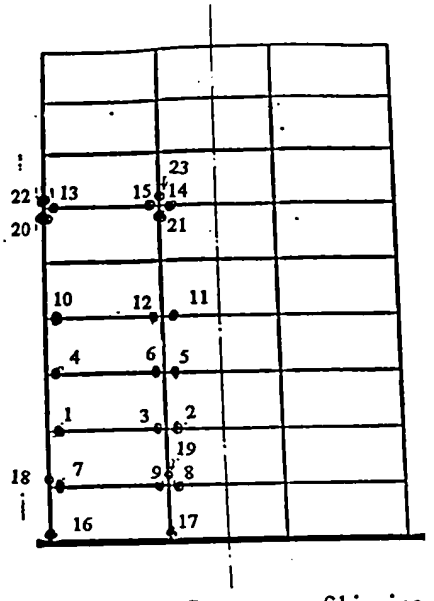

Figure 4.11; Sequence of hinging

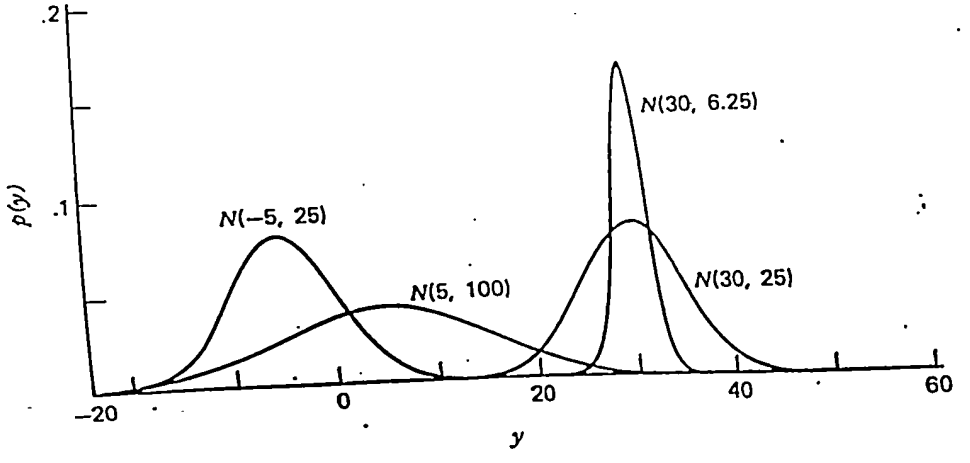

Figure 4.12 Normal distributions with variable means and variances (Box et al., 1987)

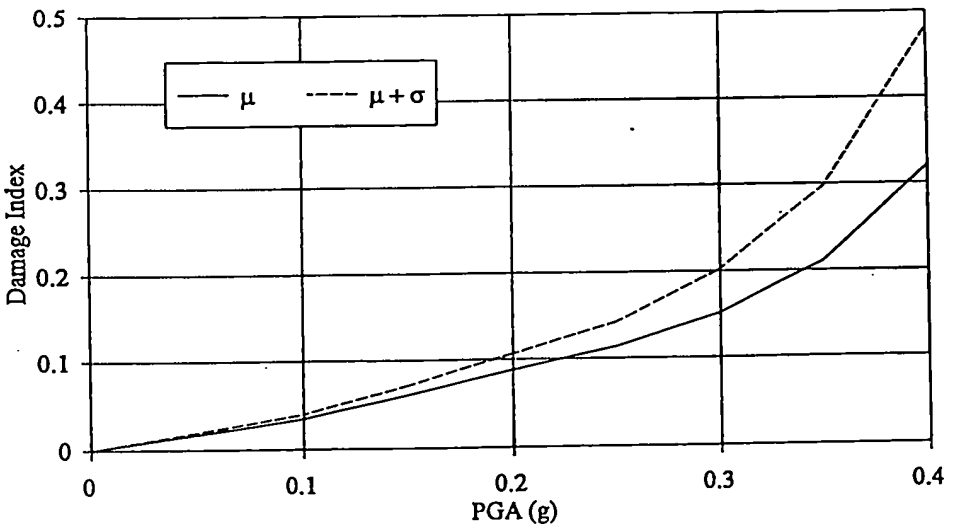

Figure 4.13 Variation of the mean and (mean + standard deviation) of the damage index with PGA

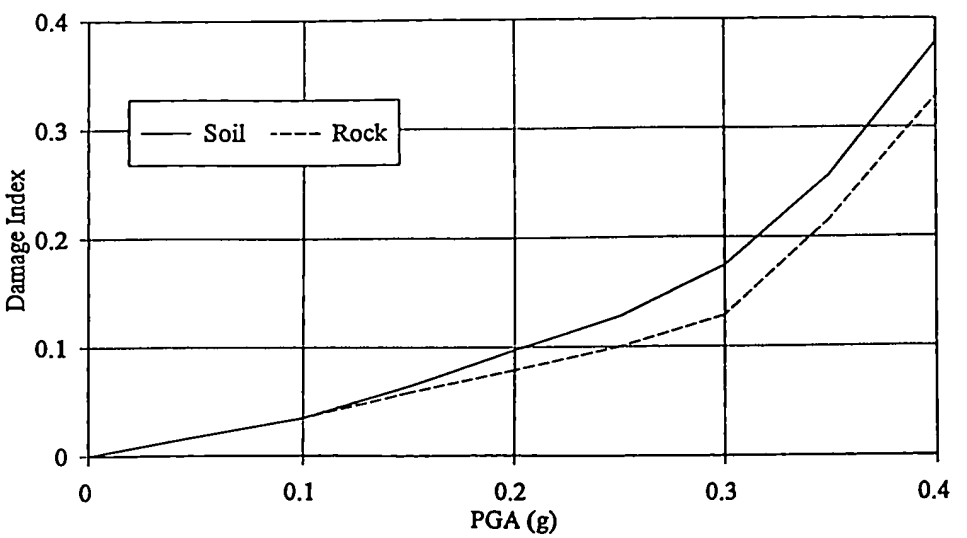

Figure 4.14 Comparison between the damage index when subjected to earthquakes simulating soft soil and rock ground motion

CHAPTER FIVE

REHABILITATED BUILDINGS

5.1 INTRODUCTION

During recent earthquakes (1995 Kobe, 1994 Northridge, and 1989 Loma Prieta Earthquakes), buildings designed in accordance with earlier codes sustained considerable damage. Therefore, it might be required to rehabilitate some of the existing buildings in order to enhance their performance during earthquakes. One of the major decisions facing civil engineers is selecting the most appropriate rehabilitation technique to enhance the seismic capacity of structures. The traditional practice in rehabilitation is not to attempt to make the existing structure comply with the current code provisions. Rather, the retrofit objectives are normally based on a performance criteria for the structures to either ensure a defined state of damage, or to prevent collapse of the building (SEAOC, 1995; Ghobarah, 1996).

The rehabilitation scheme might involve increasing the ductility of the structure, introducing systems that would increase the overall stiffness and strength, repairing deficient regions, or providing redundant load-carrying systems. More than one technique might be used simultaneously to rehabilitate a structure. The selection of a specific rehabilitation strategy should be based on the objectives as well as

economic considerations. Therefore the choice of the optimum rehabilitation strategy requires a great deal of engineering judgement. The most common techniques adopted for upgrading reinforced concrete buildings are presented in Chapter One.

Rehabilitation of columns is one of the most widely used rehabilitation techniques for reinforced concrete moment resisting frame buildings (Edno et al., 1984). Several techniques are available for rehabilitating reinforced concrete columns. Enhancing the column behaviour involves increasing the column strength, stiffness, or ductility. Normally, increasing one of the above properties affects the others. Therefore, the effect of each individual strategy on the overall behaviour of the structure in terms of its drift and damage potential when subjected to seismic loading is not very clear. Although it is not practically possible to enhance the strength without affecting the stiffness and ductility of a column, it is deemed quite important to examine the effects of changing each property independently and to investigate whether the total effect may be obtained by the summation of the two individual cases.

The effectiveness of different rehabilitation strategies for an existing reinforced concrete building was evaluated. The concrete office building designed in accordance with ACI-1963 code (discussed in Chapter Two), was analysed using various column rehabilitation techniques. The scope of the current study was limited to investigating the effect of various rehabilitation schemes for columns. Other rehabilitation systems such as bracing, beam and joint jacketing are not considered in the current study. The lateral capacity was investigated using the nonlinear pushover analysis. A

probabilistic study was performed to estimate the performance levels of the retrofitted structures in terms of their damage and drift limits. In order to evaluate the effect of each rehabilitation strategy, the results of this study were compared to the results of the study conducted on the original building. The effect of the various rehabilitation techniques on the nonlinear pushover analysis was also examined.

5.2 METHODOLOGY

A pushover analysis was conducted to investigate the response of the building in its rehabilitated forms to an increasing lateral load. The methodology was identical to the one outlined in Chapter Four. The resulting load-displacement capacity curves were used to establish the potential ductility capacity and the adequacy of the building's lateral strength.

There are several techniques to rehabilitate a reinforced concrete column. The strength, ductility and stiffness of the columns of the building were increased individually. The combined effect of increasing both the strength and the stiffness of the columns was also investigated.

In practice, rehabilitation would contribute to more than one of these properties. For example, any increase in stiffness would be associated with an increase in strength. However, in this research program, a hypothetical scheme was adopted. In this scheme, each of the three properties (strength, ductility and stiffness) were increased independent of the other two. This would give a clear insight into the effect of each rehabilitation scheme. The combined effect of increasing the strength

and stiffness was also considered.

The dynamic performance of the original and rehabilitated structures was evaluated in terms of drift and damage index and their relation to the PGA. A probabilistic analysis was carried out using the Monte Carlo Simulation, where a set of ground motion records was generated and scaled to different levels of PGA.

5.3 REHABILITATION TECHNIQUES

Selecting the optimum rehabilitation scheme depends on structural, economical, and architectural considerations. Four different techniques for rehabilitating the columns of the frame were adopted. These techniques were:

i) The original frame will be referred to as frame F.

ii) The strength of all the columns was increased by 30% (frame F1).

iii) The ductility of all the columns was increased by 100% (frame F2).

iv) The stiffness of all the columns was increased by 500% (frame F3).

v) The stiffness of all the columns was increased by 500%, accompanied by an increase in the strength of all the columns by 50% (frame F4).

Typical moment-curvature relationships for reinforced concrete columns are presented in figures 5.1a and b. The moment-curvature relationships of the columns in frame F1 were upgraded as shown in figure 5.1a to reflect a 30% increase in column strength. Figure 5.1b shows that ductility was doubled for the columns in frame F2. Columns of frame F3, as shown in Figure 5.1c, were stiffened to a level

five times higher than the original column stiffness. The combined effect of strength upgrade by 50% and stiffness increase by 500% for the columns of frame F4 is presented in figure 5.1d.

5.4 PERFORMANCE EVALUATION

The seismic performance of reinforced concrete buildings could be assessed in terms of two quantities; drift and damage. Several researchers have recognized that damage to various components of the structure may be related to drift. Several codes limit the storey drift to reduce the damage to nonstructural elements (serviceability). These limits generally depend on the type of the building and its importance. The National Building Code of Canada (NBCC, 1995) limits the storey drift to 1% for post-disaster buildings and 2% for ordinary buildings. The damage index developed by Park et al. (1985) and modified by Kunnath et al. (1992) was selected for use in the current study.

Evaluation of the rehabilitation techniques was achieved by comparing the performance of the rehabilitated structure to that of the original one. The response of the rehabilitated structure to static and dynamic loads was compared to the response of the original structure as outlined in chapter four. The high values of both storey drift and damage of the original frame suggest that the performance of the building could potentially be improved by rehabilitation.

5.5 PUSHOVER ANALYSIS

The results of the pushover analysis could be used to estimate the potential ductility of the structure, evaluate its lateral load-carrying capacity and identify the failure mechanism. The pushover analysis was carried out using the force control analysis in the IDARC2D program with two schemes of lateral load distributions;

i) an inverted triangular distribution, and

ii) a modal-adaptive distribution.

The goal of conducting a pushover analysis using a modal-adaptive load distribution was to determine the effect of higher modes on the overall response of the building.

5.5.1 Triangular Loading

The results of the analysis using a triangular load distribution is presented in figure 5.2. Each rehabilitation technique will be discussed individually.

5.5.1.1 Frame F1

Figure 5.2 shows that when subjected to a triangular lateral load, frame F1 sustained a yield load equal to about 0.069W, and an ultimate lateral load of 0.109W, where W is the weight of the building. When comparing these results with those of the original frame, no increase in the yield load was observed, but the ultimate load was increased by roughly 7%. Thus a 30% increase in strength did not affect the yield

strength, but slightly improved the ultimate strength. The fact that the yield strength remained unchanged should not be surprising, as only the ultimate strength of the columns was altered, as shown in figure 5.1a. The roof drift at the ultimate and yield loads was unaffected by the rehabilitation.

5.5.1.2 Frame F2

When subjected to a triangular lateral load, frame F2 sustained a yield load equal to about 0.069W, and an ultimate lateral load of 0.105W. Figure 5.2 shows that the paths followed by both the original frame and frame F2 were identical until frame F failed, while frame F2 sustained a higher roof drift. The roof drift at failure for frame F was 5.06%, while for frame F2 the roof drift at failure was 6.3%. Thus doubling the ductility of the columns resulted in a 24.5% increase in roof drift, and a 3% increase in the ultimate load.

5.5.1.3 Frame F3

When subjected to a triangular lateral load, frame F3 sustained a yield load equal to about 0.075W, and an ultimate lateral load of 0.1W. When comparing the loading paths for frames F and F3 as given in figure 5.2, the overall stiffness of the building was found to increase. Upon yielding, both F and F3 followed the same loading paths until ultimate failure. The ultimate load of F3, however, was slightly lower than that of the original frame. On comparing these results with those of the original frame, it can be seen that there was an 8.7% increase in the yield load, but the

ultimate load was reduced by roughly 2%. The roof drift at the ultimate load of F3 was 4.43%, indicating a 12% reduction in roof drift.

5.5.1.4 Frame F4

When subjected to a triangular lateral load, frame F4 sustained a yield load equal to about 0.08W, and an ultimate lateral load of 0.113W. On comparing these results with those of the original frame, figure 5.2 indicates that there was a significant increase in both the yield and ultimate loads. The overall stiffness of the structure was similar to that of F3. This was expected, as both frames had columns of identical stiffness. The yield load was increased by roughly 16%, while the ultimate load was increased by 10.8%. Thus, a 50% increase in strength of the columns, accompanied by a 500% increase in column stiffness, enhanced both the stiffness and the overall strength of the structure. The roof drift at the ultimate and yield loads was 4.18%. This value is 17% lower than that for the original building. This reduction in roof drift could be attributed to the fact that the ductility of the columns was identical for both F and F4.

On a general note, it was found that increasing both the stiffness and the ultimate strength of the columns was the most efficient rehabilitation technique.

5.5.2 Modal-Adaptive Loading

The results of the modal-adaptive loading are shown in figure 5.3. The results followed a similar trend as those of the triangular loading, but the yield and ultimate loads were reduced. This reduction in yield and ultimate loads could be attributed to the contribution of the higher modes. In the triangular load distribution the first mode governs the response of the building, while for the modal-adaptive load, the loads are adjusted to include the higher modes of the building. The yield loads were 0.051W, 0.051W, 0.053W, and 0.058W for frames F1, F2, F3 and F4, respectively.

5.6 SEISMIC ANALYSIS

In order to further investigate the performance of the upgraded buildings, a probabilistic analysis was carried out to determine their seismic response. Since the generated time history records simulating earthquakes typical of soil sites caused a higher response in the original building, only the time history records simulating soft soil sites were used in the analysis. The results obtained from this study were compared with those of the original building when subjected to the soil records alone. The effect of different rehabilitation schemes on the values of the damage index and the storey drift could thus be determined.

5.6.1 Frame F1

The variation of mean and (mean, μ + standard deviation, $\mu+\sigma$) of roof and storey drifts with PGA are shown in figures 5.4 and 5.5, respectively. Both the mean

and the standard deviation increase with increasing PGA. At low levels of PGA, the response of the building is linear. During that phase, the response of the building relies mainly on the structural specifics of the building. As the loading increases, the response of the building becomes non-linear. In the non-linear phase, the response of the building relies on the specific characteristics of the time history. Due to the inherent randomness of the generated time history records, the variation in results increases with increasing the PGA. This causes the variation in both the roof and maximum storey drift to increase with increasing PGA.

Figure 5.6 shows a comparison between the roof drift of the rehabilitated frame, F1, and that of the original frame, F, respectively. The roof drift for frame F1 was lower than frame F for all values of PGA. A statistical study was conducted, and the roof drift of frame F1 was found to be significantly lower than that of frame F for all levels of PGA at a confidence level of 95%.

Figure 5.7 presents a comparison between the average of the maximum storey drift of frames F and F1. The maximum drift of frame F1 was consistently lower than that of frame F. A statistical study similar to the one mentioned above was conducted to determine whether the maximum storey drift was significantly lower than that of the original building. The study verified that the maximum storey drift of frame F1 was significantly lower than that of frame F for all values of PGA.

Figure 5.8 shows the variation of the mean and the (mean + standard deviation) of the damage index for frame F1 with PGA. The figure shows that both the mean and the standard deviation of the damage index increase with the increase

of the PGA.

Figure 5.9 shows a comparison between the damage indices of frames F and F1 for different levels of PGA. The figure shows that the damage index of frame F1 was consistently lower than that of frame F for all values of PGA.

It can thus be concluded from figures 5.5, 5.6 and 5.8 that increasing the strength of the columns by 30% significantly enhanced the performance of the building.

5.6.2 Frame F2

The variation of mean and (mean + standard deviation) of roof and storey drifts with PGA are shown in figures 5.10 and 5.11, respectively. Both figures indicate that both the mean and the standard deviation increases with increasing PGA.

Figure 5.12 shows a comparison between the roof drift of the rehabilitated frame, F2, and that of the original frame, F, respectively. As shown in the figure, the roof drift for frame F2 was lower than frame F for all values of PGA. A statistical study was conducted, and the roof drift of frame F2 was found not to be significantly lower than that of frame F for all values of PGA.

Figure 5.13 presents a comparison between the average of the maximum storey drift of frames F and F2. The maximum drift of frame F2 was consistently lower than that of frame F. A statistical study was conducted to determine whether the maximum drift of frame F2 was significantly lower than that of the original frame.

The study showed that the maximum storey drift of frame F2 was not significantly lower than that of frame F for all values of PGA.

Figure 5.14 shows the variation of the mean and the (mean + standard deviation) of the damage index for frame F2 with PGA. The figure shows that both the mean and the standard deviation of the damage index increase upon increasing PGA.

Figure 5.15 shows a comparison between the damage indices of frames F and F2 for different levels of PGA. The figure shows that the damage index of frame F2 was consistently lower than that of frame F for all values of PGA. Again, the statistical study showed that the damage index of frame F2 was not lower than that of frame F for all values of PGA.

It can thus be concluded from figures 5.11, 5.12 and 5.14 that increasing the ductility of the columns by 100% did not have a significant effect on the performance of the building. This could be attributed to the flexibility of the original building, as shown by its natural modes of vibration listed in table 4.1. Thus, increasing the ductility of the columns did not enhance the seismic behaviour of the structure as significantly as the other rehabilitation techniques.

5.6.3 Frame F3

The variation of mean and (mean + standard deviation) of roof and storey drifts with PGA are shown in figures 5.16 and 5.17, respectively. The figures show

that both the mean and the standard deviation increase with increasing PGA.

Figure 5.18 shows a comparison between the roof drift of the rehabilitated frame, F3, and that of the original frame, F, respectively. The roof drift for frame F3 was lower than frame F for all values of PGA. A statistical study was conducted, and the roof drift of frame F3 was found to be significantly lower than that of frame F for all levels of PGA at a confidence level of 95%.

Figure 5.19 presents a comparison between the average of the maximum storey drift of frames F and F3. The maximum drift of frame F3 was consistently lower than that of frame F. A statistical study similar to the one mentioned above was conducted to determine whether the maximum storey drift was significantly lower than that of the original building. The study verified that the maximum storey drift of frame F3 was significantly lower than that of frame F for all values of PGA.

Figure 5.20 shows the variation of the mean and the (mean + standard deviation) of the damage index for frame F3 with PGA. The figure shows that both the mean and the standard deviation of the damage index increase upon increasing PGA.

Figure 5.21 represents a comparison between the damage indices of frames F and F3 for different levels of PGA. The figure shows that the damage index of frame F3 was consistently lower than that of frame F for all values of PGA. The statistical study was employed again, and the response of the two frames was found to be significant.

It can thus be concluded from figures 5.17, 5.18 and 5.20 that increasing the stiffness of the columns by 500% enhanced the performance of the building. This conclusion may apply in the case of moderate height buildings because of the high flexibility of the structure.

5.6.4 Frame F4

The variation of mean and (mean + standard deviation) of roof and storey drifts with PGA are shown in figures 5.22 and 5.23, respectively. The figures indicate that both the mean and the standard deviation increases with increasing PGA.

Figure 5.24 shows a comparison between the roof drift of the rehabilitated frame, F4, and that of the original frame, F, respectively. The roof drift for frame F4 was lower than frame F for all values of PGA. A statistical study was conducted, and the roof drift of frame F4 was found to be significantly lower than that of frame F for all levels of PGA at a confidence level of 95%.

Figure 5.25 presents a comparison between the average of the maximum storey drift of frames F and F4. The maximum drift of frame F4 was found to be consistently lower than that of frame F. A statistical study was conducted to determine whether the maximum drift of frame F4 was significantly lower than that of the original frame. The study verified that the maximum storey drift of frame F4 was significantly lower than that of frame F for all values of PGA.

Figure 5.26 shows the variation of the mean and the (mean + standard deviation) of the damage index for frame F4 with PGA. The figure shows that both

the mean and the standard deviation of the damage index increase upon increasing PGA.

Figure 5.27 shows a comparison between the damage indices of frames F and F4 for different levels of PGA. As can be seen from the figure, the damage index of frame F4 was consistently lower than that of frame F for all values of PGA. Again, the statistical study verified that the damage index of frame F4 was lower than that of frame F for all values of PGA.

It can be concluded from figures 5.23, 5.24 and 5.26 that the performance of the building was significantly enhanced by increasing the strength and stiffness of the columns by 50% and 500%, respectively.

5.6.5 Evaluation of Rehabilitation Techniques

As discussed above, all the rehabilitation schemes enhanced the seismic response of the original building. A comparison between the four different rehabilitation techniques was considered appropriate in order to determine which strategy had the strongest effect on the building. Figures 5.28 and 5.29 show a comparison between the roof and maximum storey drifts, respectively, at various values of PGA for the different rehabilitation schemes, along with the original frame.

Figure 5.28 shows that the roof drift of frame F4 was lower than all the other frames for all values of PGA. The roof drift of frame F1 was considerably higher than that of frame F4 for all values of PGA. The roof drift of frame F3 was slightly higher

than that of frame F1, while frame F2 was closest to that of the original frame. A similar trend was observed for the maximum storey drift, as shown in figure 5.29. For the maximum storey drift, however, the difference between frames F1 and F3 was considerably larger than in the roof drift.

A comparison between the different rehabilitation schemes in terms of damage index is presented in figure 5.30. Frame F4 sustained the least damage for all values of PGA. The damage sustained by frames F1 and F3 was almost identical until PGA exceeded 0.3g, at which point the damage sustained by frame F3 started being slightly higher than that of frame F1. Frame F2, again, showed the least improvement over the original frame.

5.7 COMPARISON WITH THE PERFORMANCE OF A THREE-STOREY FRAME

Ghobarah et al. (1997) conducted a similar study for three-storey buildings. Similar rehabilitation techniques were employed. Figure 5.31 (Ghobarah et al., 1997) shows the results of a static pushover analysis using a triangular load distribution. The figure shows that the results obtained by Ghobarah et al. (1997) showed a similar trend to those of the current study. The values of base shear/weight sustained by the three-storey building were remarkably higher than those obtained for the nine-storey one. Frame F2 showed almost 50% increase in roof drift over the original frame for the three-storey frame, while only a 24.5% increase in roof drift was observed for frame F2 for the nine-story frame.

This difference could be attributed to the difference in stiffness between the three- and nine-storey frames. The frequencies of free vibration of the original three-storey frame were 1.66Hz, 4.90 Hz and 7.79 Hz, while the frequencies of free vibration of the nine-storey frame were 0.82 Hz, 2.24 Hz and 3.79 Hz. On comparing these values, it is found that the three-storey frame was a considerably stiffer structure. Increasing the ductility of the columns would thus have a more significant effect on the three-storey building.

Another difference between the responses of the three- and nine-storey frames was observed in the response of frame F3. In the case of the three-storey building, F3 had a lower yield and ultimate loads than that of frame F (Ghobarah et al., 1997), while their yield and ultimate loads were equal for the nine-storey frame.

Figure 5.32a and b (Aly, 1997) shows the variation of the storey drift and the damage index with PGA for the three-storey frame. On comparing these figures with figures 5.28 and 5.30 for the nine-storey frame, a difference in the behaviour of frame F2 could be observed. In the case of the three-storey building, frame F2 sustained a higher storey drift than frame F. This was not the case for the nine storey frame. The variation of the damage index with PGA was similar for the three- and nine-storey buildings.

5.8 CONCLUSIONS

Various strategies were adopted to rehabilitate columns of reinforced concrete buildings, and their effectiveness was assessed. Increasing the column strength,

ductility, stiffness, and combined stiffness and strength strategies were tested. Two types of analyses were conducted, namely pushover and dynamic analyses. The results were compared in terms of roof and storey drifts, as well as a damage index.

The study showed that increasing the stiffness and strength simultaneously was the most effective technique, followed by increasing the strength alone. Increasing the stiffness alone had a lower effect on the behaviour of the building than the above techniques. Increasing the ductility alone was the least significant.

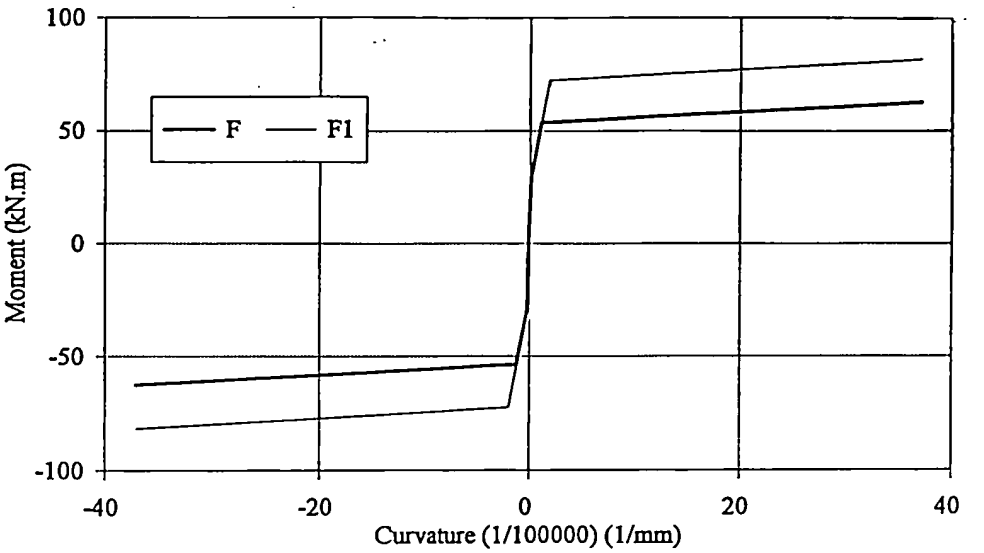

Figure 5.1a Typical moment-curvature relationships for columns of frames F and F1

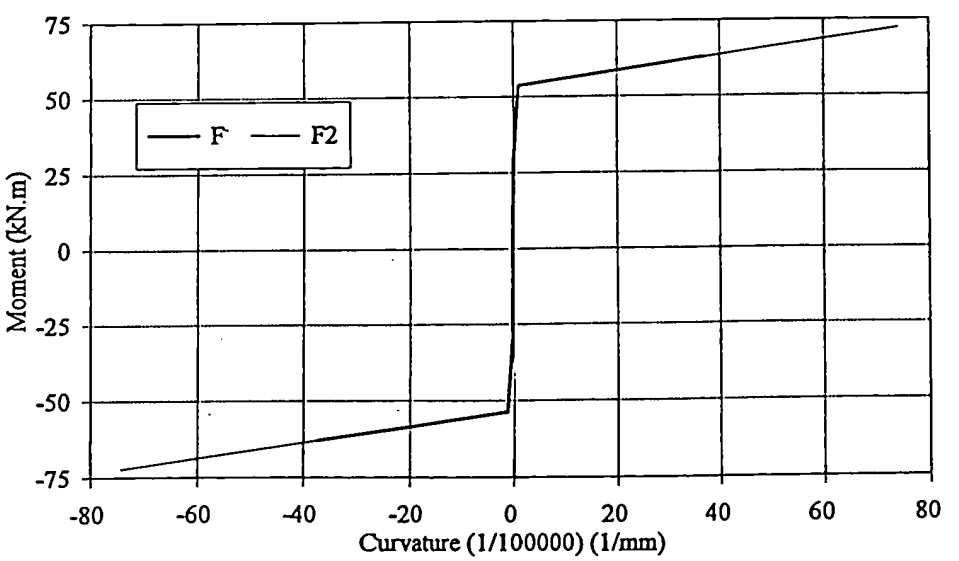

Figure 5.1b Typical moment-curvature relationships for columns of frames F and F2

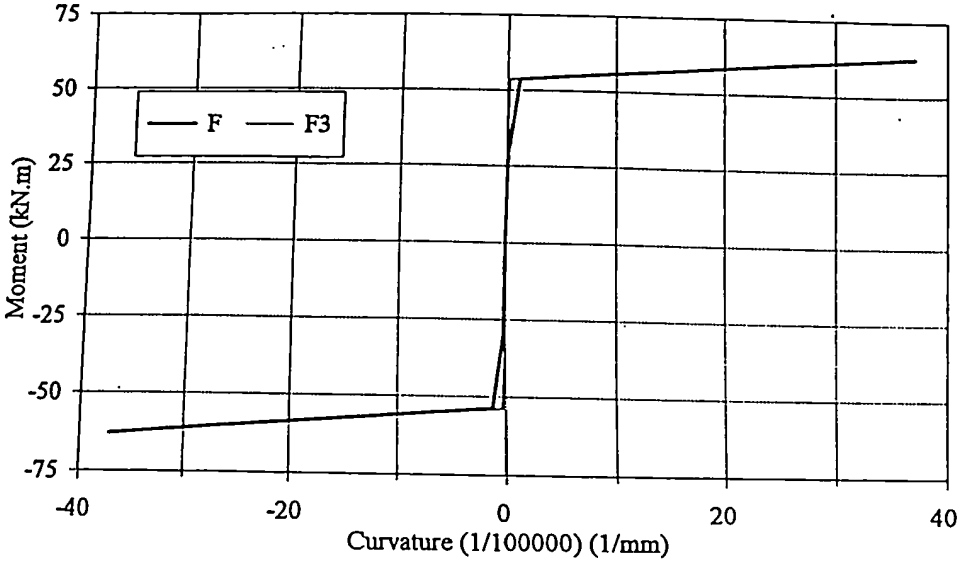

Figure 5.1c Typical moment-curvature relationships for columns of frames F and F3

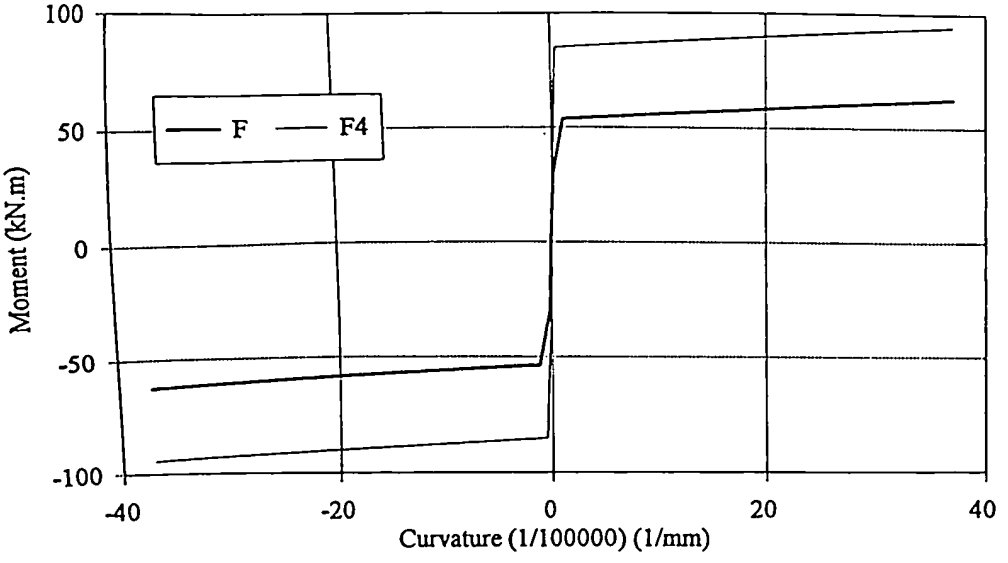

Figure 5.1d Typical moment-curvature relationships for columns of frames F and F4

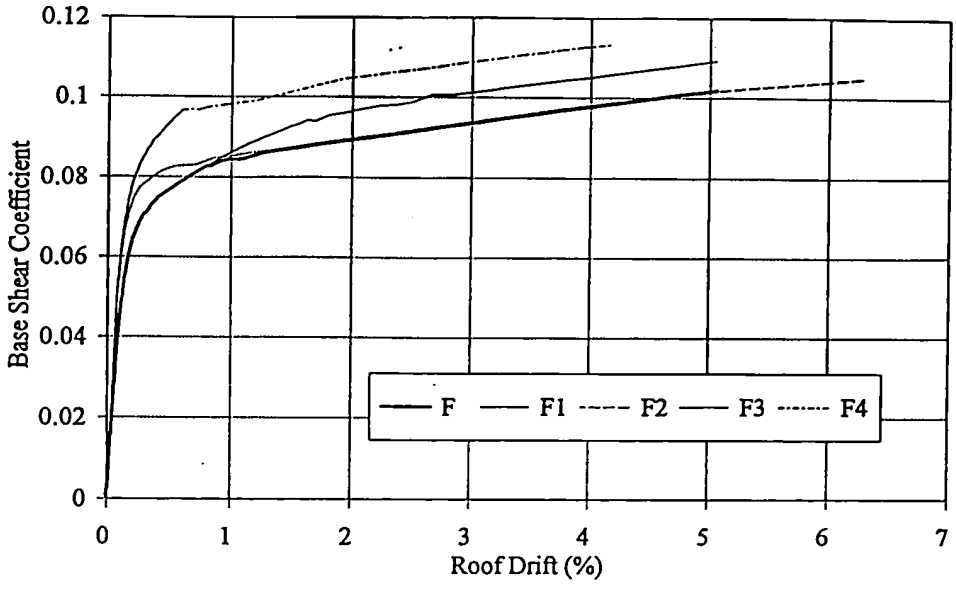

Figure 5.2 Pushover analysis for triangular load distribution

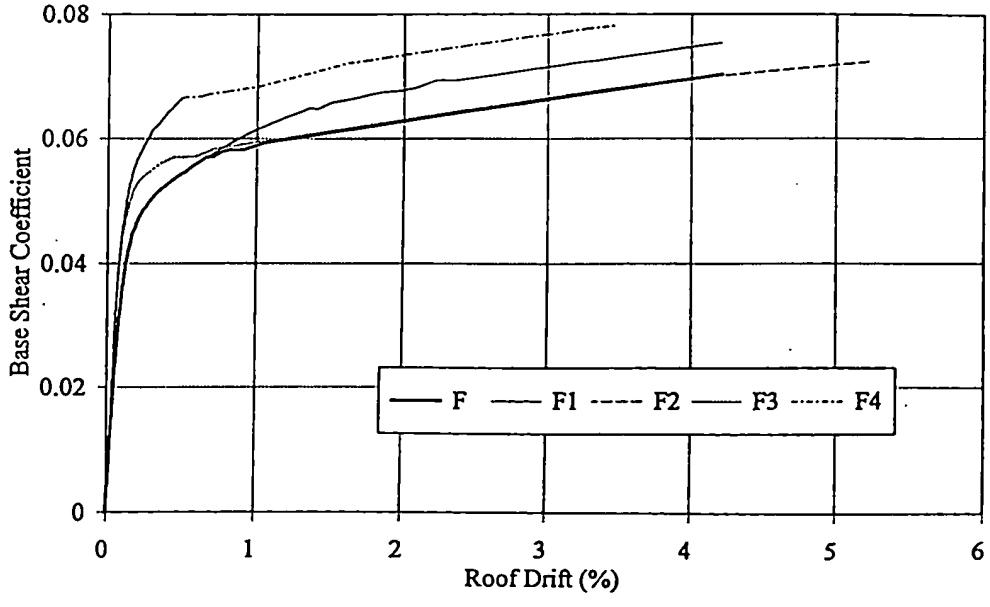

Figure 5.3 Pushover analysis for modal-adaptive load distribution

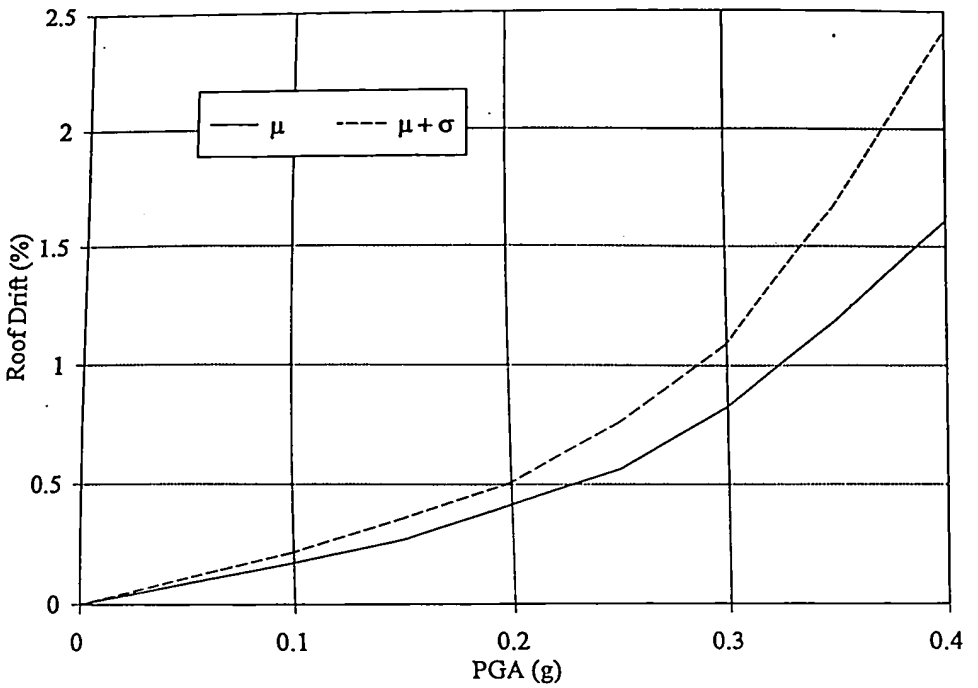

Figure 5.4 Variation of roof drift with PGA (Frame F1) for soil site conditions

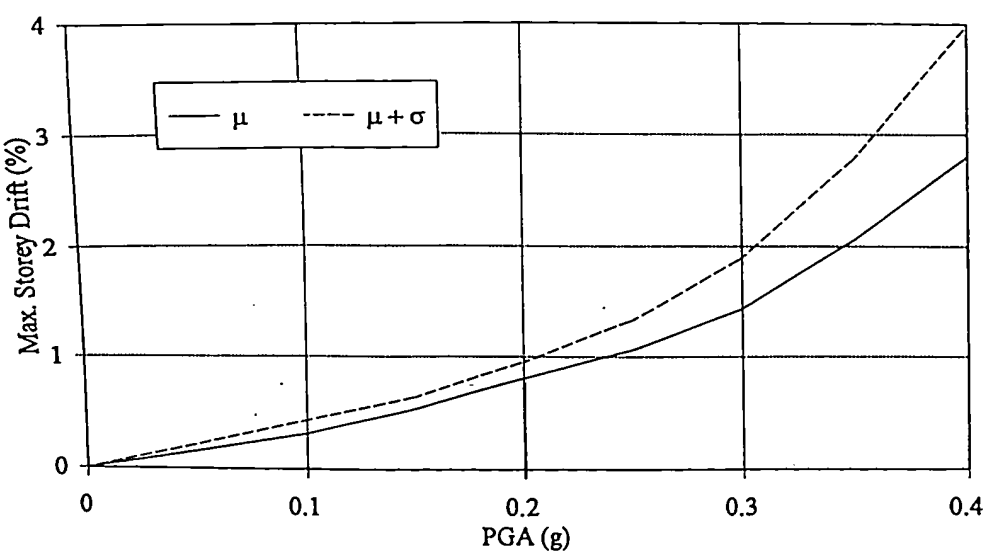

Figure 5.5 Variation of maximum storey drift with PGA (Frame F1) for soil site conditions

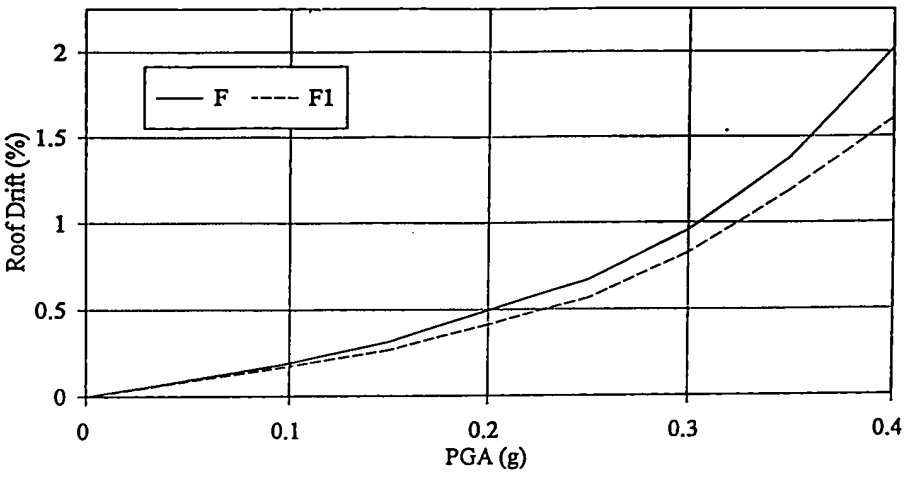

Figure 5.6 Comparison between the roof drift of frames F and F1

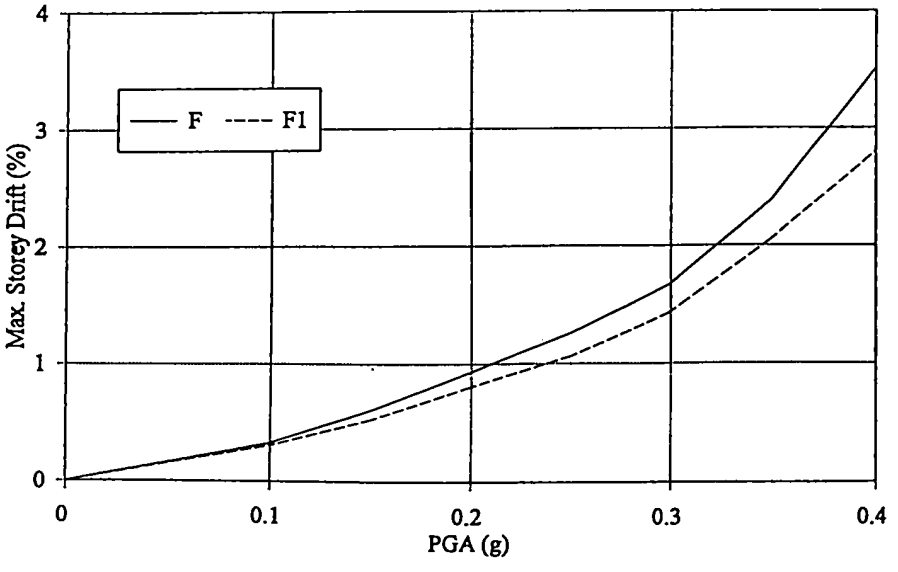

Figure 5.7 Comparison between the maximum storey drift of frames F and F1

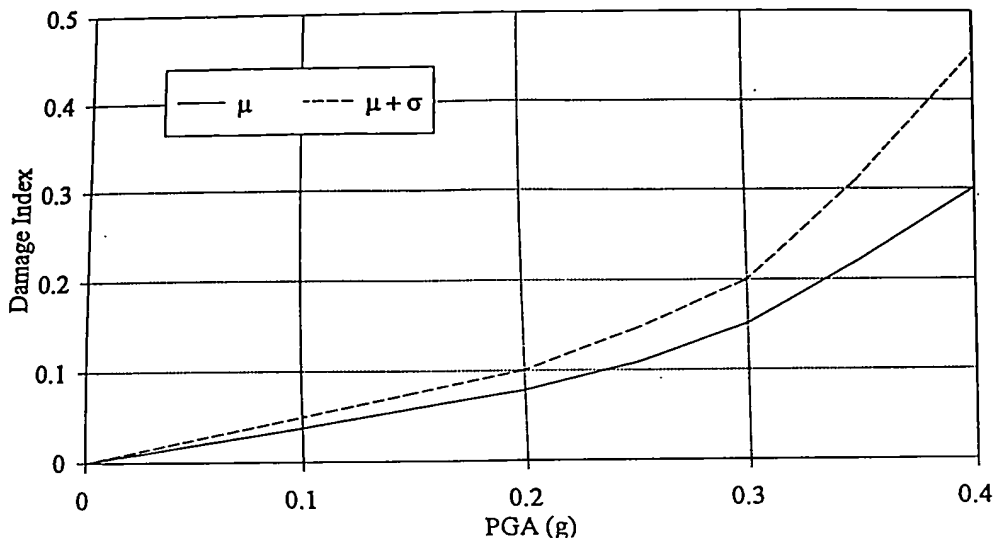

Figure 5.8 Variation of damage index with PGA (Frame F1) for soil site conditions

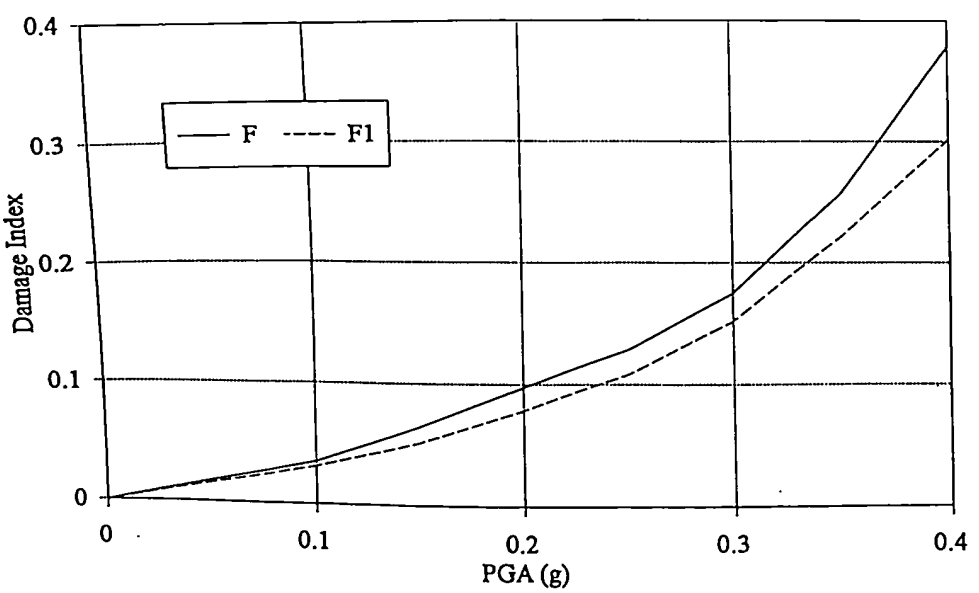

Figure 5.9 Comparison between the damage index of frames F and F1

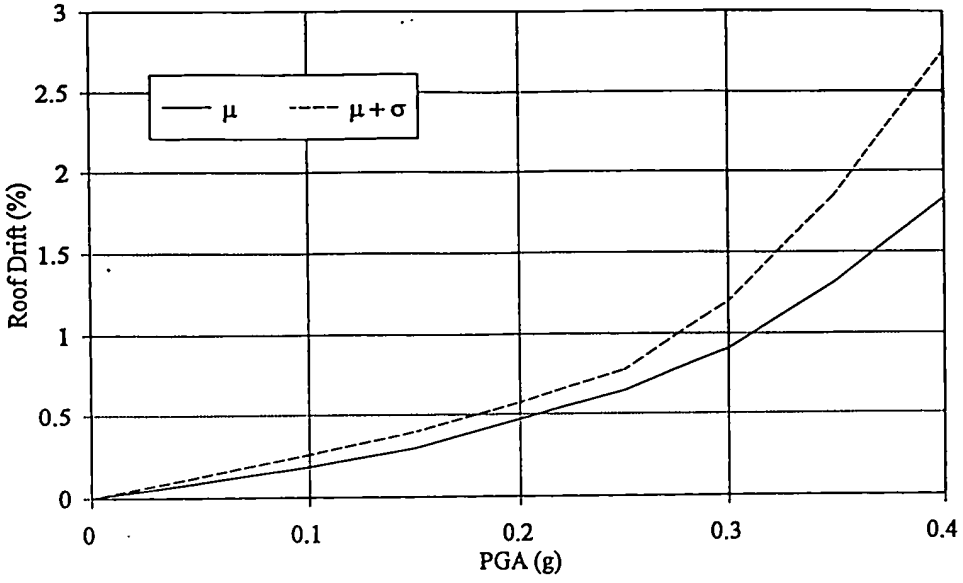

Figure 5.10 Variation of roof drift with PGA (Frame F2)

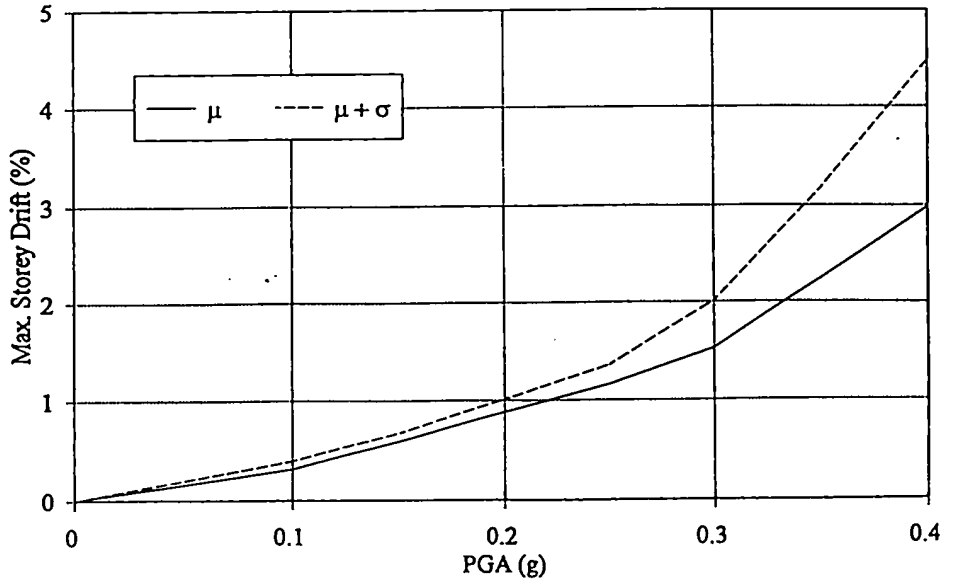

Figure 5.11 Variation of maximum storey drift with PGA (Frame F2)

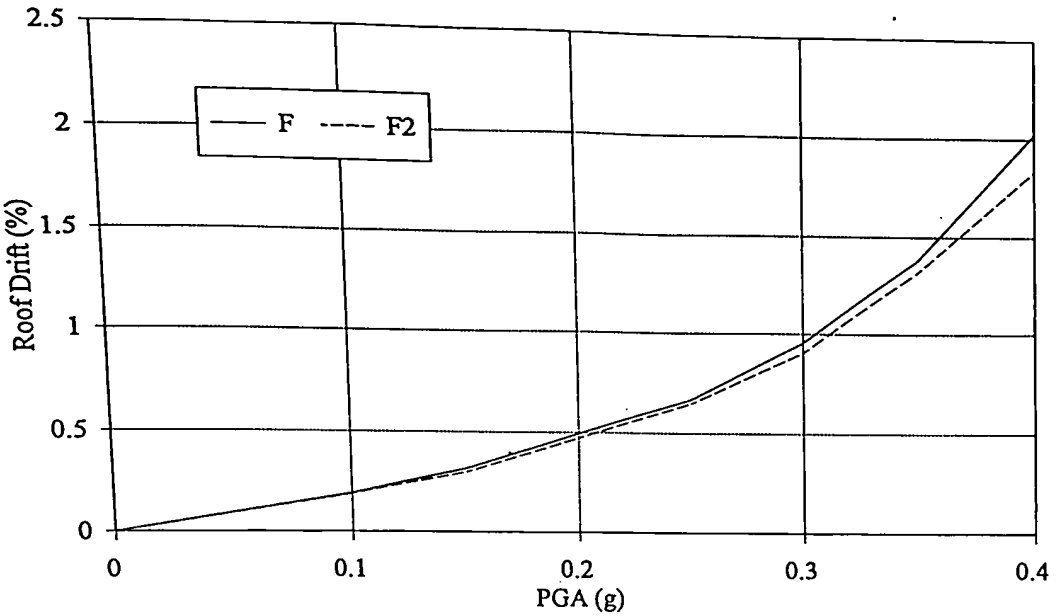

Figure 5.12 Comparison between the roof drift of frames F and F2

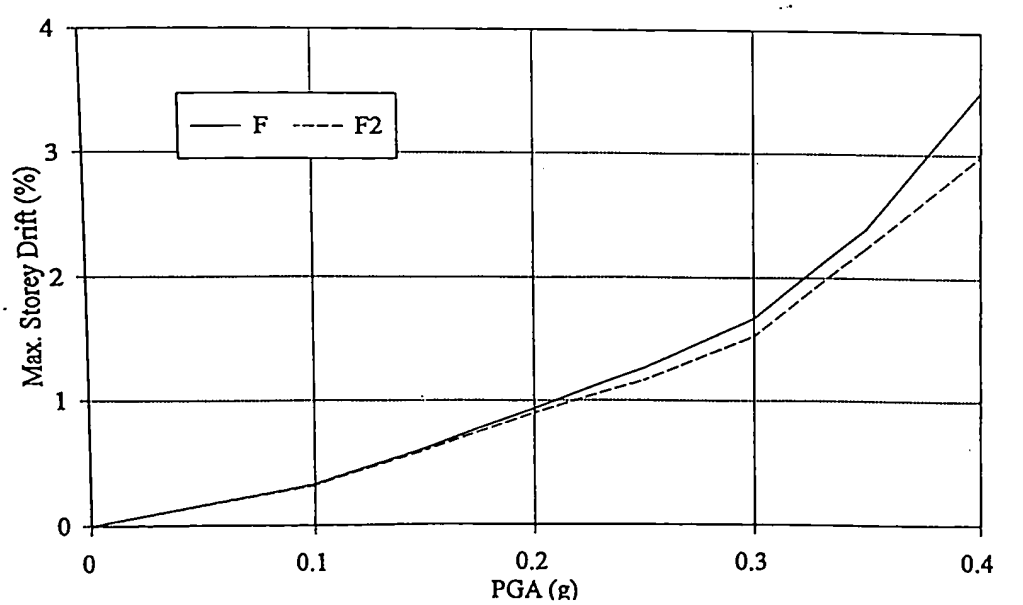

Figure 5.13 Comparison between the maximum storey drift of frames F and F2

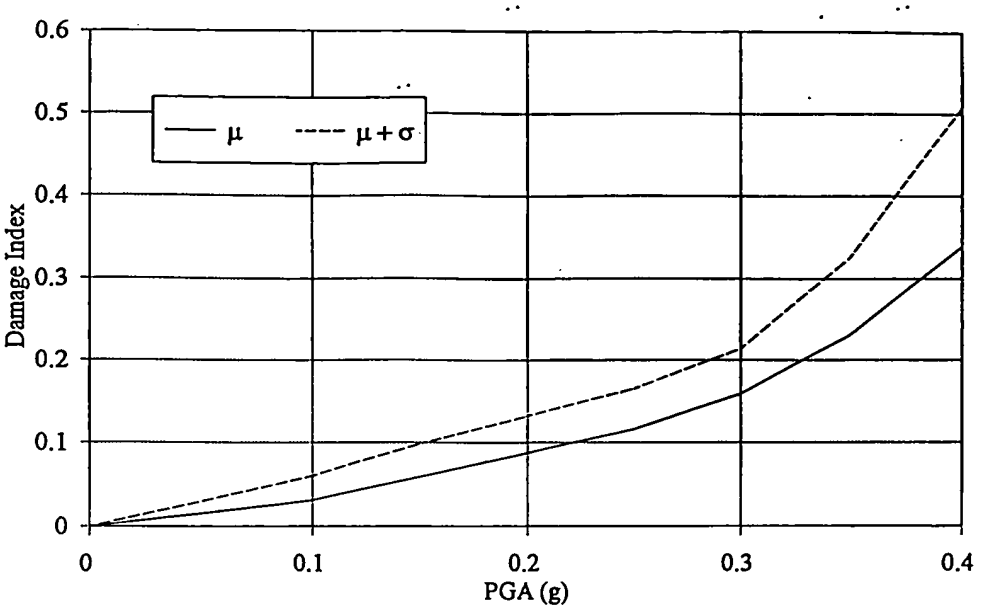

Figure 5.14 Variation of the damage index with PGA (Frame F2)

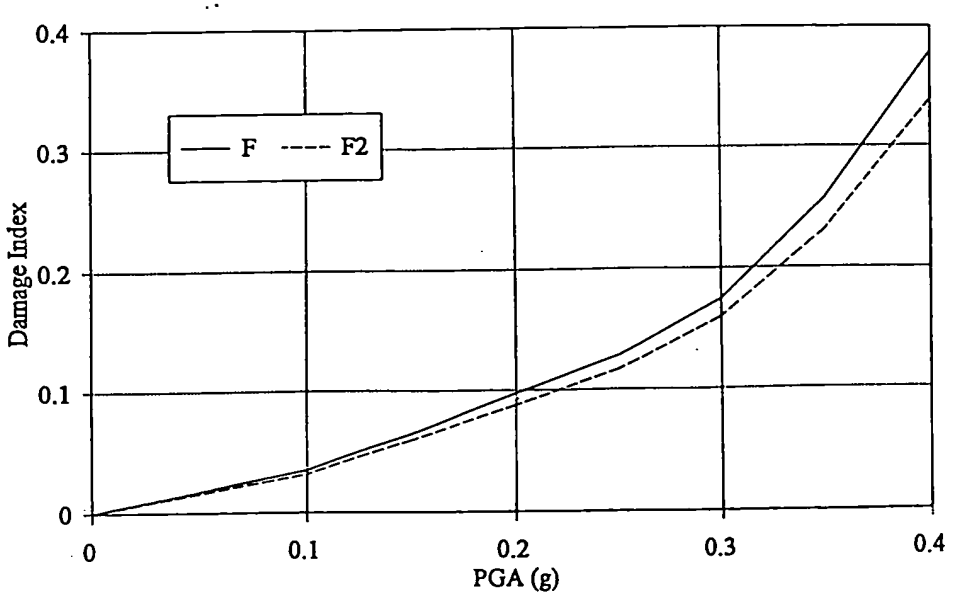

Figure 5.15 Comparison between the damage index of frames F and F2

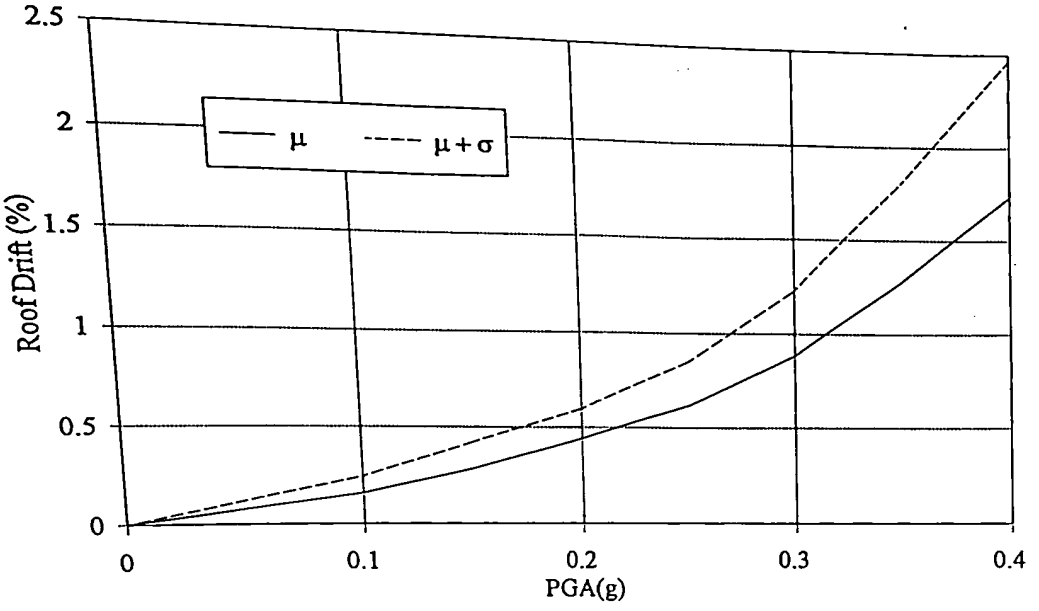

Figure 5.16 Variation of roof drift with PGA (Frame F3)

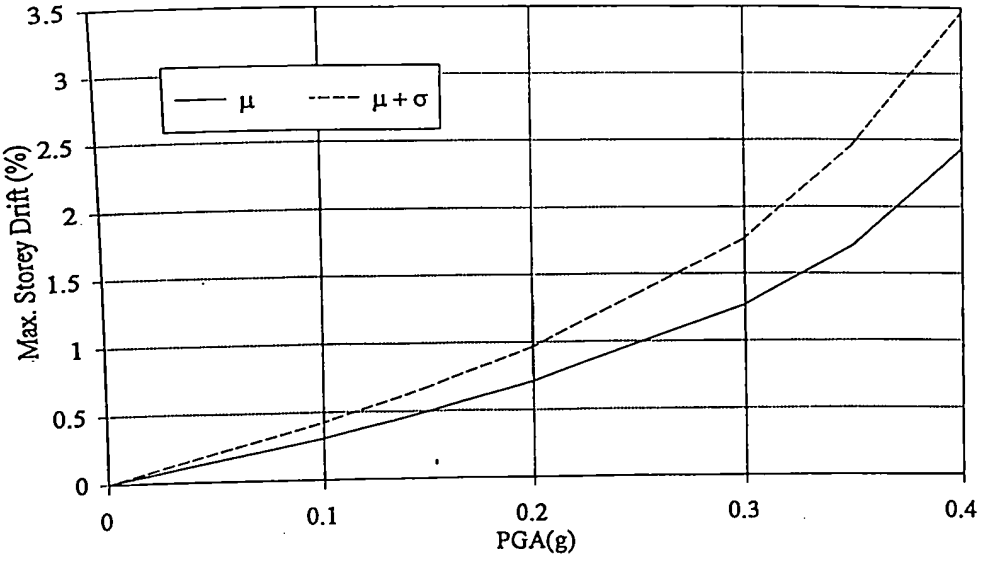

Figure 5.17 Variation of maximum storey drift with PGA (Frame F3)

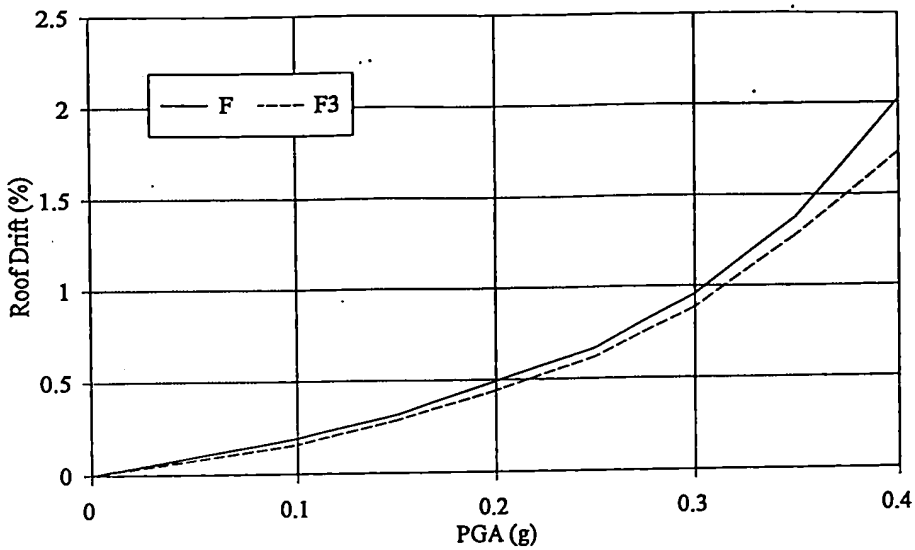

Figure 5.18 Comparison between the roof drift of frames F and F3

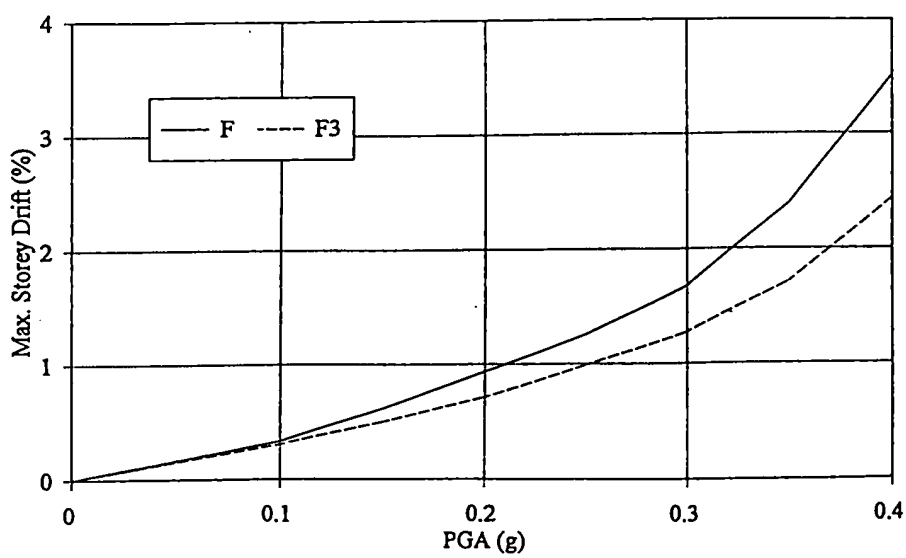

Figure 5.19 Comparison between the maximum storey drift of frames F and F3

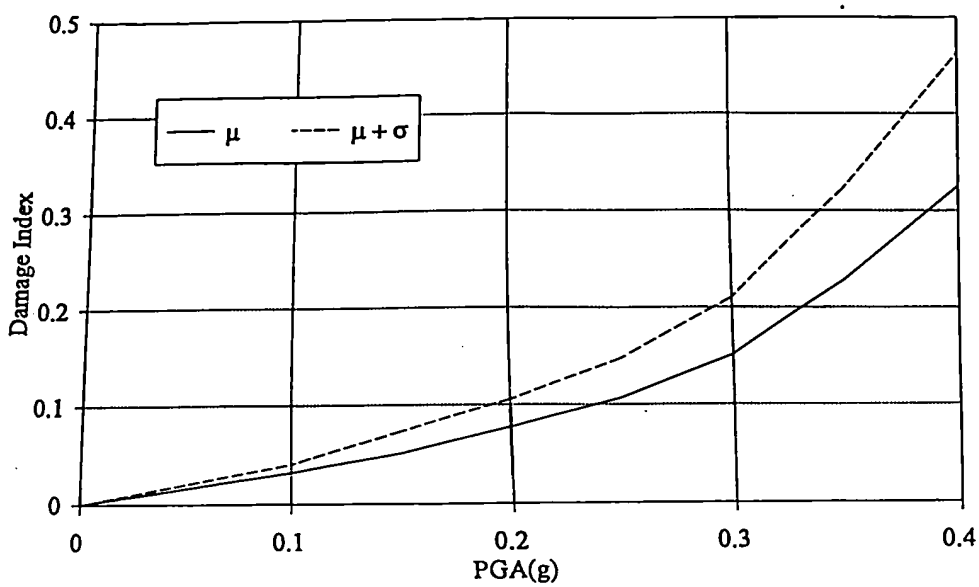

Figure 5.20 Variation of the damage index with PGA (Frame F3)

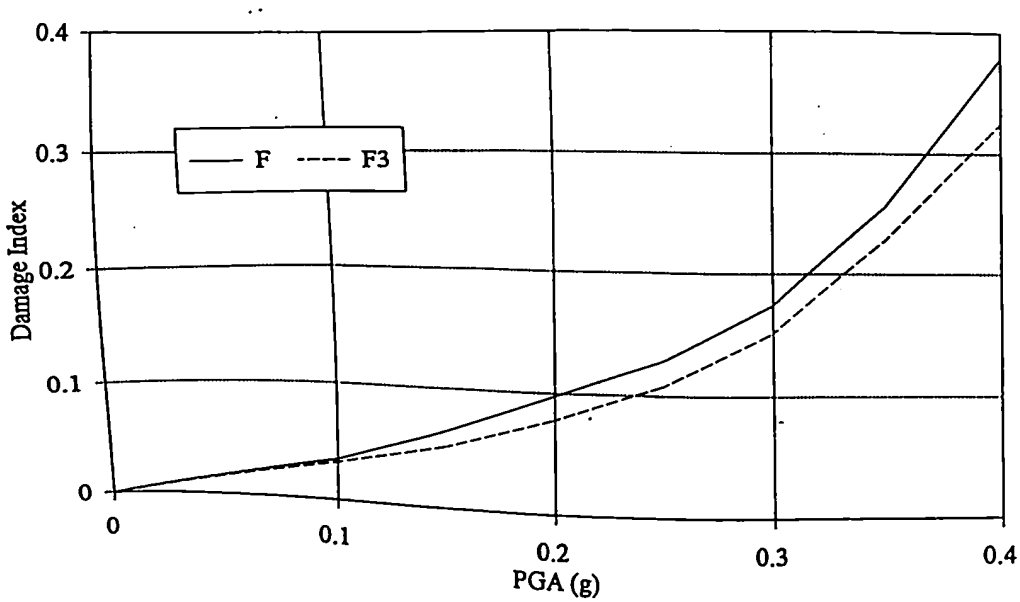

Figure 5.21 Comparison between the damage index of frames F and F3

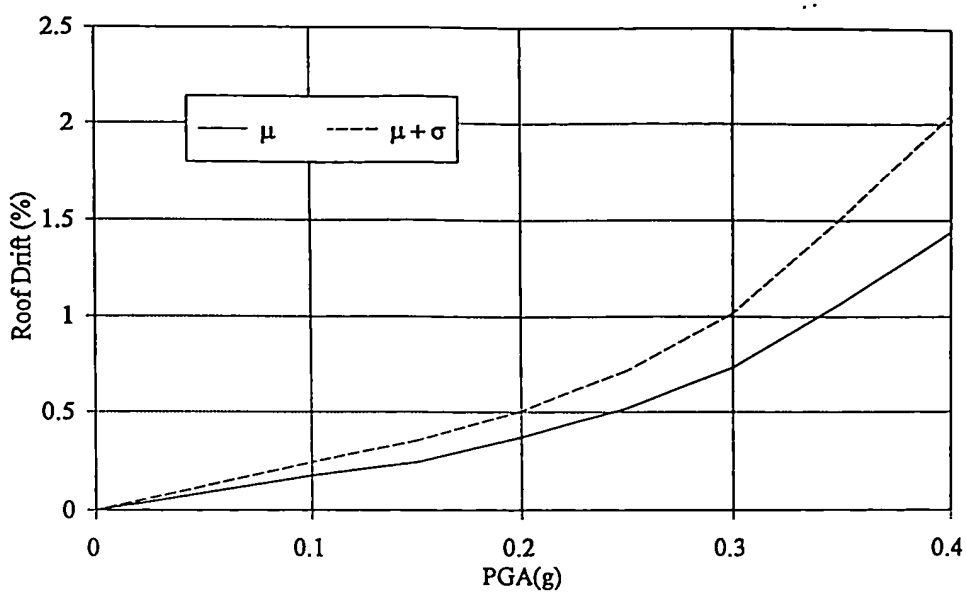

Figure 5.22 Variation of roof drift with PGA (Frame F4)

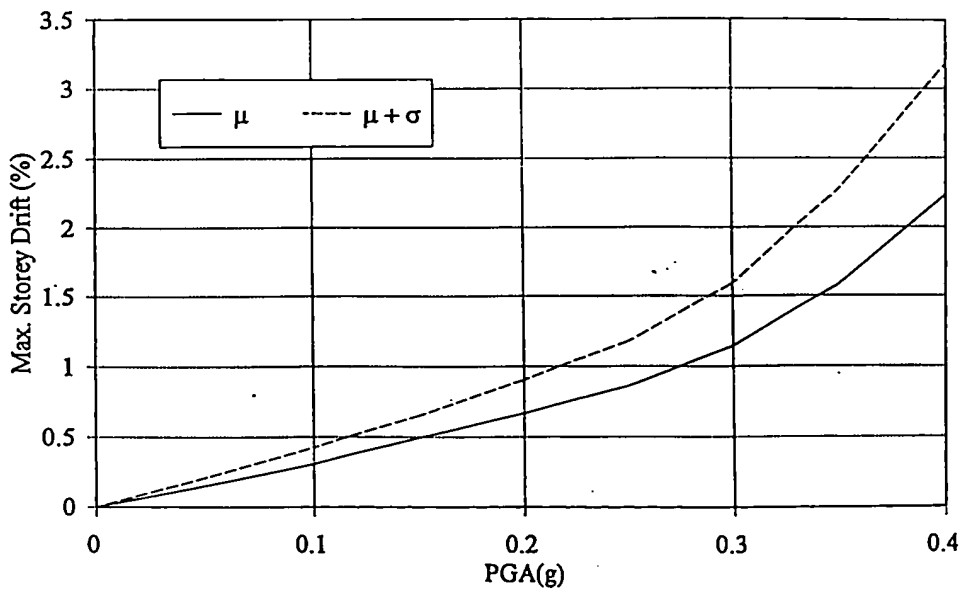

Figure 5.23 Variation of maximum storey drift with PGA (Frame F4)

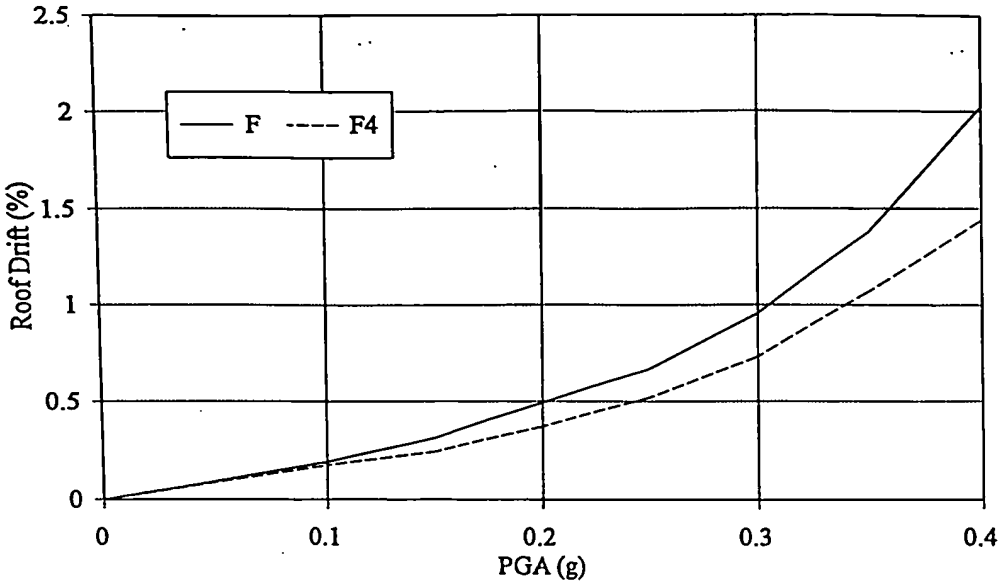

Figure 5.24 Comparison between the roof drift of frames F and F4

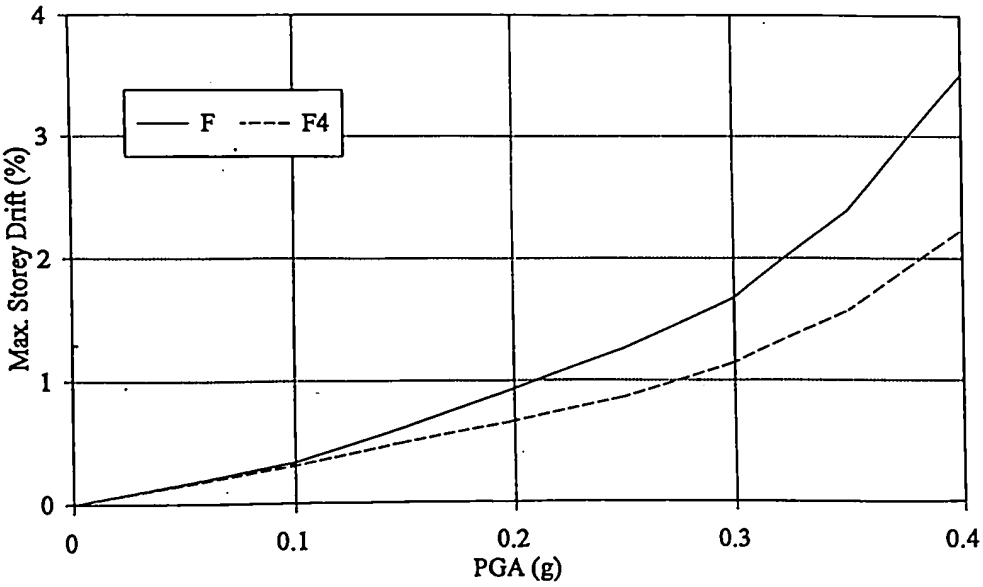

Figure 5.25 Comparison between the maximum storey drift of frames F and F4

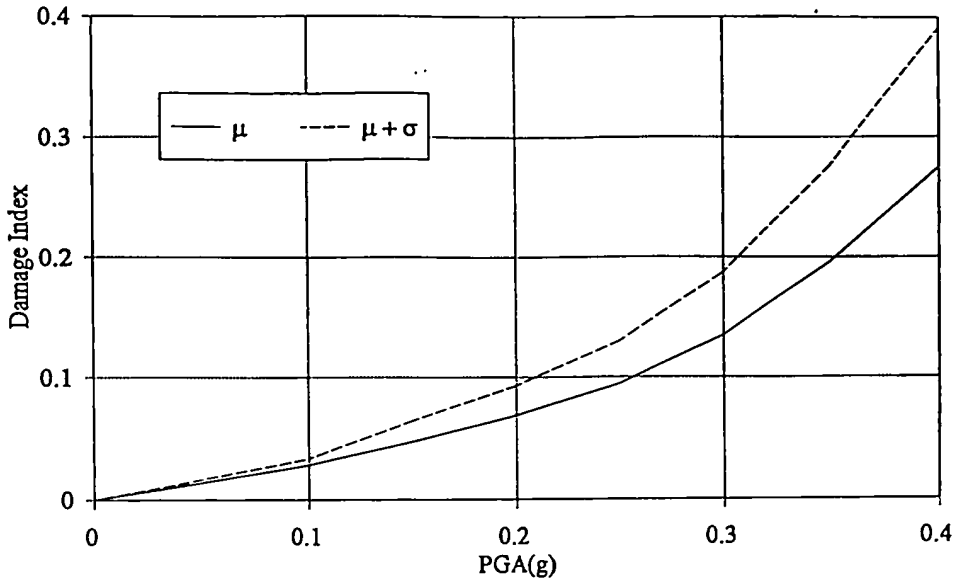

Figure 5.26 Variation of the damage index with PGA (Frame F4)

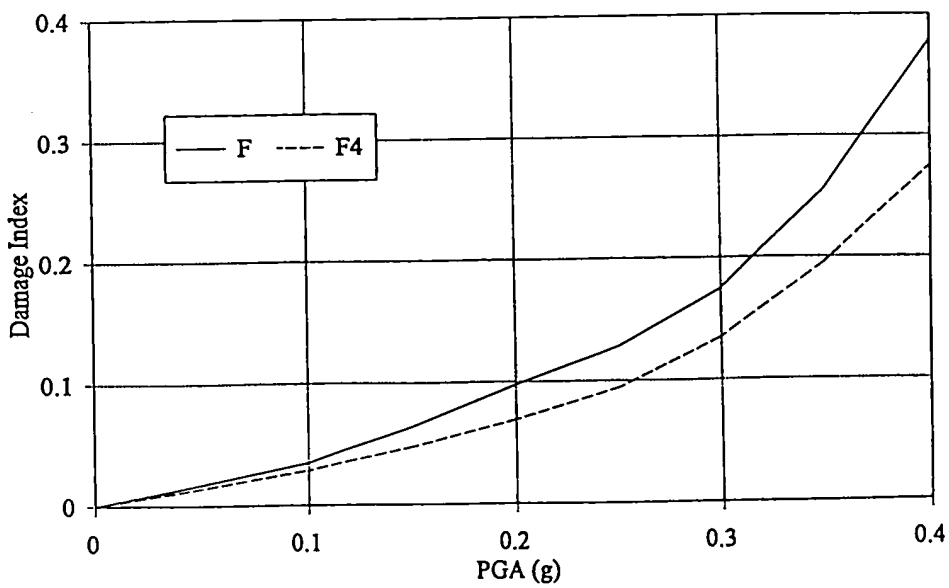

Figure 5.27 Comparison between the damage index of frames F and F4

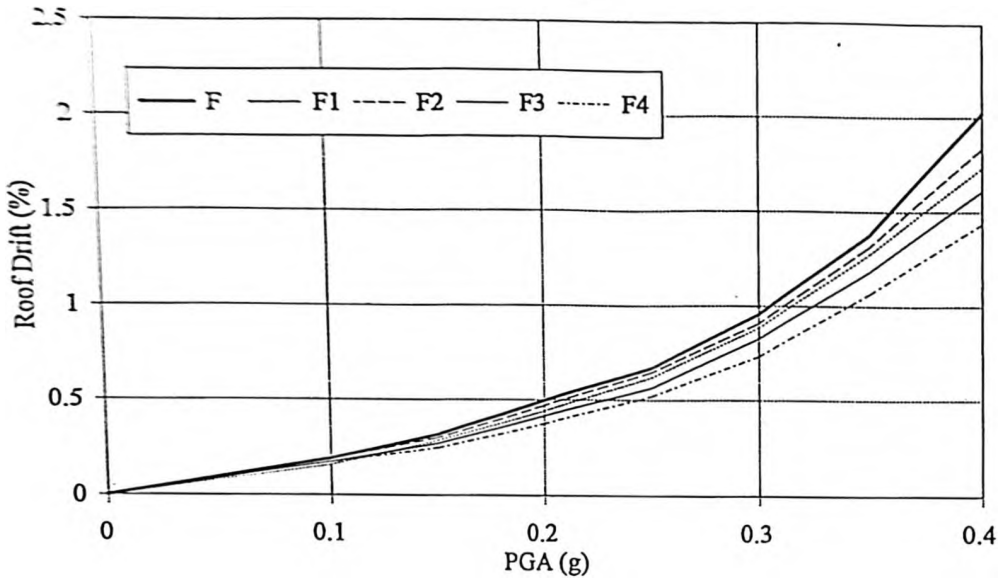

Figures 5.28 Comparison between the roof drift at various values of PGA for the different rehabilitation schemes, along with the original frame

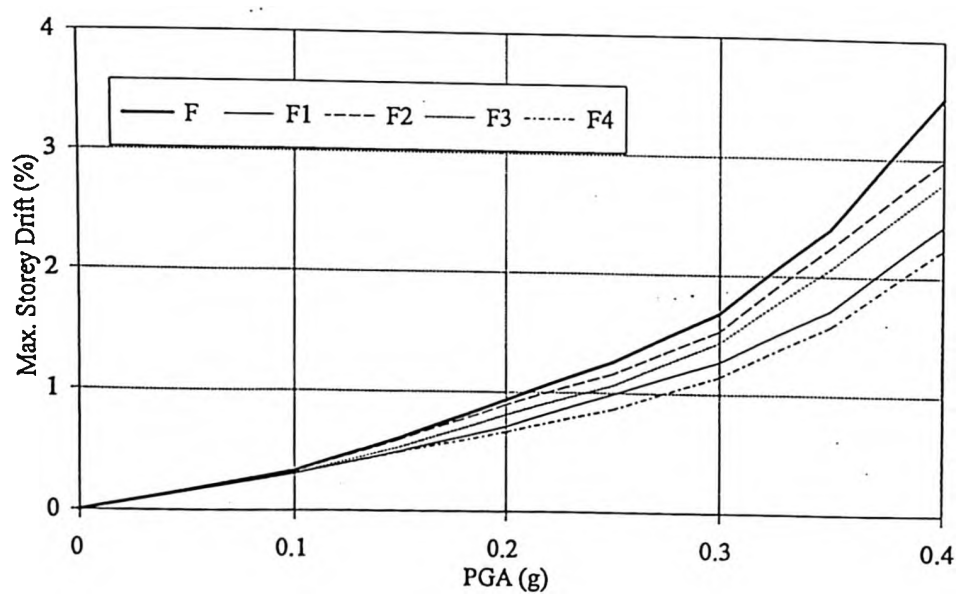

Figures 5.29 Comparison between the maximum storey drift at various values of PGA for the different rehabilitation schemes, along with the original frame

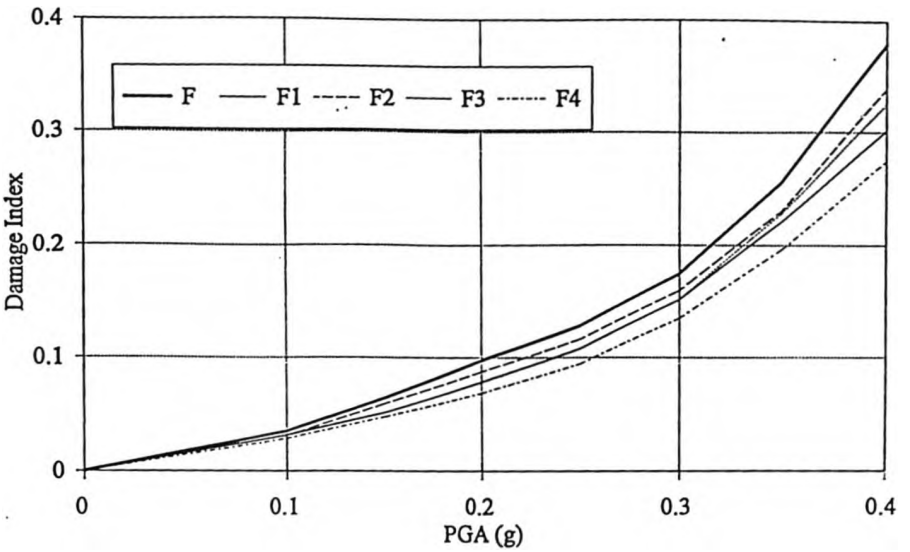

Figures 5.30 Comparison between the damage index at various values of PGA for the different rehabilitation schemes, along with the original frame

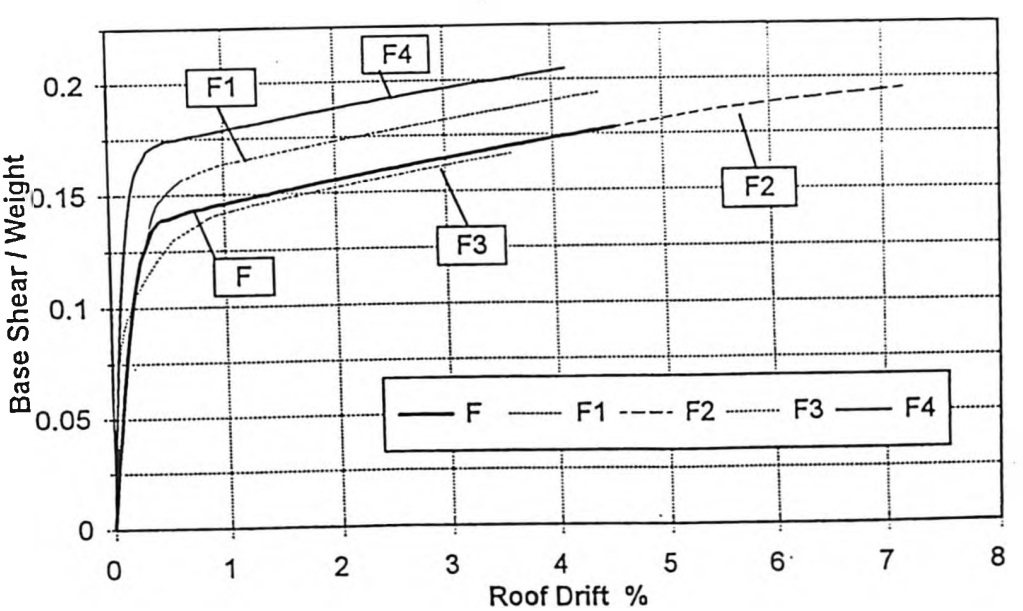

Figure 5.31 Pushover analysis using a triangular load distribution for the three-storey frame (Ghobarah et al., 1997)

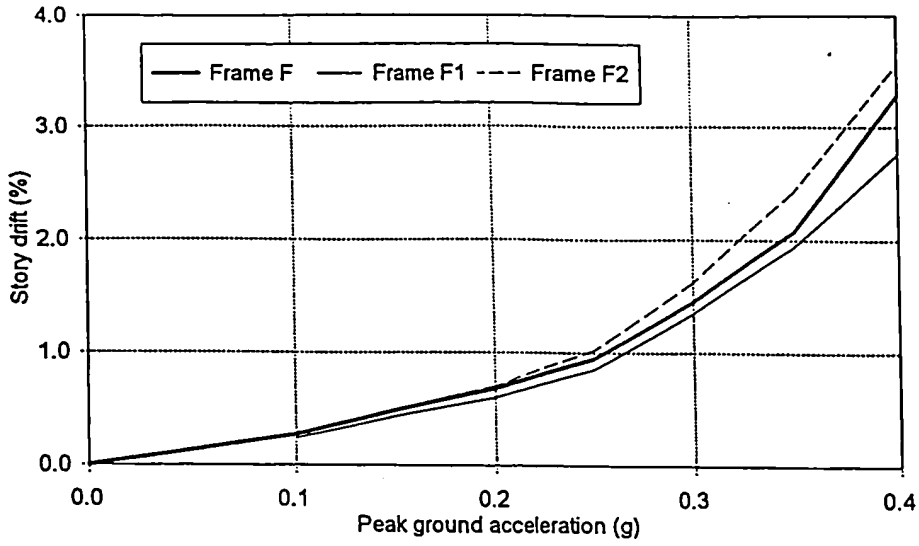

(a)

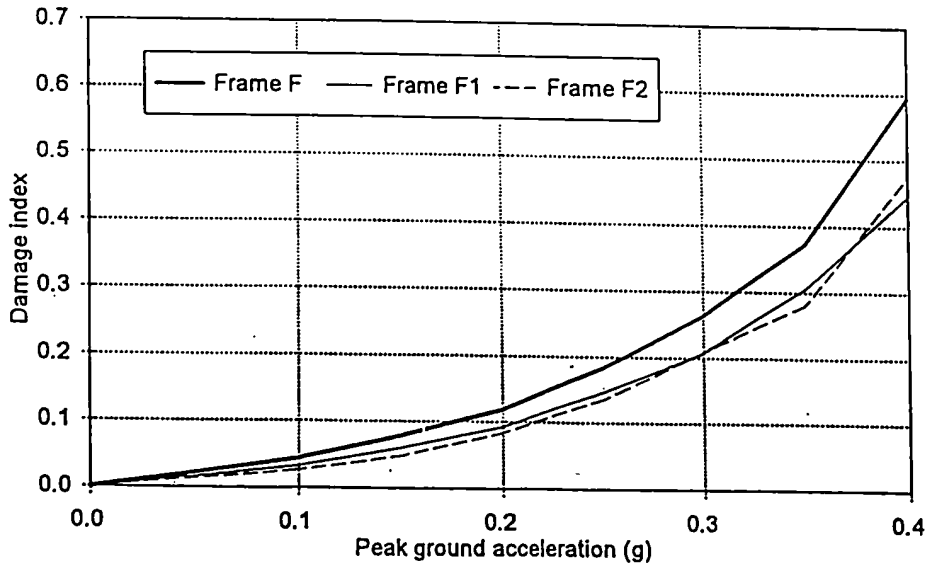

(b)

Figure 5.32 Variation of (a) storey drift and (b) damage index with PGA for the three-storey frame (Aly, 1997)

CHAPTER SIX

CONCLUSIONS AND RECOMMENDATIONS

6.1 SUMMARY

An approach for relating the various stages of damage to drift and peak ground acceleration for a nine-storey concrete building was presented. Due to inherent variation in element dimensions and material strengths, a probabilistic approach was used in which the element dimensions and material strengths were considered as random variables. The defined damage levels and their relationship to drift were used as performance-based design objectives, and in the performance assessment procedure. The static drift of the pushover analysis was related to the dynamic performance of the structure in terms of ground motion characteristics and damage level. For a given design, the pushover analysis, when related to the dynamic performance of the structure, provided the required performance evaluation procedure.

The effectiveness of different rehabilitation strategies for the reinforced concrete columns of the existing building was compared. The four retrofitting techniques tested in the current analysis were:

i) Increasing strength of all columns by 30%.

ii) Increasing ductility of all columns by 200%.

iii) Increasing stiffness of all columns by 500%.

iv) Increasing strength and stiffness of all columns by 50% and 500%, respectively.

6.2 CONCLUSIONS

Based on the results obtained from the current study, the following conclusions are arrived at:

i) Buildings designed in accordance with earlier seismic codes have limited lateral load-resisting capacity.

ii) The developed methodology provides an effective procedure for relating the performance levels to the static pushover analysis which can provide the required assessment of the lateral load carrying capacity of the existing structures as well as new designs to current code provisions.

iii) Modal-adaptive loading for the pushover analysis causes the building to fail at a lower load than for triangular loading. This could be attributed to the contribution of the higher modes in the case of the modal-adaptive loading.

iv) Increasing the strength of concrete columns is an effective rehabilitation scheme to reduce the drift and damage sustained by buildings during seismic events.

v) For a nine-storey building, increasing the columns' ductility does not have a significant effect on the behaviour of the building.

vi) The most effective rehabilitation technique for the columns of the adopted nine-storey office building was increasing the stiffness and strength simultaneously. This retrofitting scheme resulted in lower values of storey drift and damage index.

6.3 RECOMMENDATIONS FOR FUTURE RESEARCH

i) The analysis could be applied to structures other than reinforced concrete moment resisting frames. Examples would be structural walls and masonry buildings.

ii) The analysis could be expanded to include other rehabilitation schemes such as retrofitting of beams, the addition of bracing and/or base isolation.

iii) The analysis could be expanded to include models of flexible joints and shear failure, as well as the other possible failure modes of the structure.

REFERENCES

ACI, (1963a). "Building Code Requirements for Reinforced Concrete." American Concrete Institute Standard 318-63, Detroit, Michigan.

ACI, (1963b). "Commentary on Building Code Requirements for Reinforced Concrete." American Concrete Institute Committee 318 Report, ACI Publication No. SP-10, Detroit, Michigan.

ACI SP-75, (1982). "Fatigue of Concrete Structures." ACI Special Publication SP-75, American Concrete Institute, Detroit, Michigan.

Ahmadi, G., (1979). "Generation of Artificial Time-Histories Compatible with Given Response Spectra - A Review." Solid Mechanics Archives, Volume 4, No. 3, pp. 207-239.

Allen, D.E. and Rainer, J.H., (1995). "Guidelines for the Seismic Evaluation of Existing Buildings." Canadian Journal of Civil Engineering, Volume 22, pp. 500-505.

Aly, N.M., (1997). "Reliability Assessment of Seismic Performance and Retrofit of Buildings." M.Sc. Thesis, McMaster University, Hamilton, Ontario.

Ang, A.H-S. and Tang, W., (1984). "Probability Concepts in Engineering Planning and Design." John Wiley and Sons, New York.

Anicic, D., (1994). "Repair and Retrofit of Building Structures - State-of-the-Art Report." Proceedings of the Tenth European Conference on Earthquake Engineering, Vienna, Austria, Volume 3, pp. 2199- 2208.

Aoyama, H., (1981) "A Method for the Evaluation of the Seismic Capacity of Existing Reinforced Concrete Buildings in Japan." Bulletin of New Zealand National Society for Earthquake Engineering, Volume 14, No. 3, pp. 105-130.

ATC, (1985). "Earthquake Damage Evaluation Data for California." Applied Technology Council, Redwood City, California, Report No. ATC-13.

ATC, (1987). "Evaluating the Seismic Resistance of Existing Buildings." Applied Technology Council, Redwood City, California, Report No. ATC-14.

Banon, H., Biggs, J.M. and Irvine, H.M., (1981). "Seismic Damage in Reinforced Concrete Frames." Journal of Structural engineering, ASCE, Volume 107, No. ST9, pp. 1713-1729.

Bertero, V.V., (1992). "Seismic Upgrading of Existing Structures." Proceedings of the Tenth World Conference on Earthquake Engineering, Madrid, Spain, pp. 5101-5106.

Biddah, A., (1997). "Seismic Behaviour of Existing and Rehabilitated Reinforced Concrete Frame Connections." Ph.D. Thesis, McMaster University, Hamilton, Ontario.

Biddah, A., Ghobarah, A. and Aziz, T.S., (1995). " Assessment of the Capacity of Existing Beam-Column Connections." Proceedings of the Seventh Canadian Conference on Earthquake Engineering, Montreal, Canada, pp. 421-428.

Bonowitz, D., Lee, P., Amin, N. and Desai, R., (1994). "Seismic Assessment Criteria for Multiple Buildings: Lessons From San Francisco's Earthquake Safety Program." Proceedings of the Fifth U.S. National Conference on Earthquake Engineering, Chicago, Illinois, Volume 3, pp. 531-540.

Box, G.E.P., Hunter, W.G., and Hunter, J.S. (1987). "Statistics for Experimenters." John Wiley Publishers, New York.

Bracci, J.M., Reinhorn, A.M., Mander, J.B. and Kunnath, S.K., (1989). "Deterministic Model for Seismic Damage Evaluation of Reinforced Concrete Structures." National Center for Earthquake Engineering Research, Report No. NCEER-89-0033, State University of New York at Buffalo, Buffalo, New York.

Branson, D.E., (1977). "Deformations of Concrete Structures." McGraw-Hill, Inc.

Bush, T., Jones, E. and Garcia J.O., (1991). "Behaviour of a RC Frame Strengthened Using Structural Steel Bracing." Structural Division Journal, ASCE, pp. 1117-1128.

Clough, R.W. and Penzien, J., (1975). "Dynamics of Structures." McGraw-Hill, New York, NY.

Chung, Y.S., Meyer, C. and Shinozuka, M., (1989). "Modelling of Concrete Damage". ACI Structural Journal, Volume 86, No. 3, pp. 259-271.

DiPasquale, E., and Cakmak, A.S., (1990). "Seismic Damage Assessment Using Linear Models." Soil Dynamics and Earthquake Engineering, Volume 9, No. 4, pp. 194-215.

Elghadamsi, F.E., Mohraz, B. and Lee, C.T., (1988). "Time-Dependent Power Spectral Density of Earthquake Ground Motion." Soil Dynamics and Earthquake Engineering, Volume 7, pp. 15-21.

Ellingwood, B.R., (1977). "Statistical Analysis of RC Beam-Column Interaction." Journal of Structural Engineering, ASCE, Volume 103, No. 7, pp. 1377-1388.

Ellingwood, B.R., (1994). " Probability-Based Codified Design for Earthquakes." Engineering Structures, Volume 16, No. 7, pp. 498-506.

Edno, T., Okifuji, A., Sugano, S., Ayashi, T., Shimizu, T., Takahara, K., Saito, H. and Yoneyama, Y., (1984). " Practices of Seismic Retrofit of Existing Concrete Structures in Japan." Proceedings of the Eighth World Conference on Earthquake Engineering, San Francisco, California. Volume I, pp. 469-476.

Englekirk, R.E. and Sabol, T.A., (1990). "Strengthening Buildings to a Life Safety Criterion." Proceedings of the Fourth U.S. National Conference on Earthquake Engineering, Palm Springs, California. Volume 3, pp. 315-321.

FEMA, (1992a). "NHERP Handbook for Seismic Rehabilitation of Existing Buildings." Federal Emergency Management Agency, Washington, D.C., Report No. FEMA-172.

FEMA, (1992b). "NHERP Handbook for the Seismic Evaluation of Existing Buildings." Federal Emergency Management Agency, Washington, D.C., Report No. FEMA-178.

Garcia, J.O., (1994). " Divergent Issues in the Rehabilitation of Existing Buildings." Earthquake Spectra, Volume 10, No. 1, pp. 95-112

Garcia, J.O., (1996). "Strength, Ductility, and Redundancy in Rehabilitation of Reinforced Concrete Structures." Proceedings of the International Conference on Retrofitting of Structures, Columbia University, New York, pp.175-186.

Garcia, J.O., and Badoux, M., (1990). "Strategies for Seismic Redesign of Buildings." Proceedings of the Fourth U.S. National Conference on Earthquake Engineering, Palm Springs, California, Volume 3, pp. 343-251.

Ghobarah, A., (1994). "Seismic Withstand Capacity of Important Reinforced Concrete Structures." Proceedings of the Fifth International Colloquium on Concrete in Developing Countries, Cairo, Egypt, Volume 2, pp. 658-669.

Ghobarah, A., (1996). "Evaluation of the Seismic Capacity of Existing Structures and Their Rehabilitation Requirements." Proceedings of the 7th International Colloquium on Structural and Geotechnical Engineering, Ain Shams University, Cairo, Egypt, Volume 3, pp. 341-358.

Ghobarah, A., Aziz, T.S. and Biddah, A. (1996a). " Seismic Behaviour of Rehabilitated Reinforced Concrete Connections." First Cairo Conference on Concrete Structure, Cairo, Egypt. Section 1.1, pp. 1-11 to 21.

Ghobarah, A., Aziz, T.S. and Biddah, A., (1996b). " Rehabilitation of Reinforced Concrete Beam-column Joints." Proceedings of the Eleventh World Conference on Earthquake Engineering, Acapulco, Mexico, Paper No. 1394.

Ghobarah, A., Aziz T.S. and Biddah, A., (1996c). "Seismic Rehabilitation of Reinforced Concrete Beam-Column Connections." Earthquake Spectra, Volume 12, No. 4, pp. 761-780.

Ghobarah, A., Biddah, A. and Mahgoub, M., (1997). "Seismic Retrofit of Reinforced Concrete Columns Using Steel Jacketing." To appear in the European Journal of Earthquake Engineering.

Ghobarah, A., Aly, N. M. And El-Attar, M., (1997). "Performance Level Criteria and Evaluation." Workshop on Seismic Design Methodologies for the Next Generation of Codes, Bled, Slovenia, Balkema Publishers.

Hamburger, R.O., Rojahn, C., Shapiro, D., Reaveley, L.D., Holmes, W.T. and Moehle, J., (1996). "Performance-Based Guidelines for Seismic Rehabilitation of Buildings." Proceedings of the International Conference on Retrofitting of Structures, Columbia University, New York, New York, pp. 93-111.

Hirosawa, M., Sugano, S. and Kaminosono, T., (1994). "Seismic Evaluation Method and Restoration Techniques for Existing and Damaged Buildings Developed in Japan." Building Research Institute, Ministry of Construction, Tokyo.

Holmes, W.T., (1996). "Seismic Evaluation of Existing Buildings - State-of-the-Practice." Proceedings of the 11th World Conference on Earthquake Engineering, Paper No. 2008, Acapulco, Mexico.

Hwang, H.H.M. and Jaw, J-W., (1990). "Probabilistic Damage Analysis of Structures." Journal of Structural Engineering, ASCE, Volume 116, No. 7, pp. 1992-2007.

Imam, R.L. and Conover, W.J., (1980). "Small Sample Sensitivity Analysis Techniques for Computer Model, with an Application to Risk Assessment." Communications in Statistics, Volume A9, No. 17, pp. 1749-1842.

Jirsa, J.O., (1996). "Strength, Ductility, and Redundancy in Rehabilitation of Reinforced Concrete Structures." Proceedings of the International Conference on Retrofitting of Structures, Columbia University, New York, pp. 175-186

Kunnath, S.K., Reinhorn A.M., and Lobo, R.F., (1992). "IDARC version 3.0: A Program for the Inelastic Damage Analysis of Reinforced Concrete Structures." Report No. NCEER-92-0022. National Center for Earthquake Engineering Research, State University of New York at Buffalo, NY.

Lai, S-S.P., (1982). "Statistical Characterization of Strong Ground Motion Using Power Spectral Density Function." Bulletin of the Seismological Society of America, Volume 72, No. 1, pp.259-274.

Lu, R., Luo, Y. and Conte, J.P., (1994). "Reliability Evaluation of Reinforced Concrete Beams." Structural Safety, Volume 14, pp. 277-298.

Luo, Y.H., Durrani, A. and Conte, J., (1995). "Seismic Reliability Assessment of Existing R/C Flat-Slab Buildings." Journal of Structural Engineering, ASCE, Volume 121, pp. 1522-1530.

Madsen, H.O., Krenk, S. and Lind, N.C., (1986). "Methods of Structural Safety." Prentice-Hall, Inc., Englewood Cliffs, New Jersey.

Mahgoub, M., (1997). "Reinforced Concrete Column Retrofit Using Steel Jeckets." Master of Engineering Thesis, Department of Civil Engineering, McMaster University, Hamilton, Ontario.

Marshall, L. and Farzad, N., (1996). "Use of Design Spectrum-Compatible Time Histories in Analysis of Structures," Proceedings of the 11th World Conference on Earthquake Engineering, Paper No. 326, Acapulco, Mexico.

Melchers, R.E., (1987). "Structural Reliability Analysis and Prediction." Ellis Horwood Ltd., John Wiley & Sons.

Mirza, S.A. and MacGregor, J.G., (1979a). "Variations in Dimensions of Reinforced Concrete Members." Journal of Structural Engineering, ASCE, Volume 105, pp.751-765.

Mirza, S.A. and MacGregor, J. G., (1979b). "Variability of Mechanical Properties of Reinforced Bars." Journal of Structural Engineering, ASCE, Volume 105, pp. 921-937.

Mirza, S.A., Hatzinikolas, M. and MacGregor, J.G., (1979). "Statistical Descriptions of Strength of Concrete." Journal of Structural Engineering, ASCE, Volume 105, No. 6, pp. 1021-1036.

Mori, Y. and Ellingwood, B.R., (1993). "Reliability-Based Service-Life Assessment of Aging Concrete Structures." Journal of Structural Engineering, ASCE, Volume 119, No. 5, pp. 1600-1621.

Naumoski, N., (1996). "Program SYNTH - Theoritical Background." Earthquake Engineering Research Group Brochure, McMaster University, Hamilton, Ontario.

NBCC, (1995). "National Building Code of Canada 1995." National Research Council of Canada, Ottawa, Ontario.

Nilson, A.H. and Winter, G., (1991). "Design of Concrete Structures." McGraw-Hill, Inc., New York.

NRC, (1992a). "Guidelines for Seismic Evaluation of Existing Buildings." Institute for Research in Construction, National Research Council Canada, Ottawa, Ontario.

NRC, (1992b). "Manual for Screening of Buildings for Seismic Investigation." Institute for Research in Construction, National Research Council Canada, Ottawa, Ontario.

Park, Y-J., Ang, A.H-S. and Wen, Y.K., (1984). "Seismic Damage Analysis and Damage-Limiting Design of RC Buildings." Structural Research Series, Report No. UILU-ENG-84-2007, University of Illinois at Urbana-Champaign, Urbana, Illinois.

Park, Y-J. and Ang, A.H-S., (1985). "Mechanistic Seismic Damage Model for Reinforced Concrete." Journal of Structural Engineering, ASCE, Volume 111, No. 4, pp. 722-739.

Park, Y-J., Ang, A.H-S. and Wen, Y.K., (1985). "Seismic Damage Analysis of Reinforced Concrete Buildings." Journal of Structural Engineering, ASCE, Volume 111, No. 4, pages 740-757.

Park, Y-J., Ang, A.H-S. and Wen, Y.K., (1987). "Damage-Limiting Aseismic Design of Buildings." Earthquake Spectra, Volume 3, No. 1, pp. 1-26.

Rodriguez, M. and Park, R., (1991). "Repair and Strengthening of Reinforced Concrete Buildings for Seismic Resistance." Earthquake Spectra, Volume 7, pp. 439-459.

Rodriguez, M. E., (1994). "Seismic Retrofitting Strategy for Buildings." Proceedings of the Fifth U.S. National Conference on Earthquake Engineering, Chicago, Illinois, Volume 3, pp. 569-574.

Rojahn, C., (1986). "ATC Metodology and Data for Rapid Assessment of Seismic Vulnerability." Techniques for Assessment of Seismic Vulnerability. Editor: Scawthorn, C., American Society of Civil Engineers, New York.

Roufael, M.S.L. and Meyer, C., (1987). "Reliability of Concrete Frames Damaged by Earthquakes." Journal of Structural Engineering, ASCE, Volume 113, No. ST3, pp. 445-457.

Sause, R., Pessiki, S., Wu, S. and Kurama, Y., (1996). "Modelling and Seismic Behaviour of Nonductile Concrete Frame Structures and Retrofit Implications." ACI Special Publication SP 160: Seismic Rehabilitation of Concrete Structures, Paper No. SP 160-12, pp. 231-253.

SEAOC, (1995). "Vision 2000: Performance-Based Seismic Engineering of Buildings." Structural Engineers Association of California, Sacramento, California.

Shinozuka, M., (1974). "Digital Simulation of Random Process in Engineering Mechanics with the Aid of FFT Technique." Stochastic Problems in Mechanics, Editors: Ariaratnam, S.T., and Liepholz, H.E.E., University of Waterloo Press, Waterloo, Ontario.

Singhal, A. and Kiremidjian, S., (1996). "Method for Performance Evaluation of Seismic Structural Damage." Journal of Structural Division, ASCE, Volume 122, No. 12, pp. 1459-1467.

Stone, W.C. and Taylor, A.W., (1994). "IDSP: Integrated Approach to Seismic Design of Reinforced Concrete Structures." Journal of Structural Division, ASCE, Volume 120, No. ST12, pp. 3548-3566.

Sues, R.H., Wen, Y-K. and Ang, A.H-S., (1985). "Stochastic Evaluation of Seismic Structural Performance." Journal of Structural Engineering, ASCE, Volume 111, No. 6, pp. 1204-1218.

Sugano S., (1981). "Seismic Strengthening of Existing Reinforced Concrete Buildings in Japan." Bulletin of New Zealand National Society for Earthquake Engineering, Volume 14, No. 4, pp. 209-222.

Tsai, N.C., (1972). "Spectrum-Compatible Motions for Design Purposes." Journal of Engineering Mechanics Division, ASCE, Volume 98, No. EM2, pp. 345-356

Tso, W.K. and Zelman, I.M., (1970). "Concrete Strength Variation in Actual Structures." ACI Journal, Volume 87, pp. 981-988.

Valles, R.E., Reinhorn, A.M., Kunnath, S.K., Li, C. and Madan, A., (1996). "IDARC2D version 4.0: A Computer Program for the Inelastic Analysis of Buildings." Report NCEER-96-0010, State University of New York at Buffalo, New York.

Wen, Y.K., Hwang, H. and Shinozuka, M., (1994). "Development of Reliability-Based Design Criteria for Buildings Under Seismic Load." National Center for Earthquake Engineering Research, Report No. NCEER-94-0023, State University Of New York at Buffalo, Buffalo, New York.

Wilson, E.L., and Habibullah, A., (1987). "Static and Dynamic Analysis of Multistory buildings Including P-Delta Effects." Earthquake Spectra, Volume 3, No. 2, pp. 289-298.

Yao, J.T.P., (1981). "Performance of Low Rise Buildings - Existing and New." Seismic Performance of Low Rise Buildings, Editor: Gupta, A.K., American Society of Civil Engineers, New York.